Physical Aging of Sustainable Polyester Materials towards High-End Consumer Products

Weyhe, Anne Therese Husth

DOI (link to publication from Publisher):
10.54337/aau695968150

Publication date:
2024

Document Version
Publisher's PDF, also known as Version of record

PHYSICAL AGING OF SUSTAINABLE POLYESTER MATERIALS TOWARDS HIGH-END CONSUMER PRODUCTS

BY
ANNE THERESE HUSTH WEYHE

PhD Thesis 2024

AALBORG UNIVERSITY
DENMARK

PHYSICAL AGING OF SUSTAINABLE POLYESTER MATERIALS TOWARDS HIGH-END CONSUMER PRODUCTS

by

Anne Therese Husth Weyhe

AALBORG UNIVERSITY
DENMARK

PhD Thesis 2024

Submitted:	February 2024
Main Supervisors:	Associate Professor Donghong Yu, Aalborg University
	René Mikkelsen, LEGO System A/S
Co-supervisors:	Professor Jesper de Claville Christiansen, Aalborg University
	Emil Andersen, LEGO System A/S
Assessment:	Associate Professor Cristiano Varrone (chair) Aalborg University, Denmark
	Associate Professor Søren Hvidt Roskilde University, Denmark
	Professor Heikki Tenhu University of Helsinki, Finland
PhD Series:	Faculty of Engineering and Science, Aalborg University
Department:	Department of Chemistry and Bioscience

ISSN: 2446-1636
ISBN: 978-87-94563-19-2

Published by:
Aalborg University Open Publishing
Kroghstræde 1-3
DK – 9220 Aalborg Øst
aauopen@aau.dk

Printed in Denmark by Stibo Complete, 2024

ENGLISH SUMMARY

Polyesters are widely used today and are promising candidates as sustainable alternatives to fossil-based acrylonitrile-butadiene-styrene (ABS) in high-end consumer products such as LEGO bricks, where durability and long-term safety are non-negotiable criteria. The transition poses several challenges, including loss of clutch force over time, leading to functional failure. To elevate polyester materials for use in durable products, this thesis aims to tailor the function over time without compromising the impact properties. Furthermore, this work aims to increase the understanding of physical aging in polyesters designed for engineering applications.

Thermal treatment of four glycol modified PET grades at 20 to 40 °C below their glass transition temperatures (T_g), showed acceleration of physical aging measured as enthalpy loss and yield strength increase. The aging rates were found to depend on both chemical structure and co-polymeric composition, where the introduction of rigid chain segments impeded physical aging. Arrhenius and Vogel-Fulcher-Tamman models were used to fit horizontal shift factors, evaluating the time and temperature dependencies. The two models showed no significant differences in ability to describe the effects of physical aging. A difference between the Arrhenius activation energies could suggest a decoupling of physical aging observed as enthalpy relaxation and yield strength increase.

More exotic polyesters with high isosorbide content and high T_g's were investigated to explore whether a correlation between T_g and aging rate exists. These polyesters also demonstrated a difference in Arrhenius activation energies between enthalpy loss and yield strength, emphasizing the complicated relationship between the two methods. Furthermore, most of the polyesters showed increasing aging rate the closer their T_g was to the aging temperature with exception of two polyesters, exhibiting similar T_g's but different aging rates.

After accelerated aging of two glycol modified PET copolyesters, containing 1,4-cyclohexylenedimethylene and 2,2,4,4-tetramethyl-1,3-cyclobutanediol, stress relaxation tests (1.5 % strain) showed a significant decrease in relaxation rate. By modelling these relaxation curves, the concentration of active junctions (junctions sliding during stress relaxation) was found to decrease exponentially with aging time, indicating that molecular configurations with stronger inter-chain interactions are formed during physical aging. Generally, the two polyesters showed similar behaviours independent of chemical structure.

To counter poor impact toughness in especially PET, impact modification with ethylene-butyl acrylate-glycidyl methacrylate was employed. The effect of aging was investigated on impact modified PET to understand the influence, especially in relation to the LEGO function, resulting in a patent application. Incorporation of impact modifier up to 8 wt% did not show any significant effects on physical aging rate measured as enthalpy loss and yield strength increase. Furthermore, impact modification was found to increase stress relaxation and decrease initial stress level, but it did not hamper the effect of accelerated aging (reducing stress relaxation), enabling improved functional durability in LEGO bricks after thermal treatment.

DANSK RESUME

Polyestere er bredt anvendte plastmaterialer og lovende kandidater som bæredygtige alternativer til acrylnitril-butadien-styren (ABS) i produker som LEGO klodser, hvor lang levetid ift. funktion og sikkerhed ikke kan nedprioriteres. At ændre materiale medfører flere udfordringer så som tab af "clutch force" over tid, hvilket medfører faldende funktionalitet. Dette Ph.D. projekt forsøger at skræddersy funktionen over tid i polyestre uden at gå på kompromis med slagstyrke. Desuden er målet med projektet, at øge forståelsen af fysisk ældning i polyester materialer i sprøjtestøbte produkter.

Termisk behandling af fire glykol-modificerede PET materialer ved 20 - 40 °C under deres glastransitionstemperaturer (T_g) viste acceleration af fysisk ældning målt som entalpitab og stigning i trækstyrke. Ældningsraterne viste sig at afhænge både af kemisk struktur og sammensætning af co-polymererne, hvor indtroduktionen af rigide segmenter i polymer kæderne gjorde den fysiske ældning langsommere. Arrhenius og Vogel-Fulcher-Tamman modeller blev anvendt til at beskrive forholdene mellem tid og temperatur af ældningen vha. horisontale forskydningsfaktorer. De to modeller udviste ikke signifikante forskelle på deres nøjagtighed i beskrivelsen af effekterne af fysisk ældning. En forskel på Arrhenius aktiveringsenergier kunne imellemtiden tyde på en afkobling mellem entalpisk relaksation og stigning i trækstyrke.

Mere eksotiske polyestre med højt indhold af isosorbid og høje T_g'er blev også undersøgt for at udforske, om der er en sammenhæng mellem T_g og ældningsrate. Disse polyestre viste også en forskel på Arrhenius aktiveringsenergier mellem entalpitab og stigning i trækstyrke, hvilket understreger det komplekse sammenspil mellem de to metoder. Desuden viste de fleste polyestre højere ældningsrate des tættere temperaturen var på deres T_g med undtagelse af to polyestre, som havde samme T_g men forskellig ældningsrate.

Efter accelereret ældning af to glykol-modificerede PET copolymerer indeholdende 1,4-cyclohexylendimethylen og 2,2,4,4-tetramethyl-1,3-cyclobutandiol viste test af spændingsrelaksation (1.5 % tøjning) en signifikant falende relaksationsrate som funktion af ældningstid. Ved at modellerer relaksationskurverne, blev et eksponentielt fald i antallet af aktive "forbindelser" med ældningstid observeret, hvilket indikerer, at der dannes en molekylekonfiguration med stærkerer intermolekylære interaktioner under fysisk ældning. Generelt viste de to polyestre samme opførsel uafhængigt af kemisk struktur.

For at modvirke lav slagstyrke, blev PET modificeret med ethylene-butyl acrylate-glycidyl methacrylate (E-BA-GMA). Effekten af accelereret fysisk ældning på modificeret PET blev undersøgt for at forstå indflydelsen – særligt ift. funktionen af LEGO klodser, hvilket har resulteret i en patent-ansøgning. Ved modificering med op til 8 vægt% E-BA-GMA var der ingen betydelig indflydelse på ældningsraten målt som entalpitab og stigning i trækstyrke. Der blev observeret en øget spændingsrelaksation og lavere initielt stress niveau med øget mængde E-BA-GMA, men effekten af fysisk ældning blev ikke hæmmet, hvilket betyder, at spændingsrelaksationen mindskedes betydeligt efter ældning. Dette medfører, at accelereret ældning kan forbedre funktionen over tid i LEGO klodser uden at kompromittere slagstyrken.

ACKNOWLEDGEMENTS

I would like to extend my deepest gratitude to my supervisor Donghong Yu for being my guide through the academic world and for great collaboration and support. His constant believe in me and motivation has been invaluable. I also want to thank my co-supervisor Jesper de Claville Christiansen for valuable discussions and Aleksey D. Drozdov for modelling of data, their inputs have been instrumental for my understanding of material behaviours.

A great thanks is also owed to my company supervisor René Mikkelsen for choosing me for this project, for great sparring and for backing my ideas. I have always felt that my work in the R&D team mattered, for which I am very grateful. A sincere thank you also goes to Emil Andersen, for countless academic discussions and help through the entire Ph.D. project. Furthermore, I would like to thank Klaudia Chruslinska and Borbála Kovacs for always taking time to help me in the laboratories in Billund.

My international collaborators at Avantium must be thanked as well. Their interest and enthusiasm to participate in joint work has been highly motivating and has strengthened the findings of my thesis. A special thanks is owed to Bruno Bottega Pergher for providing materials and putting excellent work towards our joint paper. I have truly enjoyed our collaboration.

I would also like to thank my family for their unconditional love and support through the ups and downs of the project period. Their encouragement means the world to me.

Finally, I would like to thank my boyfriend Kristian for being very patient and overbearing with me through tough times and weird working hours, and for always believing in me and keeping my moral high. And to my dog Nuka – for having the greatest stress reducing powers there ever was.

TABLE OF CONTENTS

LIST OF ABBREVIATIONS

Abbreviations are listed in alphabetic order.

ABS	Acrylonitrile-butadiene-styrene
CHDM	1,4-cyclohexylenedimethylene
DSC	Differential scanning calorimetry
E-BA-GMA	Ethylene-butyl acrylate-glycidyl methacrylate
EG	Ethylene glycol
NMR	Nuclear magnetic resonance spectroscopy
PALS	Positron annihilation lifetime spectroscopy
PCL	Poly(ε-caprolactone)
PCTT	Poly(1,4-cyclohexylenedimethylene-*co*-2,2,4,4-tetramethyl-1,3-cyclobutanediol terephthalate)
PE	Polyethylene
PECT	Poly(ethylene-*co*-1,4-cyclohexylenedimethylene terephthalate)
PEF	Poly(ethylene furanoate)
PET	Poly(ethylene terephthalate)
PETT	Poly(ethylene-*co*-2,2,4,4-tetramethyl-1,3-cyclobutanediol terephthalate)
PIBT	Poly(isosorbide-*co*-1,4-butanediol terephthalate)
PICT	Poly(isosorbide-*co*-1,4-cyclohexanedimethanol terephthalate)
PIDT	Poly(isosorbide-*co*-diethylene glycol terephthalate)
PVAc	Polyvinyl acetate
T_a	Aging temperature
T_f	Fictive temperature
T_g	Glass transition temperature
TMCD	2,2,4,4-tetramethyl-1,3-cyclobutanediol
TNM	Tool-Narayanaswamy-Moynihan
VFT	Vogel-Fucher-Tammann

CHAPTER 1. INTRODUCTION

Polyesters, a diverse class of polymers with wide-ranging applications, have received significant attention in the fields of materials science and engineering due to their exceptional properties and versatility. From textile fibres to packaging materials and beverage bottles, polyesters have established their indispensability in various industries.

Since 1963, most LEGO bricks have been made of the terpolymer, acrylonitrile-butadiene-styrene (ABS), which provides a unique clutch force along with many other requirements such as quality, safety, and durability. However, ABS is produced from non-renewable fossil-based resources and thus have a considerable environmental impact. In 2018 the LEGO Group started making some sustainable elements of polyethylene from sugarcanes, launched as *Plants from Plants*, which was the first step on the journey to find alternative sustainable materials. Replacing currently used ABS materials with a sustainable polyester alternative, will facilitate the possibility of using sustainable and recyclable materials. However, the elements need to uphold certain non-negotiable characteristics demanded by the LEGO Group, including a specific and durable clutch force, as seen in Figure 1.1. The clutch force can be described as the force keeping bricks assembled, which origins from the stress created when a nub on top of a brick is pressed into the slightly smaller space in the bottom of another brick and thus straining the elements. It is essential for quality and great play experience that assembly and disassembly of various bricks, geometries, and materials is possible for many years. In order to optimize the development of new sustainable polyester materials, knowledge is needed on how chemical structure of polyester backbone, additives and post-treatment like aging can alter the friction, stiffness, creep and stress relaxation behaviour, which governs the clutch force over time.

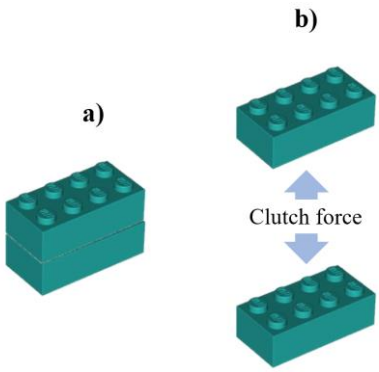

Figure 1.1 a) clutched and b) un-clutched representative LEGO bricks.

The life cycle of LEGO bricks include injection moulding, transport (by land, sea and air), storage and assembling/disassembling. Especially, during transportation and storage, the temperatures can reach up to ~60 °C [1]. Temperatures in this range are relatively close to the glass transition temperatures (T_g) of many polyesters, making significant physical aging inevitable.

By shedding light on the complex interplay between aging time, temperature, molecular structure, and properties of polyesters, this Ph.D. thesis aims to further the knowledge of physical aging mechanisms for future advancements in materials design and engineering. Regarding the properties affecting the clutch force in LEGO bricks, the tribological properties e.g. friction are not considered in this thesis, since it is believed that stress relaxation and creep have a larger influence over time in polyesters.

1.1. OBJECTIVES

The ultimate objective of this Ph.D. project is to get a better understanding of how sustainable polyester materials can be tuned to achieve the correct interconnectivity over time in LEGO bricks. This will not only support the LEGO Group in a faster and safer sustainable material implementation, but also aid other industries along with academia in this understanding. Additionally, the aim is to extend the understanding of physical aging in polyesters and to establish tools or guidelines for future material development. The following objectives serves as basis for this thesis:

1. Elucidate the effect of physical aging on thermodynamic and mechanical properties in polyester materials, relating the aging rates to chemical structure and copolymeric composition.
2. Investigate the effect of physical aging on stress relaxation and creep in polyester materials.
3. Examine the effect of impact modifiers on physical aging rate and viscoelastic properties.

1.2. OUTLINE OF THESIS

This thesis is a collection of papers and consists of seven chapters. The first introductory chapter focusses on the challenges, which this thesis aims to solve (chapter 1). The following chapter summarizes the background and previous work, high-lighting gaps in knowledge. The subsequent four chapters consist of peer-reviewed papers (chapter 3-4), basis for a pending patent (chapter 5) and a manuscript to be submitted (chapter 6). Finally, concluding remarks and perspectives are presented (chapter 7).

Scientific contributions:

I. Weyhe, A. T., Andersen, E., Mikkelsen, R., Yu, D. (2023) Accelerated physical aging of four PET copolyesters: Enthalpy relaxation and yield behaviour *Polymer* 278, 125987

II. Weyhe, A. T. H., Drozdov, A. D., Christiansen, J. C., Andersen, E., Yu, D. (2023) The effect of physical aging on the viscoelastoplastic response of glycol modified poly(ethylene terephthalate) *Materials Today Communications* 37, 107241

III. Weyhe, A. T. H., Bottega Pergher, B., Gruter, G. J., Yu, D. (2024) Physical aging of aromatic copolyesters with high isosorbide content and high glass transition temperatures (to be submitted)

IV. [Patent pending] Method for improving functional durability of toy building elements, inventors: Mikkelsen, R., Andersen, E., Weyhe, A. T.

CHAPTER 2. BACKGROUND

2.1. POLYESTERS

Polyesters are a class of polymers characterized by having ester functional groups as the primary structural component in their main chain. They can be processed by melt spinning, film extrusion and blow- and injection moulding, giving them versatile applications [2]. Generally, synthesis of polyesters is achieved by a polycondensation reaction between a diacid and a diol, allowing diverse chemical structures. One of the most common polyester, polyethylene terephthalate (PET), can be synthesized through transesterification or direct esterification between ethylene glycol (EG) and either dimethyl terephthalate or native terephthalic acid by means of step-reaction polycondensations [3,4].

Even though a large number of polyesters and copolyesters can be prepared by varying dicarboxylic acids and diols, only some of them are commercialized, such as PET, polylactic acid (PLA), polyethylene furanoate (PEF) and poly(1,4-cyclohexylenedimethylene-co-2,2,4,4-tetramethyl-1,3-cyclobutanediol terephthalate) (PCTT), as shown in Figure 2.1.

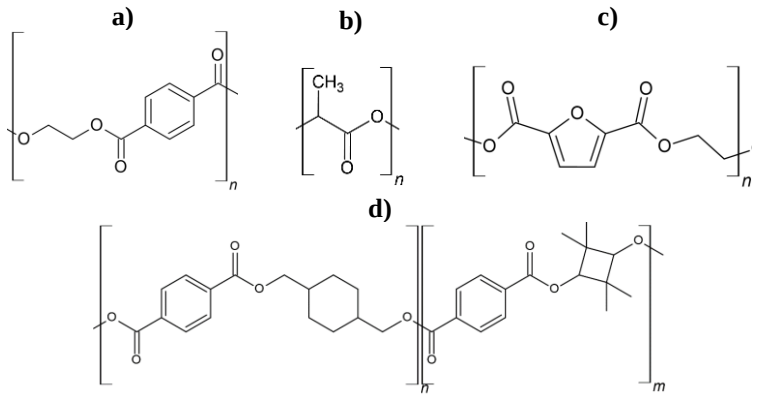

Figure 2.1 Chemical structures of examples of polyesters: a) polyethylene terephthalate (PET), b) polylactic acid (PLA), c) polyethylene furanoate (PEF) and poly(1,4-cyclohexylenedimethylene-co-2,2,4,4-tetramethyl-1,3-cyclobutanediol terephthalate) (PCTT)

Polyester research has predominantly centred on enhancing both mechanical- and barrier properties, with a particular focus on sustainability. The pursuit of sustainable polyesters has led towards derivation of monomers from bio-based resources and recycled/reused materials and monomers. Today, most PET is made using EG derived from ethylene and terephthalic acid obtained from *p*-xylene, components of crude oil. Consequently, PET itself is not considered sustainable [5]. However, PET shows great

possibilities for recycling. Mechanical recycling of post-consumer waste is already an established industrial practice, while chemical recycling shows great prospective [6]. An advantage of using recycled PET lies in the substantial amount of available PET waste. In 2020, 80 million tons of PET were produced, primarily used for bottles and packaging material [7]. Furthermore, a recent report highlights that PET constitutes approximately 12 % of the global solid waste volume [8], making it not only available for recycling but also an environmental risk if mismanaged.

Another polyester, which has gained significant attention in recent years, is PEF. Unlike PET, which is derived from fossil fuels, PEF utilizes biomass as a feedstock, thereby reducing dependency on non-renewable resources. The diacid used for PEF production, 2,5-furandicarboxylic acid, can be synthesized from bio-sources such as fructose and pectin, making it a greener alternative to PET [9]. While PEF shows great promise, there are still challenges to overcome for widespread adoption. One key challenge is the scalability of PEF production and its cost competitiveness compared to traditional polymers [10].

An option to tailor the properties of PET, is through glycol modification by substituting a portion of the ethylene glycol with another diol. Commonly used diols for commercially produced glycol modified PET (PETG) includes 1,4-cyclohexylenedimethylene (CHDM) and 2,2,4,4-tetramethyl-1,3-cyclobutanediol (TMCD), both of which can be synthesized from bio-mass [11,12]. Both diols (especially TMCD) increase the T_g and reduce the crystallization rate compared to PET [13,14], enabling production of amorphous polyesters. CHDM has also been found to enhance impact strength compared to both PET and PET modified with TMCD, owing to the flexibility of CHDM compared to the rigid TMCD. However, the combination of the two glycols has resulted in a polyester (PCTT) with superior impact strength 30 times higher than PET and a T_g above 100 °C [15]. Table 1.1 shows an overview of selected polyesters and their properties.

Recently, isosorbide (1,4:3,6-dianhydroxitol) has gained attention as monomer in different copolyesters and as glycol modification of PET (PEIT) [16,17]. Isosorbide can be derived from glucose, making it a renewable monomer. Its rigid molecular structure and chirality cause polyesters with isosorbide to exhibit high T_g and high modulus [18-20]. Isosorbide has also been used together with other monomers such as CHDM in PET copolyesters, resulting in PEICT, recently commercialized [21]. Such polyesters are promising candidates in the transition from ABS to sustainable polymers in LEGO bricks.

Table 1.1 Overview of selected polyesters and properties. PET copolyesters with TMCD and CHDM are named PETT and PECT, respectively. PCTT contains ~20 % TMCD and ~80 % CHDM [22]. It should be noted, that the properties vary depending on the diol composition

Polyester	Tg [°C]	Notched Impact strength [kJ/m^2]	Yield strength [MPa]	Research
PET	71-83	2-5	62-64	[23,24]
PBT	43-45	3	65	[23]
PEF	82-89	2	67-85	[25]
PEIT	80-91	-	-	[17]
PETT	86	3	61	[23]
PECT	78	9-30	50-54	[26]
PCTT	100-110	99	46-48	[15,23]

2.1.1. GENERAL CHALLENGES

For polyesters to be possible substitutes to ABS in LEGO bricks, several challenges must be addressed. First, polyesters are prone to different degradation pathways, including thermal and photo-induced degradation as well as hydrolysis [27]. Furthermore, polyesters are also vulnerable to recrystallization and physical aging, when exposed to temperatures below their T_g, affecting mechanical properties such as toughness and yield strength over time [22,23]. Both degradation and physical aging cause embrittlement over time, as seen in Figure 2.2 for PET, poly(ethylene-co-2,2,4,4-tetramethyl-1,3-cyclobutanediol terephthalate) (PETT), poly(ethylene-co-1,4-cyclohexylenedimethylene terephthalate) (PECT) and PETT. Before testing, these materials have been subjected to thermal treatment at T_g-20 °C for times indicated in the figure to accelerate physical aging. It is evident that toughness decreases as function of aging time in PET, PETT and PECT, where PCTT maintains its toughness up to approximately 24 h. A similar embrittlement has been shown for many other polymers such as PLA [28], epoxides [29] and polycarbonate [30]. The reduced toughness can be mitigated by means of antioxidants, UV-stabilizers and impact modifiers which have proven to elevate the impact properties of PET to an acceptable level for LEGO bricks [31]. Nevertheless, it is important to understand the influence of physical aging on the impact properties to predict the life-time and durability of the polyester based products.

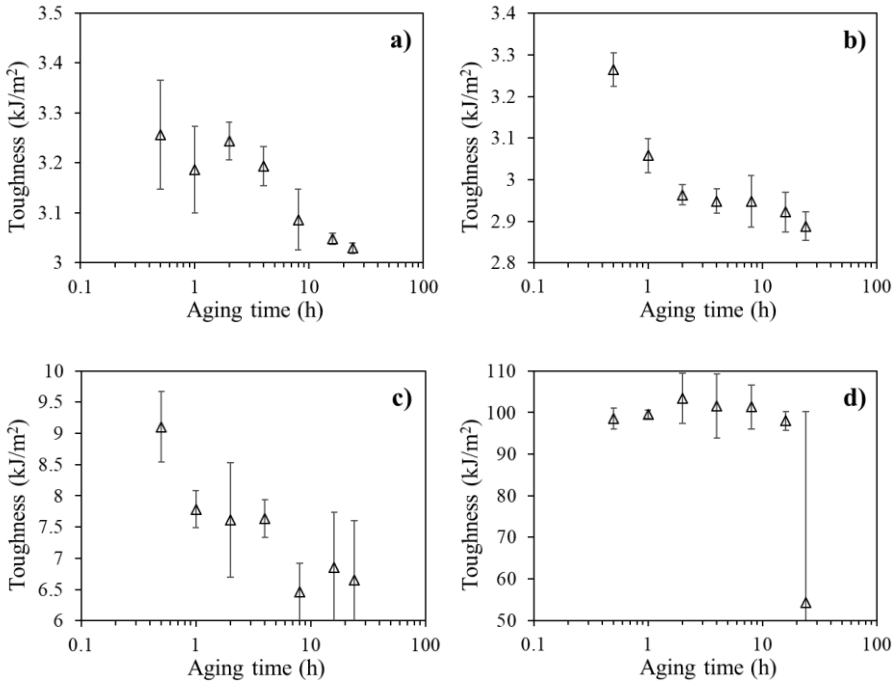

Figure 2.2 Notched impact toughness versus aging time at T_g-20 °C of a) PET, b) PETT with 30 % TMCD, c) PECT with 30 % CHDM and d) PCTT with 20 % TMCD and 80 % CHDM. The impact tests are done according to the method described in [15]

Regarding the long term durability of the LEGO function, polyesters are also challenged by their viscoelastic properties. Due to relative fast stress relaxation, the clutch force decreases drastically over time in LEGO bricks made of polyesters, causing loss of function. Physical aging is also known to affect viscoelastic properties and increase resistance to both stress relaxation and creep, thus providing a possible tool to improve the LEGO clutch force over time. In relation to both embrittlement and improvement of viscoelasticity, physical aging is a key mechanism to be better understood during the development of polyester grades for durable products. Furthermore, prediction of the long-term effect of aging is invaluable for ensuring product life-time.

2.2. PHYSICAL AGING

The state-of-the-art description of physical aging in amorphous polymers is focused on understanding the complex process of relaxation and structural changes that occur over time in these materials at temperatures below their T_g. The phenomenon originates from the fact that glassy materials, such as amorphous polymers, generally are out of equilibrium and, as any thermodynamic system, spontaneously evolve to re-establish their equilibrium state. Amorphous polymers (including some polyesters)

are an important group of glass forming materials and they are used in several high-performance applications, relying on stable properties during their service life.

The formation of a glass involves cooling/quenching a of melt below its T_g. This process is illustrated for a typical glass forming material in Figure 2.3, where the volume and enthalpy dependency on temperature is described. During cooling from the melt, the thermodynamic equilibrium will be lost at a temperature marked by T_g, depending on the cooling rate. At this temperature (or temperature range), the molecular mobility is decreasing to an extent, where the thermodynamic stable configuration, cannot be achieved anymore and thus the molecules are frozen in an out-of-equilibrium state [32] (the thermodynamic equilibrium is represented by the line corresponding to the super-cooled liquid). In this state, the material will have excess enthalpy and free volume compared to the equilibrium. When the obtained glass subsequently is kept at an aging temperature (T_a) of $T_a < T_g$, a thermodynamic stable state is slowly recovered. This process is called physical aging. It is important to highlight, that there are spontaneous fluctuations of thermodynamic variables at equilibrium, and these variables need to be pushed significantly further away from the equilibrium state than the amplitude of the natural fluctuations, for physical aging to occur.

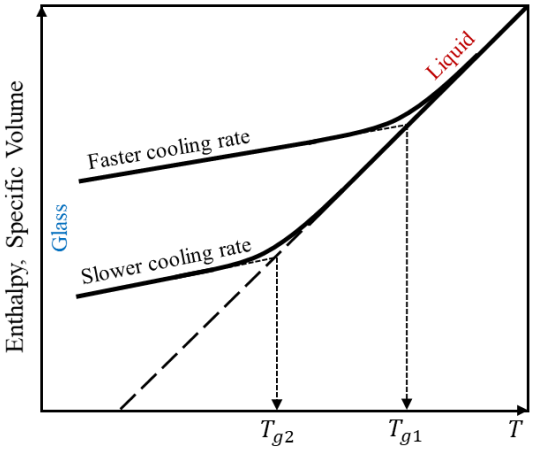

Figure 2.3 Schematic representation of the effect of cooling rate on enthalpy, specific volume and T_g of a glass forming liquid or melt. The dashed line represents the extrapolated equilibrium line

Figure 2.4 illustrates free volume between polymer chains, which affects the specific volume. Today, there is some uncertainty about how free volume is affected during physical aging. Previously, a decreasing free volume has been considered the ultimate cause for the resulting changes in mechanical, thermal and dielectric properties over time [33,34]. However, more recent studies imply that physical aging involves a

redistribution of polymer chains and free volume rather than a reduction of overall volume [35,36].

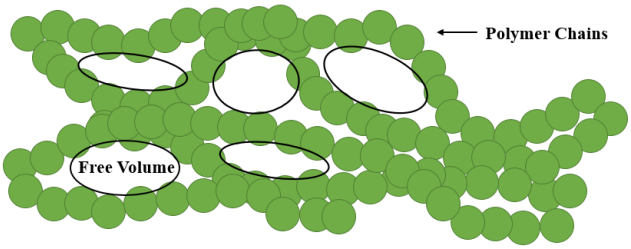

Figure 2.4 Schematic illustration of free volume, seen as gaps between polymer chains

2.3. STUDY OF PHYSICAL AGING

Throughout the years, physical aging has been studied using various methods. The most common ways of monitoring physical aging is through recovery experiments, involving enthalpy [37-39] and volume [40,41]. Apart from those, properties including refractive index [42,43], dielectric properties [39,44] and gas permeability [45-47] have been used to track the aging.

2.3.1. VOLUME RELAXATION

The work of Tool [48-51] from the 1930's and 40's effectively established the theory of volume- and enthalpy relaxation, specifically the presence of a distribution of relaxation times, and the non-linearity of the response of aging. Tool showed that after applying a temperature jump from an equilibrium state, the following isothermal recovery, could not be described by any equations in which the relaxation time only depended on the temperature. He suggested that the relaxation time in addition depended on the state or structure of the glass, which he characterized by means of fictive temperature (T_f) [51]. T_f can be defined as the temperature at which the glass/structure would be in equilibrium, thus being a measure of the structures out-of-equilibrium state. It can be described from Figure 2.5, which illustrate the cooling from equilibrium, and it can be distinguished from T_g according to the method in ref [52]. The resulting enthalpy and volume will deviate from the equilibrium line at a temperature, depending on the cooling rate [53]. Subsequent isothermal aging at a temperature, T_a, will allow the properties to reduce from their original values, V_0, H_0, and approach equilibrium at that specific temperature. After a given aging time, the properties will be, V_t, H_t, and the new T_f is defined as the temperature at which the properties would be equal to their equilibrium values, marked by T_{f2}. Based on this definition, T_f decreases from (close to) T_g to T_a during aging in a way which characterizes the kinetics of the relaxation.

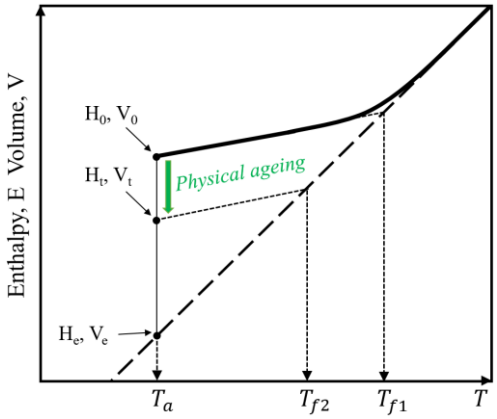

Figure 2.5 Schematic illustration of the effect of aging on thermodynamic properties enthalpy, H, volume, V, and the fictive temperature, T_f. The dashed line represents the extrapolated equilibrium line

The non-linear characteristic of the relaxation can be seen from the work of Kovac and co-workers [54]. They employed a dilatometric technique to study isothermal volume relaxation, and demonstrated a feature of structural relaxation called "memory effects". Kovac studied the volume recovery of glassy polyvinyl acetate (PVAc), subjected to a down-jump in temperature from 40 °C (T_g of PVAc) to 25-37.5 °C for isothermal aging. Another sample was subject to a down-jump to 30 °C and equilibrated followed by an up-jump to 35 °C. As seen from Figure 2.6, the amount of volume recovery increases with decreasing aging temperature, as expected from Figure 2.5. The variation can be explained by the fact that the molecular relaxation time is a function of the thermodynamic state of the glass, and thus for the larger down-jumps, a larger divergence from equilibrium result in more recoverable volume. Furthermore, it can be seen that the recovery rate decreases with decreasing temperature. When comparing the recovery curves of the samples subject to a down-jump (from 40 to 35 °C) and up-jump (from 30 to 35 °C), the shapes are significantly different. The up-jump shows a compressed and self-accelerating behaviour, whereas the down-jumps exhibit a self-retarding effect during aging resulting in stretched functions. These behaviours demonstrate, that the samples seem to have a memory of their previous thermal history and a distribution of relaxation times, which a single relaxation time theory is unable to describe. Similar studies have been published recently [55-57], e.g. showing how the dielectric properties change after different temperature jumps in a glass forming liquid, 4-vinyl-1,3-dioxolan-2-one [55]. In this study Riechers *et al.* demonstrated, that physical aging measured as changes in capacitance as function of time after small temperature jumps (100 mK), exhibited a notable non-linearity. They also saw, that jumping to the same final temperature from a higher temperature resulted in faster response than the same size jump from below, agreeing with the work of Kovac. To explain/model the behaviour, Riechers *et al.* use the concept of material time, which quantifies the rate of aging processes through an

"inner clock" of the material. The concept was proposed by Narayanaswamy in 1971, suggesting that the cause of non-linearity is the changing viscosity of the glass as T_f changes [58]. These theories can, however, be difficult to translate directly to injection moulded polymers, since these typically experience much larger temperature jumps and show more complicated behaviours [59,60].

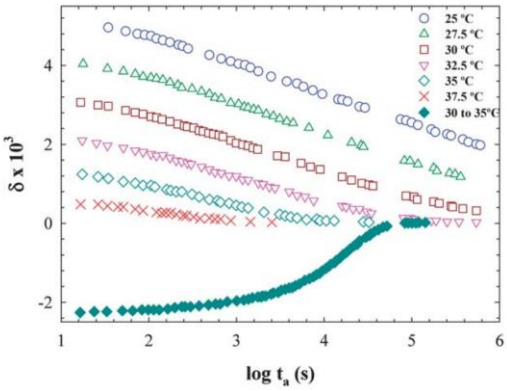

Figure 2.6 Volume recovery in terms of deviation from equilibrium in PVAc after quenching from 40 °C to the indicated temperatures (open symbols) and after equilibrating at 30 °C jumping up to 35 °C [54], [61]

Another technique, positron annihilation spectroscopy (PALS), has found increasing applications in studying physical aging of polymers based on its ability to measure both free volume and the distribution of free volume [62-65]. D.M. Bigg found a strong correlation between fractional free volume, impact strength and physical aging in polycarbonate/PET blends [66]. On the other hand McGonigle *et al.* studied PET using PALS and found no significant variation in free volume with aging time. However, they did find a reduction in dielectric permittivity and increase in storage modulus with aging time, implying the development of local order in the structure [35].

2.3.2. ENTHALPY RELAXATION

The most common technique used to study physical aging in amorphous polymers, is differential scanning calorimetry (DSC) [60,67-69]. DSC can be used to determine the enthalpy of the polymeric glass and thus characterizing its structural state. During physical aging, the enthalpy decreases as described for the volume relaxation. This change in enthalpy can be determined by integration of suitable DSC thermograms, as illustrated for PET in Figure 2.7, where an increase in the magnitude of the endothermic peak and a shift of the peak position to higher temperature is seen around T_g. The difference in enthalpy between an unaged (2nd DSC scan) and aged sample (1st scan after aging) corresponds to the enthalpy lost upon aging. It is typical to find

a linear dependence of both enthalpy loss and the peak temperature on the logarithm of aging time. The former is the enthalpy relaxation, whose linear dependence of aging time corresponds to the linear reduction in volume relaxation, with the logarithm of aging time. However, the dependence of peak temperature upon the logarithm of aging time (peak shift) has been linked to the degree of non-linearity of the relaxation behaviour [70].

Figure 2.7 (right) shows the resulting enthalpy losses as function of aging time at T_g-20 °C for two sets of PET samples. One set of samples is aged after injection moulding (290 → 20 °C during moulding) without preliminary erasing of the thermal history, whereas the other set is heated and equilibrated at 300 °C before quenching in liquid nitrogen (300 → -196 °C). The difference in cooling rate leads to different structural states and hence, the driving force for physical aging is not the same. It is evident from Figure 2.7, that the enthalpy loss is greater in the quenched samples, which can be expected given the faster cooling rate and hence the higher T_f compared to the samples aged as-moulded. This illustration of the memory effect highlights the importance of thermal history in the evaluation of enthalpy relaxation.

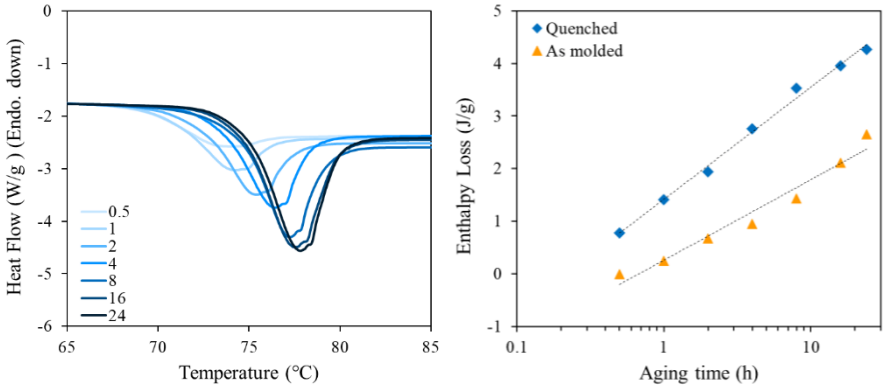

Figure 2.7 Left) DSC thermograms of PET aged at Tg-20 °C after injection moulding for times (in hours) indicated by the legends. Right) Enthalpy lost upon aging at Tg-20 °C in PET quenched from 300 °C in liquid nitrogen (-196 °C) (blue) and PET as moulded (injection moulding) (orange). The DSC experiments were performed according to the methods described in [22]

2.3.3. MECHANICAL PROPERTIES

Physical aging often leads to a transition from a more rubbery state to a glassy state, increasing the material's stiffness, yield strength and brittleness. At the same time, its damping, creep- and stress relaxation rate decrease among other properties. The effect of physical aging on viscoelastic properties of polymers were intensively studied by Struik in the 70's and 80's [33,71-73]. Through creep compliance tests, he showed that physical aging causes an almost horizontal shift of the creep curves, each

producing a shift factor, a_{t_a}. Usually, the logarithm of the shift factors varies linearly with the logarithm of aging time, t_a, and thus the shift rate, μ, (aging rate) can be defined as Eq. (2.1).

$$\mu = -\frac{d\log(a_{t_a})}{d\log(t_a)} \tag{2.1}$$

From studying a wide range of amorphous polymers, Struik concluded, that all polymers age in the same way, and that the effect on their viscoelastic- and mechanical behaviour is very similar. Thereby, he suggested that their amorphous state is the primary cause for their behaviour, and that their chemical structure is less important. However, one of his later studies suggests that backbone rigidity influences the aging rate, slowing the effects of aging in polymers with more rigid chain segments [72]. He further concluded that nearly all characteristics of physical aging can be explained from the free-volume concept, which correlate segmental mobility in the polymer chains with free volume. These statements are based on experiments at small strains and within a temperature range between T_g and the first secondary transition (β-relaxation), which means they might not transfer to polymers under other conditions.

Several more recent studies have monitored the effect of physical aging on mechanical properties and attempted to establish a relationship between these and enthalpy relaxation. Hutchinson *et al*. studied polycarbonate aged at T_g-20 °C and found a discrepancy between enthalpy loss and the effect on yield strength and creep [74]. Andersen *et al*. found a similar inconsistency between enthalpy loss and the effect on yield- and impact strength in PCTT, where the enthalpy reached a plateau before the yield strength and where the impact strength dropped more dramatically [23]. Pan *et al*. observed the same behaviour for poly(L-lactide), where the yield strength and modulus increased gradually with aging time, and the impact strength reduced suddenly [28]. Yoshida investigated the correlation between enthalpy relaxation and relaxation of the dynamic modulus in amorphous poly(ether imide) and semi crystalline poly(aryl ether ether ketone) and observed a good correlation between enthalpy relaxation time and modulus relaxation time in both polymers [75]. These and other studies prove, that the story of physical aging in amorphous polymers is more complex [76], and that chemical structure [22,77], thermal history [55,78,79], aging range [60,80], stress/strain level [81], additives [82,83], degree of crystallinity [84,85] etc. all have an influence. As a final remark, it must be noted, that the different methods for detecting physical aging has different sensitivities and some might interfere with the relaxation process itself, e.g. DSC heats the sample, which can have a rejuvenating effect. Similarly, aging can be erased in mechanical tests, if the yield point is exceeded. Therefore, care must be taken when comparing different techniques.

2.4. MODELS FOR DESCRIBING PHYSICAL AGING

The most widely recognized model for description of physical aging in amorphous polymers is probably the Tool-Narayanaswamy-Moynihan (TNM) model [53,86,87], Eq. (2.2). This model assumes, that the relaxation time for enthalpy relaxation depend on both the temperature and the structure of the glass, given by T_f, where τ is the relaxation time, x is the non-linearity parameter ($0 \leq x \leq 1$) and Δh^* is the apparent activation energy.

$$\tau = \tau_0 \exp\left[\frac{x\Delta h^*}{RT} + \frac{(1-x)\Delta h^*}{RT_f}\right] \tag{2.2}$$

The TNM equation in Eq. (2.2) describes a single relaxation time, whereas it is well known from Kovac's studies, that the kinetics of enthalpy relaxation include a distribution of relaxation times. This could be included by introduction of the stretched exponential response function (2.3), where β is the shape parameter ($0 \leq \beta \leq 1$) or by using τ_i and τ_{0i}, representing the ith element of a discrete distribution.

$$\phi(t) = \exp\left[-(t/\tau)^{\beta}\right] \tag{2.3}$$

The TNM model has its limitations, particularly when it comes to describing long-term aging behaviour. One of the criticisms often pointed at the TNM equation is that it implies an Arrhenius temperature dependence for the relaxation times in equilibrium even though it is known that most polymers are "fragile" and thus obtains a curve in a plot of the logarithm of τ versus reciprocal temperature rather than a straight line. The Vogel-Fucher-Tammann (VFT) equation [88-90], Eq. (2.4), developed for describing viscosity of liquids as function of temperature upon approaching the glass transition temperature, is generally perceived to be able to describe the super-Arrhenius behaviour of physical aging in glass forming polymers.

$$\tau(T) = \tau_0 \exp\left[\frac{D_T T_0}{T - T_0}\right] \tag{2.4}$$

Where D_T denotes the fragility strength coefficient, τ is the relaxation time and T_0 is the so-called Vogel divergence temperature, which is the temperature with infinite relaxation time and zero excess volume. However, the VFT model describes T_0 where $T_0 < T_g$ and $T > T_g$, and thus is mainly meant to describe relaxation above T_g, whereas enthalpy relaxation occurs at temperatures below. However, the relationship described by the VFT model is a key point in developing models describing the relationship between relaxation time in super-Arrhenius behaving materials and thermodynamic variables. Another example is the widely accepted Adam Gibbs model [91], which describes how the configurational entropy ($S_c(T)$) is related to the relaxation time.

$$\tau(T) = \tau_0 \exp\left[\frac{A}{TS_c(T)}\right] \quad (2.5)$$

In Eq. (2.5) the configurational entropy describes the entropy difference between the super cooled state and the crystalline phase (based on the vibrational contribution to entropy). The constant A is related to the intermolecular potential, proportional to the free energy barrier for rearrangement.

Even though the Arrhenius equation has been deemed unable to capture essential aspects of the physical aging behaviour, there might be situations, where it is an acceptable approximation. For aging temperatures below T_g, the viscosity shows a more linear dependence on the temperature compared to aging closer to T_g. Theoretical work by Di Marzio and Yang suggests a change in temperature dependence of the relaxation time at T_g, from VFT- to Arrhenius temperature dependence. Other studies have also found the Arrhenius equation able to describe the temperature dependence below T_g in polycarbonate [92], PVAc [93] and recently polyesters [15], demonstrating its applicability.

2.5. SUMMARY

Even though physical aging of polymers and some polyesters has been well studied, the studies have not yet established general application in polymer engineering. This is probably due to the highly complex relationship between chemical structure, thermal history (non-linearity and memory effect) and effect of aging on thermal- and mechanical properties, making reliable modelling difficult and time consuming. Non-the-less, estimations of product lifetime is invaluable to industries producing durable products, such as the LEGO Group, especially in the transition from using one material (ABS) to using another.

It is well recognized, that volume relaxation and enthalpy loss are directly linked, but the relationship between thermodynamic- and mechanical properties are less clear. Several studies have investigated the effect of physical aging on mechanical and viscoelastic properties, finding a shift along the time axis with varying aging temperature. Time-temperature superposition is also widely used to investigate the shift in creep and stress relaxation, but this method, does not bring a lot of understanding about the underlying mechanisms. For this purpose other models might be considered.

The chemical structure was deemed of lesser importance from Struik's studies of more than 35 different polymers and organic glasses [33], but his later research acknowledge, that chemical structure cannot be ignored [72]. However, only few studies investigate the correlation between structure and aging rates/temperature in polymers. Furthermore, there is a lack of enthalpy studies of "real" samples from injection moulding with complex thermal history, complicating the link to engineering

applications. Injection moulding in itself poses a new level of complexity, since different areas of an injection moulded sample exhibit different thermal history and molecular orientation etc. This problem will not be treated in this thesis, but it must be mentioned, since all experiments are performed on moulded samples.

CHAPTER 3. PHYSICAL AGING IN POLYESTERS

This chapter presents the study of four different polyesters, assessing how the rate of physical aging depends on the chemical structure and composition of CHDM and TMCD segments present in the polyesters. Another primary objective of this study is to investigate whether different material properties age at the same rate during physical aging in amorphous polymers, specifically, the thermal properties, represented by enthalpy relaxation, and the mechanical properties, represented by the increase in yield strength. The practical need for this knowledge is based on the desire to predict the effects of aging on several properties from the aging kinetics of one. Furthermore, understanding the complex relationships between aging, structure and properties, can aid in designing more robust and reliable products with extended lifetimes.

3.1. PAPER I

This study is based on results obtained through DSC studies and tensile tests, investigating the effect of accelerated physical aging on four PET-based copolyesters (PETT, two PECT's (with different amounts of CHDM) and PCTT) thermally treated at T_g-20, 30 and 40 °C.

The results indicate that the physical aging rates indeed depend on both the chemical structure and composition of the CHDM and TMCD segments in the polyesters. The introduction of TMCD was found to retard physical aging, indicating a dependency of aging behaviour on the specific chemical components present in the polymer matrix, and especially the rigidity of the polymer backbone.

The increase in both enthalpy loss and yield strength followed VFT and Arrhenius temperature dependencies with Arrhenius activation energies of 118-244 kJ/mol. However, differences in activation energies for enthalpy and yield strength suggest that the aging of these properties may be decoupled, leading to variations in the rates of property changes over time. Overall, the study highlights the need to consider multiple material properties when assessing physical aging in amorphous polymers.

Polymer 278 (2023) 125987

Contents lists available at ScienceDirect

Polymer

journal homepage: www.elsevier.com/locate/polymer

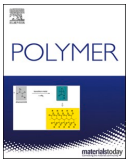

Accelerated physical aging of four PET copolyesters: Enthalpy relaxation and yield behaviour

Anne Therese Weyhe [a,b], Emil Andersen [b], René Mikkelsen [b], Donghong Yu [a,*]

[a] Department of Chemistry and Bioscience, Aalborg University, Fredrik Bajers Vej 7H, DK-9220, Aalborg East, Denmark
[b] LEGO System A/S, Åstvej 1, DK-7190, Billund, Denmark

ARTICLE INFO

Keywords:
Enthalpy relaxation
Physical aging
Polyester
Polymer stability
Vogel-fulcher-tamman
Arrhenius

ABSTRACT

Assessing suitability of amorphous polymers in durable products requires understanding of long-term effects of physical aging on the material properties. This work shows four polyesters with varying diol composition (poly (ethylene-co-1,4-cyclohexylenedimethylene terephthalate) (PETG1 and PETG2 with ~30 and ~60% 1,4-cyclohexylenedimethylene (CHDM), respectively), poly(ethylene-co-2,2,4,4-tetramethyl-1,3-cyclobutanediol terephthalate) (PETT) with ~30% 2,2,4,4-tetramethyl-1,3-cyclobutanediol (TMCD) and poly(1,4-cyclohexylenedimethylene-co-2,2,4,4-tetramethyl-1,3-cyclobutanediol terephthalate) (PCTT) with ~80% CHDM and ~20% TMCD) exposed to thermal treatment at 20, 30 and 40 °C below their respective glass transition temperatures for up to 504 h to accelerate physical aging. The enthalpy relaxation was investigated by differential scanning calorimetry and compared to mechanical changes manifested as tensile yield strength increase. The physical aging rates were found to depend on both chemical structure and composition of CHDM and TMCD segments, where the introduction of TMCD inhibited physical aging. Arrhenius and Vogel-Fulcher-Tamman models were used to fit horizontal shift factors and evaluate the time and temperature dependencies for each polyester. From this study, the two models showed no significant differences in ability to describe the effects of physical aging. The Arrhenius activation energies, E_a, were all in the range 118–244 kJ mol^{-1}, were both PETG1 and PETG2 showed no significant difference between E_a for enthalpy relaxation and yield strength increase, whereas PETT and PCTT showed ~19 and ~107% difference between the two, respectively, suggesting that the relationship between the two phenomena is not independent of chemical structure. The difference between the activation energies suggests that the time scales for physical aging are different when observed as enthalpy relaxation and yield strength.

1. Introduction

Amorphous and semi-crystalline polymers are an essential part of daily life and their significance in engineering applications increases as intensive research in this scientific area continuously improve material performance and properties [1–5]. Being a representative class of commercial polymers showing great potential regarding both sustainability [6,7] and mechanical properties [8], polyesters such as poly (ethylene terephthalate) (PET) has gained much attention. PET is used in beverage bottles, food packaging, and fibres, due to e.g. excellent food-safety and recycling properties [9,10] and, furthermore, the chemical modification of PET with different diols, can lead to improved mechanical [11] and barrier properties [12]. Incorporating 1,4-cyclohexylenedimethanol (CHDM) into PET backbone as illustrated in Fig. 1a, first reported by Kibler et al. in 1959 [13], have led to ternary copolyesters with low crystallization rates and improved optical transparency, mechanical toughness and chemical resistance [14], which can be readily introduced into polyesters via high-temperature, melting state, and/or transition metal catalysed process with superior impact property owning to its conformation transition [14,15]. The glycol ratio of 30% CHDM and 70% EG has originally been chosen for commercialization as it exhibits the lowest crystallization rate compared to other CHDM/EG compositions [14]. This means that increasing the CHDM content further decreases the amorphous window and increases the ability to form ordered structures. Another promising diol, 2,2,4,4-tetramethyl-1,3-cyclobutanediol (TMCD), has also been used to modify PET Fig. 1b increasing the glass transition temperature (T_g) due to the rigid structure of the cyclobutyl ring [16]. Incorporation with TMCD and

* Corresponding author.
E-mail address: yu@bio.aau.dk (D. Yu).

https://doi.org/10.1016/j.polymer.2023.125987
Received 26 January 2023; Received in revised form 20 April 2023; Accepted 24 April 2023
Available online 2 May 2023

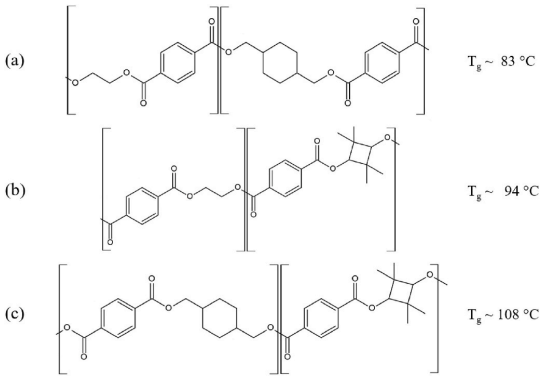

Fig. 1. Chemical structure of (a) poly(ethylene-co-1,4-cyclohexylenedimethylene terephthalate), (b) poly(ethylene-co-2,2,4,4-tetramethyl-1,3-cyclobutanediol terephthalate) (PETT) and (c) poly(1,4-cyclohexylenedimethylene-co-2,2,4,4-tetramethyl-1,3-cyclobutanediol terephthalate) (PCTT) along with their corresponding T_g.

CHDM monomer into a copolyester backbone also led to films with improved toughness and tear resistance compared to traditional polyester films [17]. On the other hand both CHDM and TMCD have been found as renewably sourced materials based on its naturally occurring camphor [18]. However, polyesters are often challenged in high temperature applications [19,20] and in durable products with long lifetime expectancies [21].

Physical aging is a central mechanism, which must be understood in the lifetime prediction of polyesters. Polymers in their glassy state, i.e. below T_g, are not in thermodynamic equilibrium, and their structures continuously approach a meta-stable or an equilibrium state [22]. This time and temperature dependent relaxation process is known as physical aging, causing both micro- and macroscopic changes on materials physical properties. On a molecular level, motions of individual atoms, molecules or segments cause secondary bond breakage and reformation during the structural relaxation [23]. Hence, various types of bonds and interactions are involved in the physical aging process that occurs after glass formation, which, due to the complexity, remain poorly understood. Macroscopically, physical aging of polymers causes an observable change in material properties e.g. enthalpy, free volume, viscosity, fracture toughness, E-modulus [24] and yield strength [20]. The description of the macroscopic relaxation behaviour has often been achieved through phenomenological models such as the Tool-Narayanaswamy-Moynihan (TNM) model, which takes the lead in describing complex relaxation features [25–27]. The TNM model describes the relaxation time as function of fictive temperature (T_f) rather than T_g, where T_f is defined as the temperature at which the glass is in the same state as the relaxed structure [25]. However, both T_g and T_f are readily used in literature to describe the temperature dependence of physical aging rate in glassy materials.

The possibility to predict the rate of physical aging and the effect on material properties is invaluable for the plastic industry. These changes can further influence the functionality of amorphous polymers and govern their applicability [14,16]. Therefore, the use of such amorphous polymers in durable products requires development of experimental methods and numerical models to characterize the long-term effects of physical aging on the mechanical properties to e.g. predict functionality, stability and ultimately lifetime. Several experimental investigations have already been carried out to understand the changes of mechanical properties during physical aging [23,24,28–30]. Differential scanning calorimetry (DSC) is a widely used technique to describe the influence of cooling rate and sub-T_g annealing time on enthalpy relaxation [23,28]. After annealing, the magnitude and peak position of endotherm overshoot around T_g increases, resulting in a quantitative measure of enthalpy lost upon annealing [29]. Another commonly used method to characterize physical aging is to measure the stress-strain response of specimens after different thermal treatments [24,30]. Hutchinson et al. showed that the yield strength of amorphous polycarbonate annealed for 1000 h at 125 °C (≈T_g-20 °C) increased by approximately 20% compared to samples without annealing [30]. Yield strength increase and enthalpy loss are both ascribed to secondary bonds and attractions between polymeric segments, which must be broken in the glass transition upon heating or to reach the yield point of a stress-strain experiment. Therefore, it is realistically assumed, that the two phenomena are coupled and follow similar time and temperature dependency. However, several studies present contradictory results, where the enthalpic response and the change in mechanical properties do not follow each other. It has also been demonstrated that enthalpy and specific volume change do not follow the same kinetics at shorter aging times ($t < t_{eq}$) in polycarbonate, polystyrene and polyvinyl acetate, where t_{eq} is the annealing time necessary to remove the prior thermal history of the sample [19,30]. At $t < t_{eq}$ the specific volume was found to decrease while the enthalpy stayed constant, whereas the two follow the same kinetics at longer aging times ($t > t_{eq}$) [31].

To evaluate the temperature acceleration of aging and to extrapolate results to make long-term predictions, the Arrhenius approach has been traditionally used [32]. The method is based on the assumption, that aging is a thermally activated process with its rate proportional to exp ($-E_a/RT$), where E_a is the activation energy, R is the gas constant and T is the exposed temperature. The Arrhenius equation is expressed as:

$$k = A \exp\left[\frac{E_a}{RT}\right] \tag{1}$$

where k is the rate constant. If the aging process follows Arrhenius behaviour, shift factors will be related to E_a by the expression:

$$a_T = \exp\left[\frac{E_a}{R}\left(\frac{1}{T_{ref}} - \frac{1}{T}\right)\right] \tag{2}$$

where a_T is the shift factor corresponding to the shift from a test temperature, T, to a reference temperature, T_{ref}. The Arrhenius activation energies may be limited by the assumption, that they are temperature-independent, and hence, the activation energies might not be identical for all ranges of annealing temperatures with different proximity to T_g. Therefore, care needs to be taken, when extrapolating outside the tested time and temperatures [33]. Another widely used model to describe relaxation processes is the Vogel-Fulcher-Tamman (VFT) law [29,34], described by the function:

$$\tau = B \exp\left[\frac{D}{T - T_0}\right] \tag{3}$$

where τ is the relaxation time, B is the pre-exponential factor, D is a material dependent constant, the so-called Vogel activation energy, and T_0 is defined as the temperature with zero free volume or infinite relaxation time. Earlier studies by DiMarzio and Yang [35] and O'Connell and McKenna [36] show that changes in viscosity and viscoelastic properties follow VFT temperature dependence above T_g, but transitions to an Arrhenius type dependence as T_g is approached. Furthermore, several studies reported in more recent years show that physical aging experiments (below T_g) deviate from VFT behaviour to a milder temperature dependence in both mechanical and dielectric measurements [37] and for volume and enthalpy loss [38]. However, some studies have also showed that VFT law is retained even at temperatures below T_g. Boucher et al. and Richert both reported VFT behaviour in polyvinyl acetate in relaxation time [39] and time domain experiments [40], respectively. These studies were however carried out in closer proximity to T_g.

In this work we aim to increase the understanding of aging behaviour in new types of polyester. We apply DSC studies to quantify enthalpy relaxation in four different glycol modified PET grades after aging below their respective T_g values. Changes in tensile properties after aging are compared to those in enthalpy relaxation to investigate if the two properties exhibit similar time and temperature dependency, hence if the changes are caused by the same mechanism and can be extrapolated similarly for long-term predictions. Arrhenius and VFT law are used to evaluate the shift factors of the two separate properties. Finally, this work seeks to investigate how glycol modification of PET alters physical aging and whether chemical structure influences the correlation between enthalpy loss and yield strength increase.

2. Materials and methods

2.1. Materials

Granulate of poly(ethylene-co-2,2,4,4-tetramethyl-1,3-cyclobutanediol terephthalate) (PETT) (GMX201, Eastman, USA), poly (ethylene-co-1,4-cyclohexylenedimethylene terephthalate) (PETG1, PETG2) (GN007, DN011, Eastman, USA) and poly(1,4-cyclohexylenedimethylene-co-2,2,4,4-tetramethyl-1,3-cyclobutanediol terephthalate) (PCTT) (TX1001, Eastman, USA) (all structures shown in Fig. 1). The polyesters were injection moulded (Arburg 470E 600-290 Arburg, GER) to tensile test specimens (1BA, ISO 527–2:2012) under various conditions according to Table 1.

2.2. Nuclear magnetic resonance spectroscopy

10 mg of PETT, PETG1, PETG2 and PCTT were dissolved for 2 h in 0.8 mL a co-solvent of 25 vol% deuterated trifluoroacetic acid (99.5% TFAA-d, Sigma Aldrich, GER) and 75 vol% CDCl3 (99.8% Chloroform-d, Sigma Aldrich, GER). NMR spectrometer (Ascend 400 MHz, Bruker, USA) recorded 16 scans for ^{1}H spectra and 1024 scans for ^{13}C NMR spectra. Data analysis was performed in TopSpin (V. 4.1.3, Bruker, GER).

2.3. Attenuated total reflectance infrared spectroscopy

Spectra were collected from the grip section of tensile bars on FT-IR spectrophotometer (Thermo Scientific, iS50, USA) equipped with ZnSe ATR (iD5, Thermo Scientific, USA). Spectra averaged 8 scans in the wavenumber interval of 500–4000 cm^{-1}, with baseline corrected in OMNIC (v. 8.2.388., TA Scientific, USA).

2.4. Gel permeation chromatography

To determine average molecular weights and their distribution, gel permeation chromatography (GPC) was used. Calibration was performed with poly(methylmethacrylate) standards. A solution of 0.5 M potassiumtrifluoroacetate in hexafluoroisopropanol was used as both the eluent and solvent of samples (3 mg/mL at room temperature). All solutions were filtered through a 1 μm filter and 50 μL of those were injected by an autosampler (PSS SECcurity 1260 autosampler) at a flow rate of 1.00 mL/min into columns (PSS PFG, 7 μm, Guard, ID 8.00 mm × 50.00 mm) and 2x(PSS PFG linear M, 7 μm, ID 8.00 mm × 300.00 mm) at 30 °C.

2.5. Thermal treatment

Tensile bars and DSC samples were annealed in ovens at T_g-20, -30 and −40 °C for 0.5, 1, 2, 4, 8, 16 and 24 h, while samples at T_g-30 and -40 °C were treated for 168, 336 and 504 h, additionally. After thermal treatment, all samples were stored at room temperature for a least 24 h before testing.

2.6. Differential scanning calorimetry

Samples of 5–10 mg were cut from tensile bars, placed in pans (Tzero hermetic pan 901683.901, TA Instruments, USA) and covered with lids (Tzero hermetic lid 901683.901, TA Instruments, USA). Samples were measured in a DSC (Q2000, TA Instruments, USA) with nitrogen flow (50 mL/min). All samples were heated twice from 20 to 300 °C at 10 °C/min with their cooling to 20 °C at 10 °C/min in between. Samples were tested in triplicates.

The enthalpy loss ($\Delta H(T_g)$), caused by aging, was determined by the area difference of the endotherm peaks between annealed sample and the references at T_g [19].

2.7. Tensile testing

Test specimens were mounted with the inlet in the lower pneumatic grip in a universal testing machine (Z005, ZwickRoall, GER) with a 25 mm gauge length extensometer (180102/2008, ZwickRoell, GER) controlled by testXpert II (Zwick, GER). Test and data extraction were performed according to ISO 527–1 (tests were done in triplicates). Yield strength (σ_Y) was evaluated at 100 mm/min at 23 ± 2 °C.

2.8. Arrhenius and VFT fit

Arrhenius and VFT plots were prepared from shift factors (a_T) as function of reciprocal temperature of exposure. Horizontal shift factors for both yield strength and enthalpy relaxation were determined with T_g-40 °C as reference temperature (all data was shifted to match the best fit curve for the T_g-40 °C data set). Both sets of shift factors were subsequently fit with Arrhenius and VFT equations.

3. Results and discussion

3.1. Structural analysis

The chemical structures of the four different PET copolymers were characterized by means of ^{1}H NMR, ^{13}C NMR and ATR-FTIR, Figs. S1–17 and Tables S1–9. Glycol ratios of CHDM, TMCD and EG, determined by integrals of their corresponding peaks from ^{1}H NMR spectra, are

Table 2
Chemical composition of PETT, PETG1, PETG2 and PCTT along with number average molecular weight (Mn) determined by GPC.

	CHDM	TMCD	EG	M_n [kDa]
PETT	–	0.29	0.71	14.0
PETG1	0.31	–	0.69	14.8
PETG2	0.63	–	0.37	14.8
PCTT	0.78	0.22	–	13.4

Table 1
Moulding parameters for tensile bars of PETT, PETG1, PETG2, and PCTT.

	Moisture content [%]	Drying temp. [°C]	Drying time [h]	Melt temp. [°C]	Injection pressure [bar]	Mould temp. [°C]	Cooling time [s]
PETT	0.03	80	8	295	1150	80	20
PETG1	0.02	80	8	272	800	60	26
PETG2	0.02	80	8	275	800	60	25
PCTT	0.03	85	6	285	936	80	18

presented in Table 2 along with number average molecular weight (M_n) determined by GPC.

Both PETG1 and PETG2 contain CHDM and EG, where PETG2 contain roughly double the amount of CHDM compared to PETG1 (63 and 31%, respectively). PETT contain 29% TMCD, and thus contain approximately the same amount of EG as PETG1 (71 and 69%, respectively). PCTT contains no EG but only CHDM and TMCD. The M_n values are similar varying from 13.4 to 14.8 kDa, which does not affect thermodynamic properties more than 0–1%, according to the Flory Fox equation [41,42] Eq. S11-13.

Table 3 gathers values of T_g, T_f and ΔC_p determined from the first heating scans from DSC. PCTT exhibits the highest T_g, which can be expected from the increased steric hindrance in especially TMCD but also CHDM compared to EG. Furthermore, the high structural stiffness of TMCD is expressed in the T_g of PETT, which is ~13 °C higher compared to the T_g of PETG1 both containing ~30% glycol modification. Since the CHDM and TMCD segments disrupt the ordered structure of PET, when partially replacing EG, crystallinity was not expected in any of the samples. The amorphous nature was confirmed by DSC and x-ray diffraction spectroscopy, Figs. S9–13, showing no melting/crystallization or crystalline peaks, respectively, in any of the copolyesters.

The difference between T_g and T_f is 2 °C for PETT and the PETGs, whereas the difference is only 1 °C for PCTT. This means that the so-called structural temperature is close to T_g in all the polyesters, and that T_g and T_f are equally good references for physical aging in this study. The obtained values of ΔC_p are similar for all the polyesters and correspond well with previous studies [43]. From these values it can be presumed that the excess energy related to free volume is similar [44,45] suggesting that the thermodynamic force for enthalpy relaxation sub-T_g is likewise similar in the four polyesters [44].

3.2. Enthalpy relaxation

Sets of DSC traces for samples of PETT (a), PETG1 (b), PETG2 (c) and PCTT (d) annealed at Tg-20 °C are shown in Fig. 2. The figure presents an endotherm peak at T_g, which corresponds to the enthalpy lost during annealing. Enthalpy loss increases with annealing time in all polyesters along with T_g-onset and peak position, which has been observed previously [23,28,30]. PETG1 and PETG2 show a steady increase in peak height and T_g-onset while the T_g-onset of PETT and PCTT increase non-linearly. Generally, enthalpy loss is first observed after approx. 2 h of annealing, which agrees with the previously reported conclusion that enthalpy stays constant at short annealing times [31]. This indicates that the polyesters undergo some structural rearrangement with constant enthalpy.

The enthalpy loss as function of annealing time at T_g-20, -30 and −40 °C is shown in Fig. 3, illustrating that enthalpy loss increases linearly with the logarithm of annealing time, which is typical behaviour for glassy polymers [30]. A temperature-dependent rate and inhibition time increase, where the enthalpy loss is zero, is also observed.

A small difference is found when comparing the polyesters containing TMCD (PETT and PCTT) to the ones that only contain CHDM (PETG1 and PETG2) as glycol modification . The enthalpy loss in PCTT and particularly in PETT is lower than in PETG1 and PETG2, presenting that TMCD may inhibit enthalpy relaxation. After 24 h at T_g-20 °C the enthalpy loss of PETT and PCTT are 1.2 ± 0.04 and 2.0 ± 0.04 J/g, respectively, where PETG1 and 2 are 2.8 ± 0.02 and 2.8 ± 0.07 J, respectively. This shows that the rate of enthalpy relaxation is 58 and 27% lower for PETT and PCTT than the PETG1 and PETG2. There are no significant differences between enthalpy relaxation in PETG1 and PETG2 in the tested temperature span, suggesting that the increase in CHDM content from PETG1 to PETG2 does not affect the enthalpy relaxation rate. However, considering the increased enthalpy loss in PCTT compared to PETT, backbone containing CHDM accelerates physical aging compared to that involving EG.

Table 3
Values of T_g, T_f and ΔC_p determined from the first heating scan from DSC.

	T_g [°C]	T_f [°C]	ΔC_p (T_f) [J g^{-1} $°C^{-1}$]
PETT	94.0 ± 1.4	92.0 ± 1.4	0.173 ± 0.01
PETG1	80.7 ± 2.1	78.8 ± 0.1	0.235 ± 0.02
PETG2	84.5 ± 0.2	82.4 ± 0.7	0.173 ± 0.03
PCTT	108.2 ± 0.3	107.1 ± 0.4	0.210 ± 0.01

Horizontal shift factors for enthalpy relaxation in PETT obtained by time-temperature superposition are shown in Fig. 4. Similar plots for PETG1, PETG2 and PCTT can be found in Figs. S18–20. The VFT and Arrhenius fitted curves do not illustrate significant differences in ability to capture the trend in shift factors. Even though Arrhenius provides a slightly better fit, the difference is not large enough to confirm from the data presented here.

The VFT parameters and Arrhenius activation energies can be found in Table 4. PETT exhibits the lowest activation energy suggesting that the enthalpy relaxation in this polyester is less accelerated when annealed in the range T_g-40 to T_g-20 °C compared to the CHDM containing polyesters.

3.3. Yield strength

The yield strength data are shown in Fig. 5 as a function of the annealing time at different temperatures. The yield strength increases linearly with the logarithm of annealing time. It can furthermore be seen that higher annealing temperature shifts the curves to shorter annealing times. For PETT, PETG1 and PETG2 an inhibition period is observed, decreasing with increasing annealing temperature. This period is seen most clearly for T_g-40 °C, where it makes up the first 2 h for PETT and the first 24 h for PETG1 and PETG2. For PCTT a yield strength difference is recorded after just 0.5 h of annealing at all the three temperatures. PETT displays the highest yield strength before aging of ~60 MPa and achieves the highest value after aging, ~72 MPa, after 504 h at T_g-30 °C, suggesting strong secondary interactions induced by TMCD compared to CHDM. In PETG1 a similar increase of 11 MPa is found after 504 h at T_g-30 °C, but the yield strength remained below 66 MPa.

Horizontal shift factors for PETT produced by time-temperature superposition with T_g-40 °C as reference temperature is depicted in Fig. 6 with fitted Arrhenius and VFT models. Similar plots for PETG1, PETG2 and PCTT can be found in Figs. S18–20. The VFT parameters and Arrhenius activation energies are shown in Table 4. The decrease in activation energy of 46–90% in polyesters with TMCD compared to polyesters with only CHDM as glycol modification suggests an inhibiting effect of TMCD on physical aging.

3.4. Summary

The temperature dependencies of physical aging manifested by yield strength increase and enthalpy loss have been investigated and fitted with the Arrhenius equation and VFT law. The obtained activation energies and VFT parameters are presented in Table 3. From the studies carried out here, it is unclear if physical aging in the four polyesters exhibit Arrhenius or VFT behaviour, as the two models are almost identical in the tested temperature range.

The Arrhenius activation energies obtained from yield strength increase and enthalpy loss are generally comparable. For PETG1 and PETG2 the difference is only ~3%, which implies a link between the two dynamics. However, for PETT and PCTT, the activation energy for enthalpy relaxation are ~19 and ~107% higher than for yield strength increase, respectively, suggesting a decoupling of the two. The observation of different activation energies obtained from enthalpic and mechanical measurements, especially of PCTT, suggests that the two types of relaxation have different interactions with the structure. For PETT and PCTT the mechanical change is less affected by temperature than the loss of enthalpy, which suggests that the two relaxations are

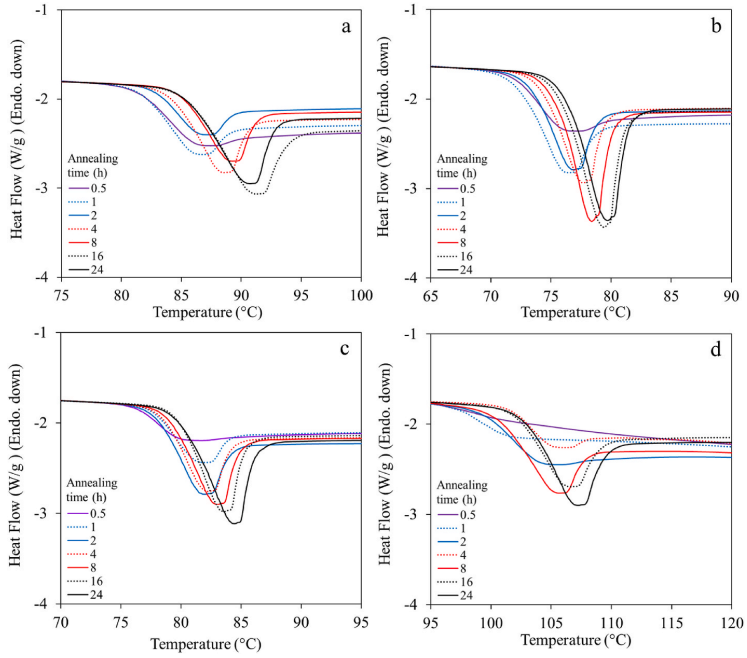

Fig. 2. DSC traces representing first heating scan after annealing of samples, PETT (a), PETG1 (b), PETG2 (c) and PCTT (d). Samples were annealed at T_g-20 °C for the times indicated in the figure legend. Curves are shifted vertically to align the plateau below T_g. Partial scans (25 °C around the T_g's) are shown here and full scans in Figure A.10-13.

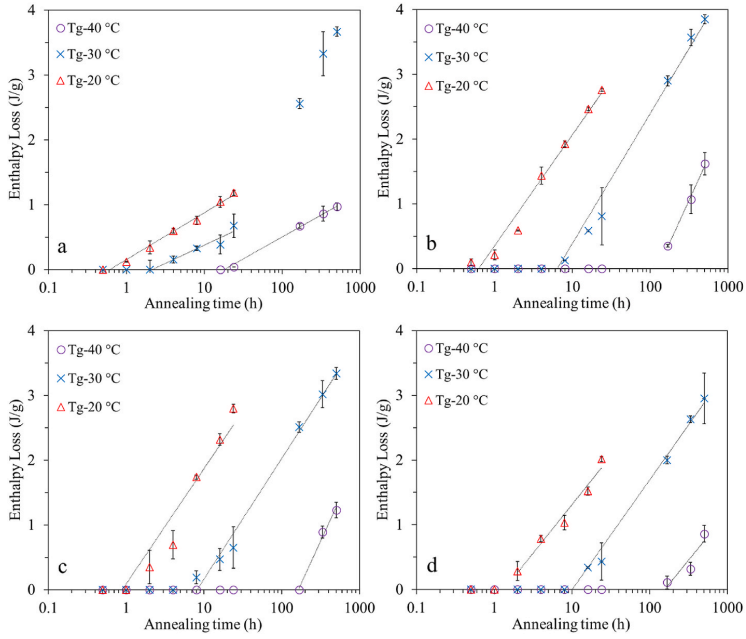

Fig. 3. Enthalpy loss ΔH(Tg) calculated from DSC traces of PETT (a), PETG1 (b), PETG2 (c) and PCTT (d) after annealing at T_g-20, -30 and −40 °C.

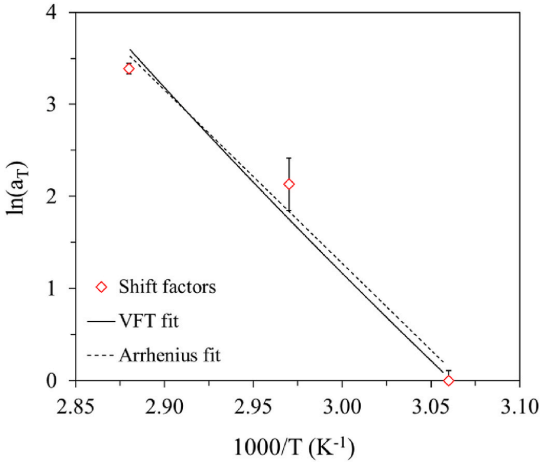

Fig. 4. The logarithm of shift factors versus 1000/T for enthalpy relaxation of PETT.

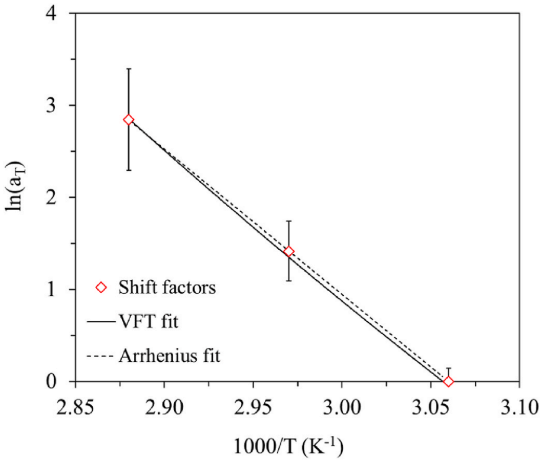

Fig. 6. The logarithm of shift factors versus 1000/T for yield strength increase of PETT.

Table 4
VFT parameters and Arrhenius activation energies, E_a, achieved from fitting yield strength increase and enthalpy loss as function of annealing time and temperature.

	E_a(Yield strength) [kJ mol^{-1}]	E_a (Enthalpy loss) [kJ mol^{-1}]	B(Yield strength)	B (Enthalpy loss)	D(Yield strength)	D (Enthalpy loss)	T_0(Yield strength)[K]	T_0(Enthalpy loss) [K]
PETT	134 ± 20.8	159 ± 5.0	1.05 10^{-17}	3.56 10^{-21}	0.102	0.120	0.0005	0.0005
PETG1	224 ± 12.5	218 ± 12.5	6.74 10^{-19}	1.17 10^{-19}	0.072	0.795	0.0015	0.0014
PETG2	195 ± 15.8	201 ± 11.6	2.90 10^{-21}	2.48 10^{-21}	0.100	0.101	0.0010	0.0010
PCTT	118 ± 13.3	244 ± 15.0	3.49 10^{-18}	1.54 10^{-20}	0.116	0.077	0.0001	0.0012

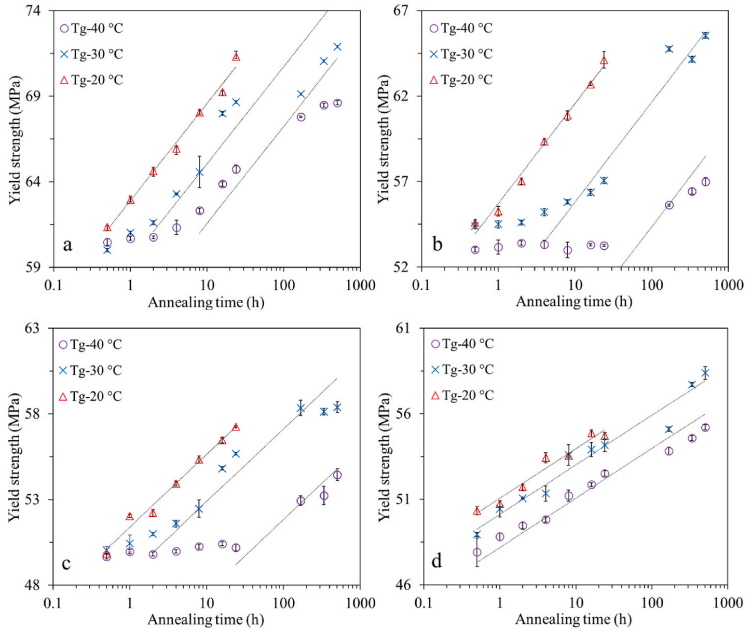

Fig. 5. Tensile yield strength of PETT (a), PETG1 (b), PETG2 (c) and PCTT (d) after annealing at T_g-20, -30 and −40 °C. Lines are created from best logarithmic fit to T_g-20 °C of each polyester and fitted to T_g-30 and -40 °C by changing the intersect.

coupled to the underlying amorphous structure differently. Furthermore, a difference in inhibition period is found between enthalpy and yield strength change, suggesting that structural changes occur before they are measurable in enthalpic experiments. This means, that while the enthalpy stays constant in the early stages of physical aging, the structure rearranges causing mechanical changes. How these rearrangements are permitted and why the enthalpy does not change correspondingly is yet unknown. Since longer annealing times provide a better fit between the two kinetics, expressed as similar Arrhenius activation energies, it is plausible that thermal history of the materials controls the first stage of physical aging.

From this study the correlation between yield strength and enthalpy loss is clearer for the polyesters glycol modified with CHDM instead of TMCD. Furthermore, the thermodynamic equilibrium states of the amorphous phases differs between the investigated copolyesters, suggesting that the mechanical and enthalpic contribution is fundamentally different and that enthalpy loss does not correlate to the yield strength increase.

4. Conclusion

Two related sets of experiments have been carried out independently to investigate the effect of physical aging in four different PET-based copolyesters induced at T_g-20, 30 and 40 °C. We have reported enthalpy relaxation during physical aging, studied by DSC, compared to the effect of physical aging on tensile yield strength. The rates of changes in enthalpy and yield strength depend on both temperature of exposure and backbone rigidity.

The physical aging rate depend on the chemical structure and composition of CHDM and TMCD segment. In the results presented here, structural stiffness and bulkiness decreased physical aging rate measured as both yield strength increase and enthalpy loss. Especially the introduction of TMCD inhibited physical aging.

Generally, the increase in yield strength and enthalpy loss follow Arrhenius and VFT behaviour for all four copolyesters in the tested temperature range. Based on the obtained Arrhenius activation energies, the correlation between yield strength and enthalpy loss is more evident for the polyesters glycol modified with CHDM instead of TMCD suggesting that the relationship between the two phenomena is not independent of chemical structure. Furthermore, this implies that rate and temperature acceleration of physical aging depend on the method of observation.

CRediT authorship contribution statement

Anne Therese Weyhe: Conceptualization, Methodology, Investigation, Formal analysis, Writing – original draft, Writing – review & editing, Funding acquisition. **Emil Andersen:** Conceptualization, Methodology, Writing – original draft, Funding acquisition. **René Mikkelsen:** Supervision, Resources, Funding acquisition. **Donghong Yu:** Supervision, Writing – original draft, Writing – review & editing.

Declaration of competing interest

The authors declare that they have no known competing financial interests or personal relationships that could have appeared to influence the work reported in this paper.

Data availability

Data will be made available on request.

Acknowledgements

This work is partly funded by the Innovation Foundation Denmark under file number0153-00105B. The authors wish to give special thanks to Borbála Kovacs and Nanna Kirkegaard for their great help with handling the materials.

Appendix A. Supplementary data

Supplementary data to this article can be found online at https://doi.org/10.1016/j.polymer.2023.125987.

References

[1] R.M. Cywar, N.A. Rorrer, C.B. Hoyt, G.T. Beckham, E.Y.-X. Chen, Bio-based polymers with performance-advantaged properties, Nat. Rev. Mater. 7 (2) (2022) 83–103, https://doi.org/10.1038/s41578-021-00363-3. Feb.

[2] H. Nakajima, P. Dijkstra, K. Loos, The recent developments in biobased polymers toward general and engineering applications: polymers that are upgraded from biodegradable polymers, analogous to petroleum-derived polymers, and newly developed, Polymers 9 (12) (2017) 523, https://doi.org/10.3390/polym9100523. Oct.

[3] A. Pellis, M. Malinconico, A. Guarneri, L. Gardossi, Renewable polymers and plastics: performance beyond the green, N. Biotech. 60 (Jan. 2021) 146–158, https://doi.org/10.1016/j.nbt.2020.10.003.

[4] M.H. Hassan, et al., The potential of polyethylene terephthalate glycol as biomaterial for bone tissue engineering, Polymers 12 (12) (2020) 3045, https://doi.org/10.3390/polym12123045. Dec.

[5] Z.I. Khan, U. Habib, Z.B. Mohamad, A.M. Raji, Enhanced mechanical properties of a novel compatibilized recycled polyethylene terephthalate/polyamide 11 (rPET/PA11) blends, Express Polym. Lett. 15 (12) (2021) 1206–1215, https://doi.org/10.3144/expresspolymlett.2021.96.

[6] P. Sarda, J.C. Hanan, J.G. Lawrence, M. Allahkarami, Sustainability performance of polyethylene terephthalate, clarifying challenges and opportunities, J. Polym. Sci. 60 (1) (Jan. 2022) 7–31, https://doi.org/10.1002/pol.20210495.

[7] A.K. Singh, R. Bedi, B.S. Kaith, Composite materials based on recycled polyethylene terephthalate and their properties – a comprehensive review, Compos. B Eng. 219 (2021) 108928, https://doi.org/10.1016/j.compositesb.2021.108928. Aug.

[8] W. Loyens, Ultimate mechanical properties of rubber toughened semicrystalline PET at room temperature, Polymer 43 (21) (2002) 5679–5691, https://doi.org/10.1016/S0032-3861(02)00472-X. Oct.

[9] M.K. Eriksen, J.D. Christiansen, A.E. Daugaard, T.F. Astrup, Closing the loop for PET, PE and PP waste from households: influence of material properties and product design for plastic recycling, Waste Manag. 96 (2019) 75–85, https://doi.org/10.1016/j.wasman.2019.07.005. Aug.

[10] A.M. Al-Sabagh, F.Z. Yehia, Gh Eshaq, A.M. Rabie, A.E. ElMetwally, Greener routes for recycling of polyethylene terephthalate, Egypt. J. Pet. 25 (1) (Mar. 2016) 53–64, https://doi.org/10.1016/j.ejpe.2015.03.001.

[11] H. Gao, Y. Bai, H. Liu, J. He, Mechanical and gas barrier properties of structurally enhanced poly(ethylene terephthalate) by introducing 1,6-hexylenediamine unit, Ind. Eng. Chem. Res. 58 (47) (2019) 21872–21880, https://doi.org/10.1021/acs.iecr.9b04953. Nov.

[12] S.K. Burgess, J.E. Leisen, B.E. Kraftschik, C.R. Mubarak, R.M. Kriegel, W.J. Koros, Chain mobility, thermal, and mechanical properties of poly(ethylene furanoate) compared to poly(ethylene terephthalate), Macromolecules 47 (4) (2014) 1383–1391, https://doi.org/10.1021/ma5000199. Feb.

[13] C.J. Kibler, A. Bell, J.G. Smith, Linear Polyesters and Polyester-Amides from 1,4-cyclohexanedimethanol, vol. 25, 1959, 2901466, Aug.

[14] S.R. Turner, Development of amorphous copolyesters based on 1,4-cyclohexanedimethanol, J. Polym. Sci. Part Polym. Chem. 42 (23) (2004) 5847–5852, https://doi.org/10.1002/pola.20460. Dec.

[15] Y. Yu, C. Pang, X. Jiang, Z. Yang, J. Ma, H. Gao, Copolycarbonates based on a bicyclic diol derived from citric acid and flexible 1,4-cyclohexanedimethanol: from synthesis to properties, ACS Macro Lett. 8 (4) (Apr. 2019) 454–459, https://doi.org/10.1021/acsmacrolett.9b00184.

[16] D.R. Kelsey, B.M. Scardino, J.S. Grebowicz, H.H. Chuah, High impact, amorphous terephthalate copolyesters of rigid 2,2,4,4-Tetramethyl-1,3-cyclobutanediol with flexible diols, Macromolecules 33 (16) (2000) 5810–5818, https://doi.org/10.1021/ma000223+. Aug.

[17] K.A. Iyer, Chain mobility, secondary relaxation, and oxygen transport in terephthalate copolyesters with rigid and flexible cyclic diols, Polymer 129 (Oct. 2017) 117–126, https://doi.org/10.1016/j.polymer.2017.09.049.

[18] S. Zhao, J. Zhang, X. Wang, L. Wang, J. Wang, C. Pang, Semiaromatic polyesters from a rigid diphenyl-terephthalic acid: from synthesis to properties, ACS Appl. Polym. Mater. 5 (4) (2023) 2408–2416, https://doi.org/10.1021/acsapm.2c02101. Apr.

[19] E. Andersen, R. Mikkelsen, S. Kristiansen, M. Hinge, Accelerated physical ageing of poly(1,4-cyclohexylenedimethylene- *co* -2,2,4,4-tetramethyl-1,3-cyclobutanediol terephthalate), RSC Adv. 9 (25) (2019) 14209–14219, https://doi.org/10.1039/C9RA00925F.

[20] E. Andersen, R. Mikkelsen, S. Kristiansen, M. Hinge, Real-time ageing of polyesters with varying diols, Mater. Chem. Phys. 261 (2021) 124240, https://doi.org/10.1016/j.matchemphys.2021.124240. Mar.

[21] T. Sang, C.J. Wallis, G. Hill, G.J.P. Britovsek, Polyethylene terephthalate degradation under natural and accelerated weathering conditions, Eur. Polym. J. 136 (2020) 109873, https://doi.org/10.1016/j.eurpolymj.2020.109873. Aug.

[22] L.C.E. Struik, Physical aging in plastics and other glassy materials, Polym. Eng. Sci. 17 (3) (Mar. 1977) 165–173, https://doi.org/10.1002/pen.760170305.
[23] R. Svoboda, J. Málek, Description of enthalpy relaxation dynamics in terms of TNM model, J. Non-Cryst. Solids 378 (Oct. 2013) 186–195, https://doi.org/10.1016/j.jnoncrysol.2013.07.008.
[24] A.V. Cugini, A.J. Lesser, Aspects of physical aging, mechanical rejuvenation, and thermal annealing in a new copolyester, Polym. Eng. Sci. 55 (8) (2015) 1941–1950, https://doi.org/10.1002/pen.24035. Aug.
[25] A.Q. Tool, Viscosity and the extraordinary heat effects in glass, J. Res. Natl. Bur. Stand. 37 (2) (1946) 73, https://doi.org/10.6028/jres.037.033. Aug.
[26] C.T. Moynihan, A.J. Easteal, M.A. Bolt, J. Tucker, Dependence of the fictive temperature of glass on cooling rate, J. Am. Ceram. Soc. 59 (1–2) (Jan. 1976) 12–16, https://doi.org/10.1111/j.1151-2916.1976.tb09376.x.
[27] O.S. Narayanaswamy, A model of structural relaxation in glass, J. Am. Ceram. Soc. 54 (10) (Oct. 1971) 491–498, https://doi.org/10.1111/j.1151-2916.1971.tb12186.x.
[28] N. Doulache, M.W. Khemici, A. Gourari, M. Bendaoud, DSC study of polyethylene terephtalate's physical ageing, in: 2010 10th IEEE International Conference on Solid Dielectrics, IEEE, Potsdam, 2010, pp. 1–4, https://doi.org/10.1109/ICSD.2010.5568072. Juls.
[29] G.D. Liu, J.P. Wu, H.M. Dong, H.Q. Zhang, Nonlinear modification of vogel-fulcher-tamman (VFT) model and its application in enthalpy relaxation of glassy polystyrene, J. Non-Cryst. Solids 528 (2020) 119761, https://doi.org/10.1016/j.jnoncrysol.2019.119761. Jan.
[30] J.M. Hutchinson, S. Smith, B. Horne, G.M. Gourlay, Physical aging of polycarbonate: enthalpy relaxation, creep response, and yielding behavior, Macromolecules 32 (15) (1999) 5046–5061, https://doi.org/10.1021/ma981391t. Jul.
[31] J. Rault, Ageing of glass: role of the vogel fulcher tamman law, J. Phys. Condens. Matter 15 (11) (2003) S1193–S1213, https://doi.org/10.1088/0953-8984/15/11/338. Mar.
[32] K.T. Gillen, R. Bernstein, D.K. Derzon, Evidence of non-Arrhenius behaviour from laboratory aging and 24-year field aging of polychloroprene rubber materials, Polym. Degrad. Stabil. 87 (1) (Jan. 2005) 57–67, https://doi.org/10.1016/j.polymdegradstab.2004.06.010.
[33] K.T. Gillen, M. Celina, R.L. Clough, J. Wise, Extrapolation of accelerated aging data - Arrhenius or erroneous? Trends Polym. Sci. 5 (1997) 250–257.
[34] V. F. Janas and R. L. McCullough, 'The Effects of Physical Aging on the Viscoelastic Behavior of a Thermoset Polyester', p. 20.
[35] E.A. Di Marzio, A.J.M. Yang, Configurational entropy approach to the kinetics of glasses, J. Res. Natl. Inst. Stand. Technol. 102 (2) (1997) 135, https://doi.org/10.6028/jres.102.011. Mar.
[36] P.A. O'Connell, G.B. McKenna, Arrhenius-type temperature dependence of the segmental relaxation below Tg, J. Chem. Phys. 110 (22) (1999) 11054–11060, https://doi.org/10.1063/1.479046. Jun.
[37] J. Zhao, G.B. McKenna, Temperature divergence of the dynamics of a poly(vinyl acetate) glass: dielectric vs. mechanical behaviors, J. Chem. Phys. 136 (15) (2012) 154901, https://doi.org/10.1063/1.3701736. Apr.
[38] S.L. Simon, J.W. Sobieski, D.J. Plazek, Volume and enthalpy recovery of polystyrene, Polymer 42 (6) (2001) 2555–2567, https://doi.org/10.1016/S0032-3861(00)00623-6. Mar.
[39] V.M. Boucher, D. Cangialosi, A. Alegría, J. Colmenero, Time dependence of the segmental relaxation time of poly(vinyl acetate)-silica nanocomposites, Phys. Rev. E 86 (4) (2012), https://doi.org/10.1103/PhysRevE.86.041501, 041501, Oct.
[40] R. Richert, Scaling vs. Vogel–Fulcher-type structural relaxation in deeply supercooled materials, Phys. Stat. Mech. Its Appl. 287 (1–2) (2000) 26–36, https://doi.org/10.1016/S0378-4371(00)00451-9. Nov.
[41] T.G. Fox, P.J. Flory, The glass temperature and related properties of polystyrene. Influence of molecular weight, J. Polym. Sci. 14 (75) (Sep. 1954) 315–319, https://doi.org/10.1002/pol.1954.120147514.
[42] T.G. Fox, P.J. Flory, Second-order transition temperatures and related properties of polystyrene. I. Influence of molecular weight, J. Appl. Phys. 21 (6) (Jun. 1950) 581–591, https://doi.org/10.1063/1.1699711.
[43] T. Hatakeyama, H. Hatakeyama, Effect of chemical structure of amorphous polymers on heat capacity difference at glass transition temperature, Thermochim. Acta 267 (Dec. 1995) 249–257, https://doi.org/10.1016/0040-6031(95)02483-2.
[44] J. Shin, S. Nazarenko, C.E. Hoyle, Effects of chemical modification of Thiol−Ene networks on enthalpy relaxation, Macromolecules 42 (17) (2009) 6549–6557, https://doi.org/10.1021/ma9001403. Sep.
[45] B. Wunderlich, Study of the change in specific heat of monomeric and polymeric glasses during the glass transition, J. Phys. Chem. 64 (8) (1960) 1052–1056, https://doi.org/10.1021/j100837a022. Aug.

Accelerated Physical Aging of Four PET Based Polyesters: Enthalpy Relaxation and Yield Behaviour

Anne Therese Weyhe [a,b], Emil Andersen [b], René Mikkelsen [b], Donghong Yu [a,*]

[a] *Department of Chemistry and Bioscience, Aalborg University, Fredrik Bajers Vej 7H, DK-9220 Aalborg East, Denmark*
[b] *LEGO System A/S, Åstvej 1, DK-7190 Billund, Denmark*

Appendix A

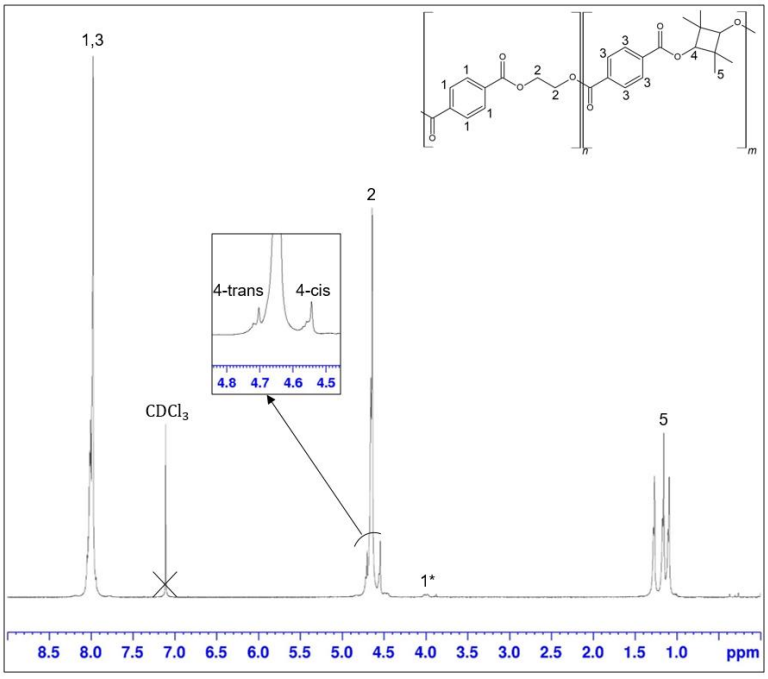

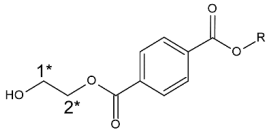

Figure S1. ^{1}H-NMR spectrum of poly(ethylene-co-2,2,4,4-tetramethyl-1,3-cyclobutanediol terephthalate) (PETT).

Table S1. ^{1}H-NMR shifts and assignment of the poly(ethylene-co-2,2,4,4-tetramethyl-1,3-cyclobutanediol terephthalate) (PETT) molecule. See Figure S1 for assignment #.

Chemical shift [ppm]	Assignment #	Ratio
7.98	1,3	76.7
7.11	$CDCl_3$	
4.70	4-trans	5.4
4.62	2	55.1
4.55	4-cis	5.9
4.46	2*	0.9
4.02	1*	1
1.27-1.09	5	52.4

Eq. S1 $$\%\,TMCD = \frac{(peak\ 4trans + peak\ 4cis)\cdot 2}{(peak\ 4trans + peak\ 4cis)\cdot 2 + peak\ 2} \cdot 100\ \%$$

Eq. S2 $$\%\,TMCD = \frac{(5.4+5.9)\cdot 2}{(5.4+5.9)\cdot 2+55.1} \cdot 100\ \% = 29.08\%$$

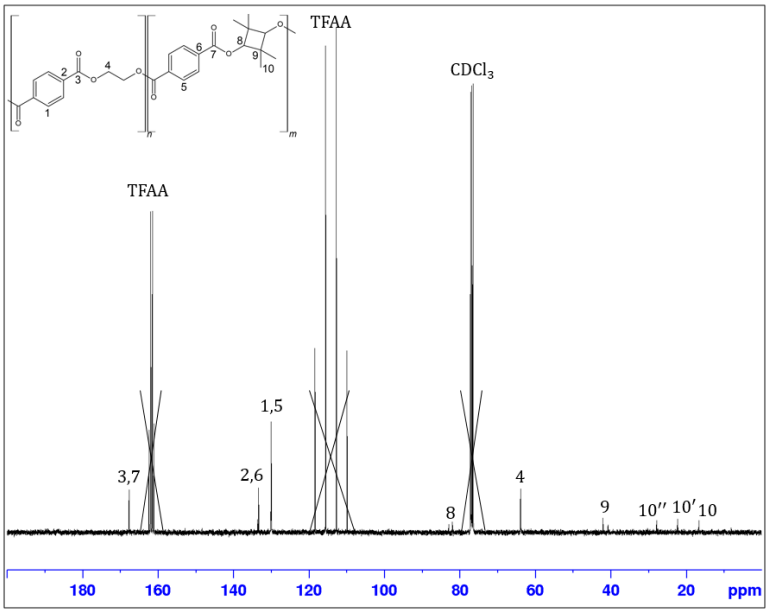

Figure S2. ^{13}C-NMR spectrum of poly(ethylene-co-2,2,4,4-tetramethyl-1,3-cyclobutanediol terephthalate) (PETT).

Table S2. ^{13}C-NMR shifts and assignment of the poly(ethylene-co-2,2,4,4-tetramethyl-1,3-cyclobutanediol terephthalate) (PETT) molecule. See Figure S2 for assignment #.

Chemical shift [ppm]	Assignment
167.68	3,7
133.22	2,6
130.12	1,5
82.91	8
81.92	8
63.85	4
42.01	9
40.69	9
27.77	10''
22.21	10'
16.54	10

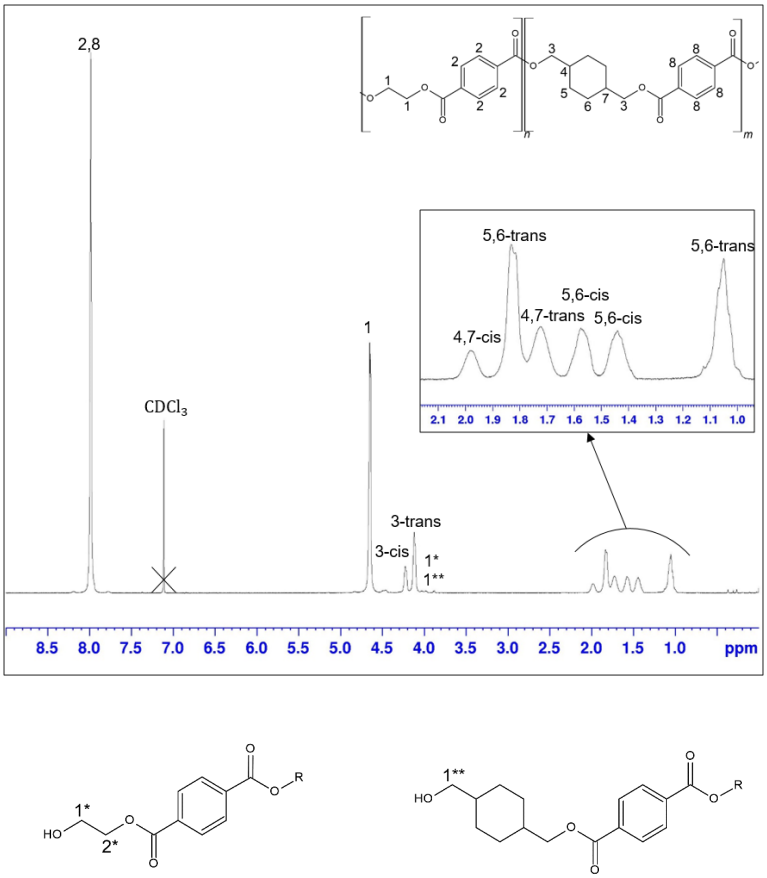

Figure S3. ^{1}H-NMR spectrum of poly(ethylene-co-1,4-cyclohexylenedimethylene terephthalate) (PETG1).

Table S3. ^{1}H-NMR shifts and assignment of the poly(ethylene-co-1,4-cyclohexylenedimethylene terephthalate) (PETG1) molecule. See Figure S3 for assignment #.

Chemical shift [ppm]	Assignment	Ratio
7.98	2,8	70.6
7.11	$CDCl_3$	-
4.65	1	46.8
4.22	3-cis	6.7
4.12	3-trans	14.6
4.03	1*, 1**	1
1.98	4,7-cis	3.8
1.83	6,5-trans	14.9
1.72	4,7-trans	7.8
1.58	6,5-cis	7.0
1.44	6,5-cis	6.9
1.05	6,5-trans	15.1

Eq. S3 $$\%\, CHDM = \frac{(peak\ 3cis + peak\ 3trans)}{(peak\ 3cis + peak\ 3trans) + peak\ 1} \cdot 100\,\%$$

Eq. S4 $$\%\, CHDM = \frac{(6.7+14.6)}{(6.7+14.6)+46.8} \cdot 100\,\% = 31.28\%$$

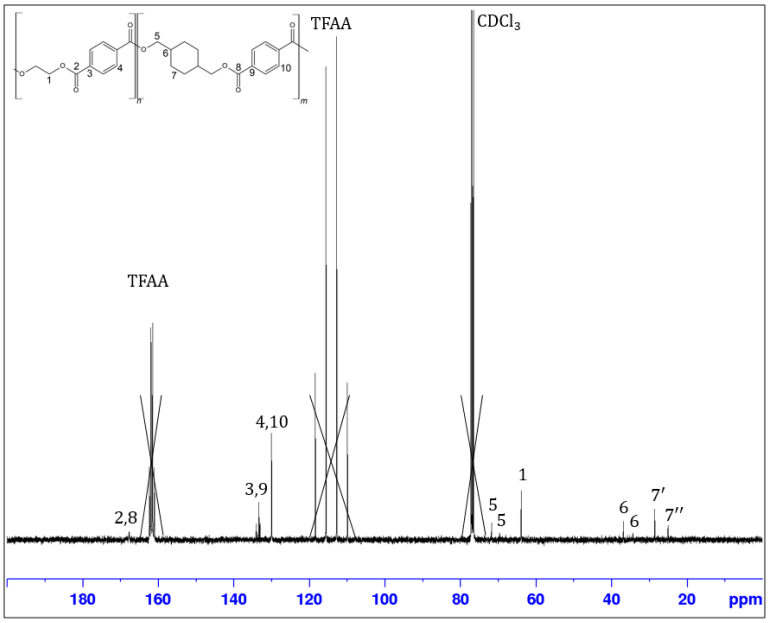

Figure S4. ^{13}C-NMR spectrum of poly(ethylene-co-1,4-cyclohexylenedimethylene terephthalate) (PETG1).

Table S4. ^{13}C-NMR shifts and assignment of the poly(ethylene-co-1,4-cyclohexylenedimethylene terephthalate) (PETG1) molecule. See Figure S4 for assignment #.

Chemical shift [ppm]	Assignment
167.69	2,8
133.32	3,9
130.02	4,10
71.69	5
69.56	5
63.84	1
36.79	6
34.27	6
28.49	7’
24.96	7’’

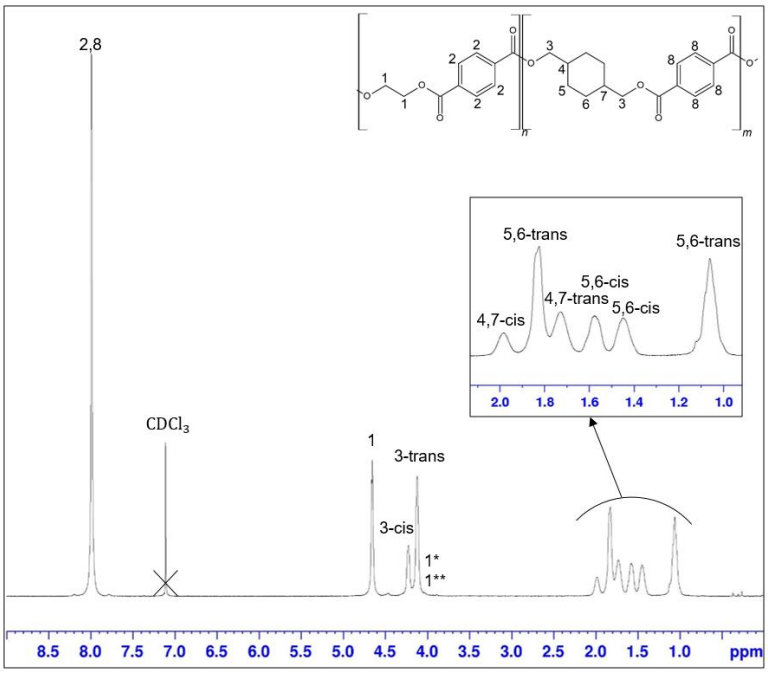

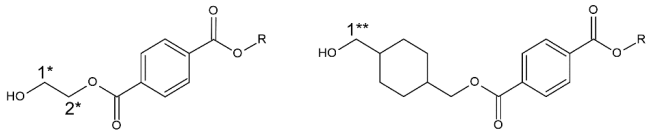

Figure S5. [1]H-NMR spectrum of poly(ethylene-co-1,4-cyclohexylenedimethylene terephthalate) (PETG2).

Table S5. ^{1}H-NMR shifts and assignment of the poly(ethylene-co-1,4-cyclohexylenedimethylene terephthalate) (PETG2) molecule. See Figure S5 for assignment #.

Chemical shift [ppm]	Assignment	Ratio
7.99	2,8	61.3
7.11	$CDCl_3$	-
4.66	1	22.4
4.23	3-cis	12.1
4.12	3-trans	25.5
4.03	1*, 1**	1
1.98	4,7-cis	6.5
1.82	6,5-trans	25.9
1.73	4,7-trans	13.7
1.58	6,5-cis	11.9
1.45	6,5-cis	11.8
1.06	6,5-trans	26.5

Eq. S5 $$\%\, CHDM = \frac{(peak\ 3cis + peak\ 3trans)}{(peak\ 3cis + peak\ 3trans) + peak\ 1} \cdot 100\,\%$$

Eq. S6 $$\%\, CHDM = \frac{(12.1 + 25.5)}{(12.1 + 25.5) + 22.4} \cdot 100\,\% = 62.67\,\%$$

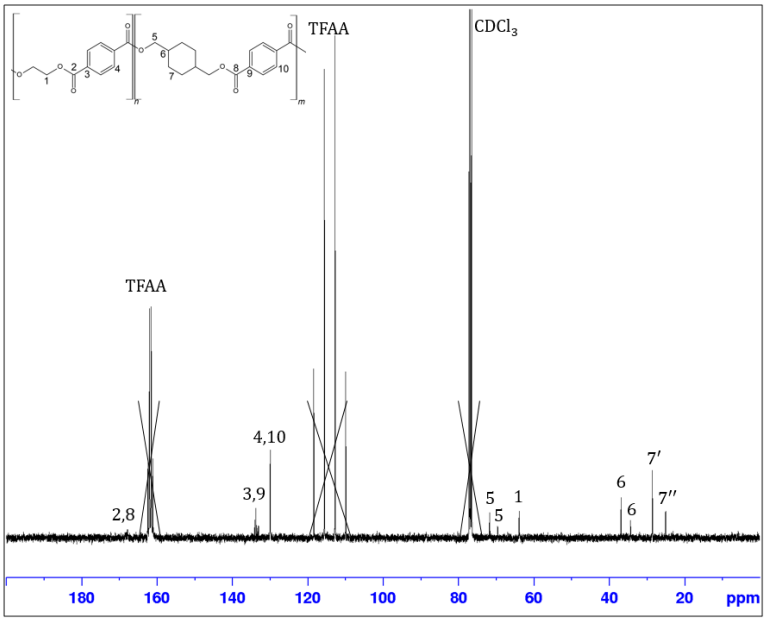

Figure S6. ^{13}C-NMR spectrum of poly(ethylene-co-1,4-cyclohexylenedimethylene terephthalate) (PETG1).

Table S6. ^{13}C-NMR shifts and assignment of the poly(ethylene-co-1,4-cyclohexylenedimethylene terephthalate) (PETG1) molecule. See Figure S6 for assignment #.

Chemical shift [ppm]	Assignment
168.41	2,8
133.75	3,9
130.01	4,10
71.68	5
69.55	5
63.86	1
36.81	6
34.28	6
28.51	7’
24.98	7’’

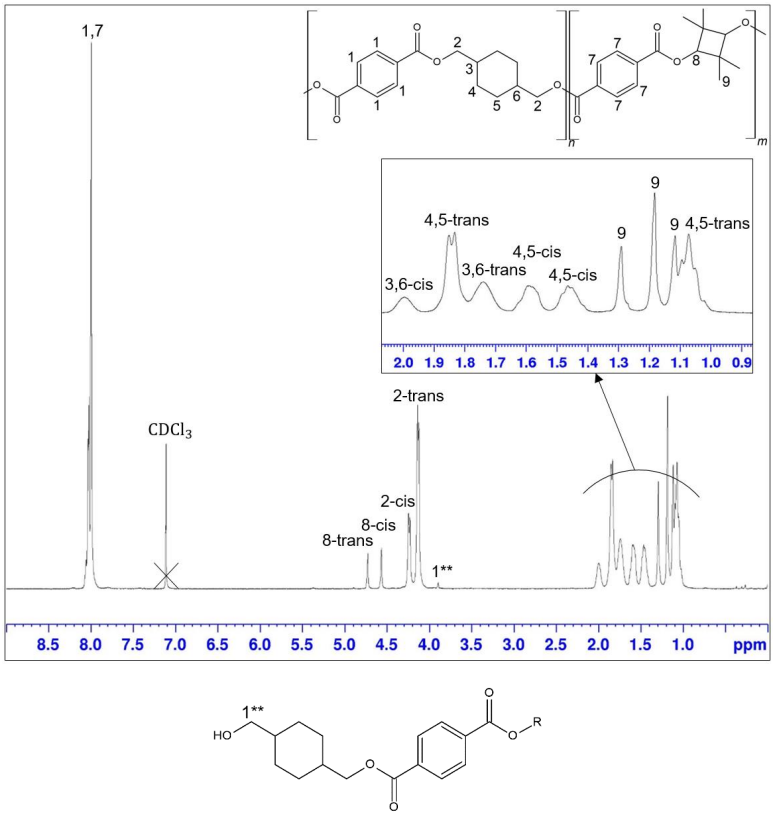

Figure S7. ^{1}H-NMR spectrum of poly(1,4-cyclohexylenedimethylene-co-2,2,4,4-tetramethyl-1,3-cyclobutanediol terephthalate) (PCTT).

Table S7. ^{1}H-NMR shifts and assignment of the poly(1,4-cyclohexylenedimethylene-co-2,2,4,4-tetramethyl-1,3-cyclobutanediol terephthalate) (PCTT) molecule. See Figure S7 for assignment #.

Chemical shift [ppm]	Assignment	Ratio
8.00	1,7	54.2
7.12	$CDCl_3$	-
4.72	8-trans	2.7
4.56	8-cis	3.3
4.24	2-cis	12.6
4.14	2-trans	29.5
3.90	1**	1
1.99	3,6-cis	6.9
1.85	4,5-trans	29.1
1.74	3,6-trans	15.8
1.59	4,5-cis	13.0
1.46	4,5-cis	13.3
1.29	9	39.2
1.07	4,5-trans	29.2

Eq. S7 $$\%\,CHDM = \frac{(peak\ 2cis + peak\ 2trans)}{(peak\ 2cis + peak\ 2trans) + (peak\ 8trans + peak\ 8cis)\cdot 2} \cdot 100\ \%$$

Eq. S8 $$\%\,CHDM = \frac{(12.6+29.5)}{(12.6+29.5)+(2.7+3.3)\cdot 2} \cdot 100\ \% = 77.82\ \%$$

Eq. S9 $$\%\,TMCD = \frac{(peak\ 8trans + peak\ 8cis)\cdot 2}{(peak\ 2cis + peak\ 2trans) + (peak\ 8trans + peak\ 8cis)\cdot 2} \cdot 100\ \%$$

Eq. S10 $$\%\,CHDM = \frac{(2.7+3.3)\cdot 2}{(12.6+29.5)+(2.7+3.3)\cdot 2} \cdot 100\ \% = 22.18\ \%$$

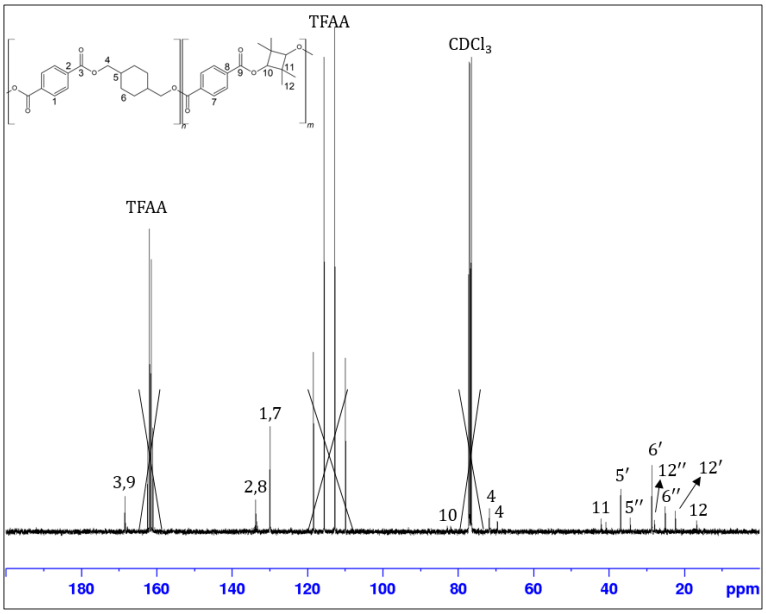

Figure S8. ^{13}C-NMR spectrum of poly(1,4-cyclohexylenedimethylene-co-2,2,4,4-tetramethyl-1,3-cyclobutanediol terephthalate) (PCTT).

Table S8. ^{13}C-NMR shifts and assignment of the poly(1,4-cyclohexylenedimethylene-co-2,2,4,4-tetramethyl-1,3-cyclobutanediol terephthalate) (PCTT) molecule. See Figure S8 for assignment #.

Chemical shift [ppm]	Assignment
168.43	3,9
133.70	2,8
130.02	1,7
81.92	10
71.68	4
69.55	4
42.02	11
40.73	11
36.83	5’
34.83	5’’

28.53	6’
27.84	12’’
25.00	6’’
22.30	12’
16.63	12

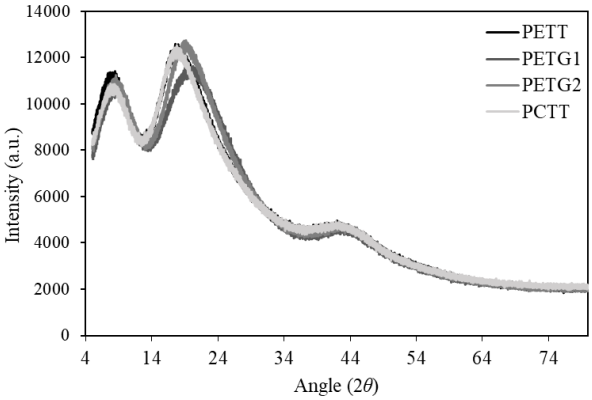

Figure S9. XRD spectra of poly(ethylene-co-2,2,4,4-tetramethyl-1,3-cyclobutanediol terephthalate) (PETT), poly(ethylene-co-1,4-cyclohexylenedimethylene terephthalate) (PETG1)(PETG2) and poly(1,4-cyclohexylenedimethylene-co-2,2,4,4-tetramethyl-1,3-cyclobutanediol terephthalate) (PCTT) showing three amorphous peaks for all four polyesters.

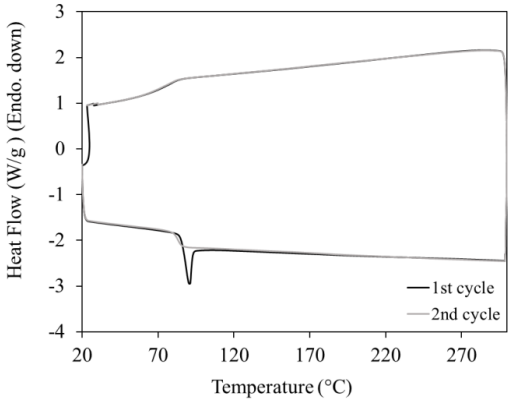

Figure S10. Sequential DSC scans of poly(ethylene-co-2,2,4,4-tetramethyl-1,3-cyclobutanediol terephthalate) (PETT) showing glass transition (T_g ~ 94 ºC) and enthalpic overshoot.

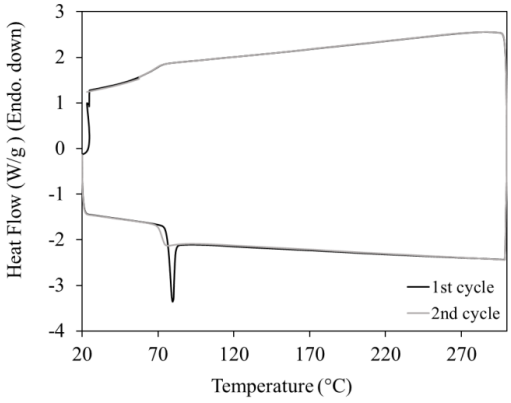

Figure S11. Sequential DSC scans of poly(ethylene-co-1,4-cyclohexylenedimethylene terephthalate) (PETG1) showing glass transition (T_g ~ 80 ºC) and enthalpic overshoot.

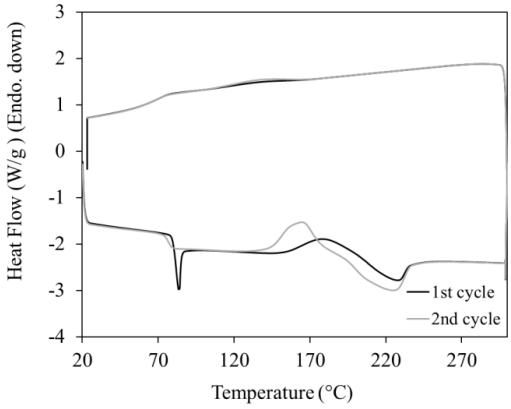

Figure S12. Sequential DSC scans of poly(ethylene-co-1,4-cyclohexylenedimethylene terephthalate) (PETG2) showing glass transition (T_g ~ 85 ºC) and enthalpic overshoot.

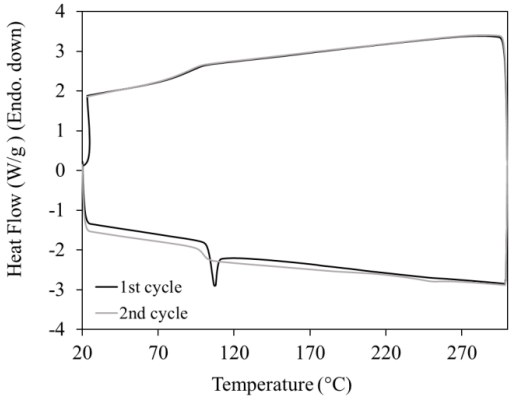

Figure S13. Sequential DSC scans of poly(1,4-cyclohexylenedimethylene-co-2,2,4,4-tetramethyl-1,3-cyclobutanediol terephthalate) (PCTT) showing glass transition (T_g ~ 110 ºC) and enthalpic overshoot.

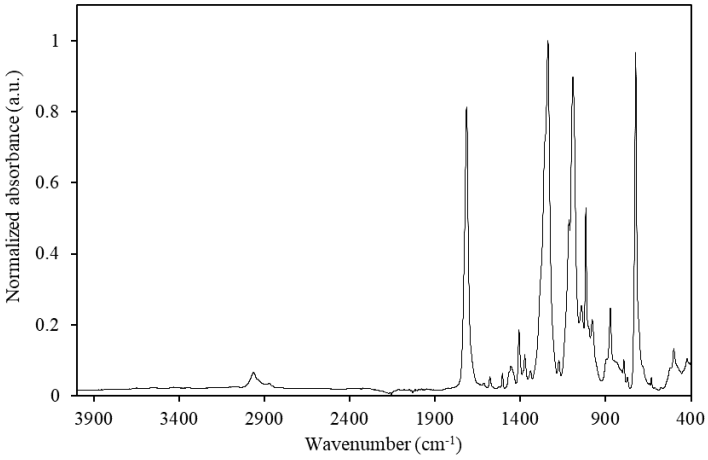

Figure S14. ATR-FTIR spectrum of poly(ethylene-co-2,2,4,4-tetramethyl-1,3-cyclobutanediol terephthalate) (PETT). Peak assignment can be found in Table S9.

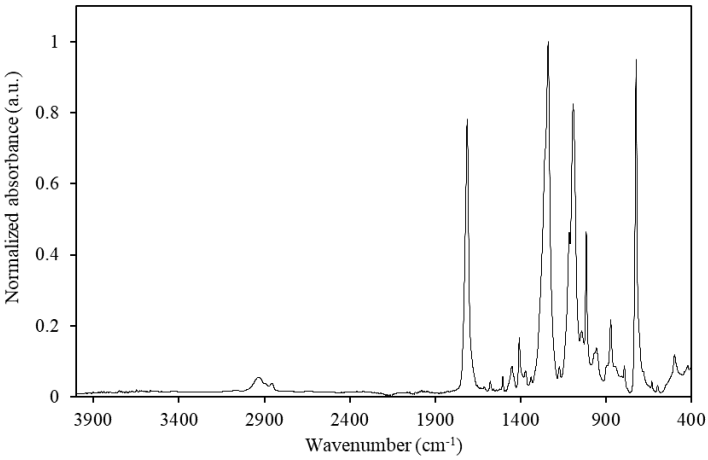

Figure S15. ATR-FTIR spectrum of poly(ethylene-co-1,4-cyclohexylenedimethylene terephthalate) (PETG1). Peak assignment can be found in Table S9.

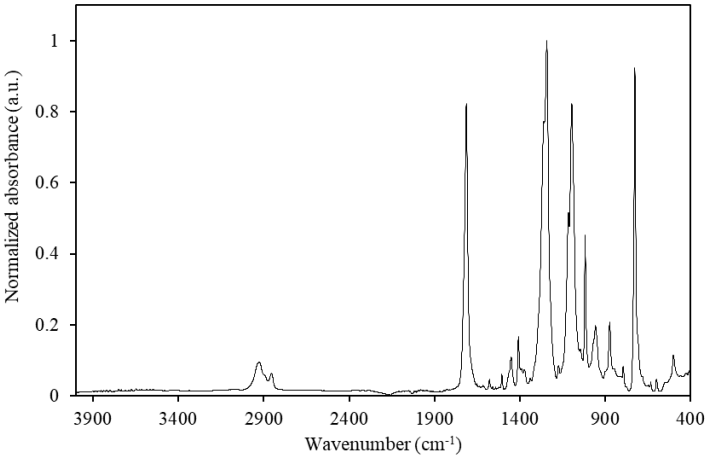

Figure S16. ATR-FTIR spectrum of poly(ethylene-co-1,4-cyclohexylenedimethylene terephthalate) (PETG2). Peak assignment can be found in Table S9.

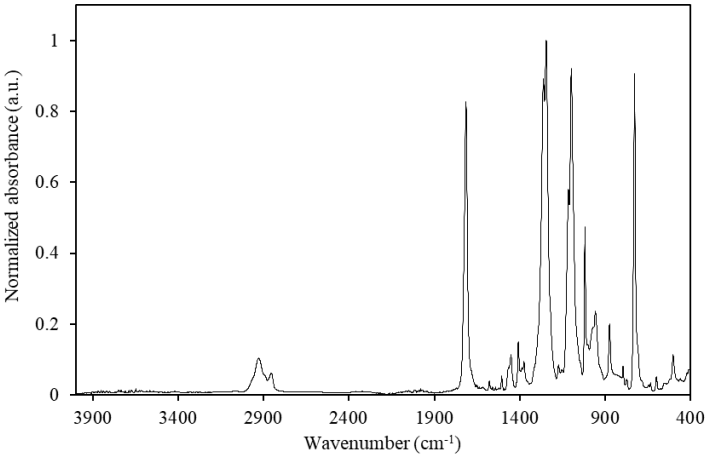

Figure S17. ATR-FTIR spectrum of poly(1,4-cyclohexylenedimethylene-co-2,2,4,4-tetramethyl-1,3-cyclobutanediol terephthalate) (PCTT). Peak assignment can be found in Table S9.

Table S9. Assignment of ATR-FTIR peaks.

Assignment	PETT [cm^{-1}]	PETG1 [cm^{-1}]	PETG2 [cm^{-1}]	PCTT [cm^{-1}]
OH-stretch	3435	3430	3430	3429
Saturated C-H stretch	3055	3054	3053	3064
CH_2 stretch	2965	2936	2932	2931
Symmetric C-H stretch	2872	2856	2856	2856
C=O stretch	1724	1723	1722	1722
Vibrations aromatic skeleton with C=C stretch	1578	1578	1578	1578
C-O stretching, deformation of OH group	1456	1452	1451	1451
Wagging ethylene glycol	1409	1409	1409	1408
CH_2 bending gouch	1374	1372	1373	1375
CH_2 bending trans	1340	1339	1337	-
Ester group	1264	1266	1270	1269
CH_2 wagging	1174	1173	1172	1172
Terephthalate group	1118	1119	1119	1118
Methylene group, vibrations of C-O	1101	1101	1102	1102
1,4-disubstituted aromatic ring	874	874	874	874
Vibrations of two adjacent aromatic H atoms	794	794	794	794
1,4-parasubstituted, C-H out-of-plane stretch/rocking	728	729	729	730

Appendix B

The Flory Fox equation Eq. S11, where $T_{g,\infty}$ is the asymptotic glass transition temperature at the theoretically highest T_g and K is a constant. The following calculations show the difference in Tg as a result of varying molecular weight in poly(ethylene-co-1,4-cyclohexylenedimethylene terephthalate) (PETG1) (Eq. S12) and poly(1,4-cyclohexylenedimethylene-co-2,2,4,4-tetramethyl-1,3-cyclobutanediol terephthalate) (PCTT) (Eq. S13)

Eq. S11 $$T_g(M_n) = T_{g,\infty} - \frac{K}{M_n}$$

Eq. S12 $$T_g(14.8\ kDa) = 359\ K - \frac{100000}{14800} = 352.2\ K$$
$$T_g(13.4\ kDa) = 359\ K - \frac{100000}{13400} = 351.5\ K$$
$$\text{Difference} = 0.2\ \%$$

Eq. S13 $$T_g(14.8\ kDa) = 388\ K - \frac{100000}{14800} = 381.2\ K$$
$$T_g(13.4\ kDa) = 388\ K - \frac{100000}{13400} = 380.5\ K$$
$$\text{Difference} = 0.2\ \%$$

Appendix C

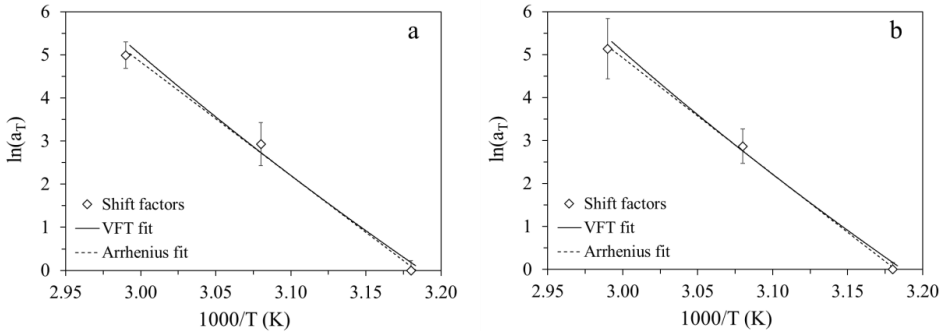

Figure S18. Shift factors versus 1000/T for enthalpy relaxation (a) and yield strength (b) of poly(ethylene-co-1,4-cyclohexylenedimethylene terephthalate) (PETG1) obtained from data in Figure 4 and 6. The solid curve represents the VFT fit and the dashed line represents the Arrhenius fit.

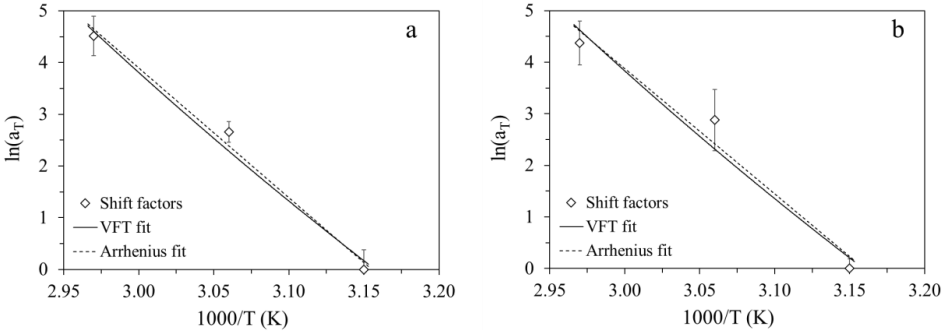

Figure S19. Shift factors versus 1000/T for enthalpy relaxation (a) and yield strength (b) of poly(ethylene-co-1,4-cyclohexylenedimethylene terephthalate) (PETG2) obtained from data in Figure 4 and 6. The solid curve represents the VFT fit and the dashed line represents the Arrhenius fit.

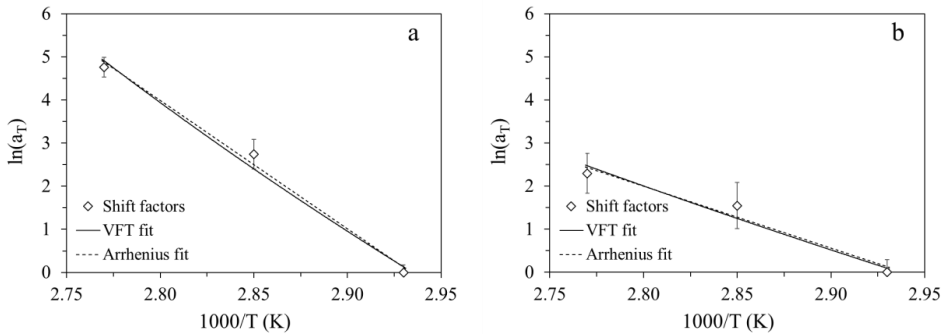

Figure S20. Shift factors versus 1000/T for enthalpy relaxation (a) and yield strength (b) of poly(1,4-cyclohexylenedimethylene-co-2,2,4,4-tetramethyl-1,3-cyclobutanediol terephthalate) (PCTT) obtained from data in Figure 4 and 6. The solid curve represents the VFT fit and the dashed line represents the Arrhenius fit.

CHAPTER 4. EFFECT OF PHYSICAL AGING ON VISCOELASTICITY

Early studies of physical aging in amorphous polymers showed that the creep and stress relaxation behaviour of the polymers changes with physical aging. As the material ages, its resistance to creep deformation increases, and the rate of stress relaxation decreases. This has special significance for applications where constant load or strain is involved, since aging alters the time-dependent stress/strain response and thus governs the application lifetime in such designs. In some cases, accelerated physical aging might be used to improve functionality of e.g. press fits over time, which would otherwise loose connectivity faster.

This chapter presents the study of two glycol modified PET grades, PECT and PETT, containing CHDM and TMCD, respectively, as glycol modification. The focus of the work is to deepen the understanding, of how physical aging influences stress relaxation behaviour and creep response in polyesters, and to investigate the effects of chemical structure. The importance of this work is linked to the need to control and improve function over time in durable products under load/strain. Especially, the wish to improve and predict lifetime of the press fit function in LEGO bricks (the so-called clutch force) made of polyester, has driven the need for this study.

4.1. PAPER II

The study presents the use of a constitutive model to describe the viscoelastic response in two glycol modified PET polymers, PETT and PECT, with different thermal history (accelerated aging). As hypothesised from previous studies, the results first of all show that the aging time has a significant influence on the viscoelastic behaviour, increasing the resistance to creep and stress relaxation. The chosen model is able to describe the stress relaxation for up to 24 h at 1.5 % strain of PETT and PECT thermally treated at T_g-20 °C for up to 504 h. Furthermore, the model can describe creep at 28.6 MPa, corresponding to an initial strain of 1.5 %, for 24 h in aged PECT but it underestimates the strain in the unaged samples.

The effect of aging time on model parameters is described, where κ (concentration of active polymer junctions) is most affected. The concentration of active junctions decreases exponentially with aging time, indicating that molecular arrangements with stronger interchain interactions form during physical aging, rendering the entanglements “fixed” when strained. Since the effect of aging time on every model parameter can be described by a function, the effect of other aging times on stress relaxation can be predicted. Such a tool could possibly help determine a level of physical aging needed to retain a given function over time in polyesters.

Both polyesters showed similar stress relaxation behaviours at 30 °C, suggesting that the chemical structure of the glycol units tested here does not have significant effect on stress relaxation. The results also imply that PETT and PECT age with similar rates at Tg-20 ºC, which contradicts the previous work (paper I), where PECT was found to age faster at Tg-20 ºC than PETT when measured as enthalpy loss and yield strength increase. When stress relaxation is tested at elevated temperatures, the structural differences are more visible, yielding higher activation energies (describing the rate of the rearrangement of interchain interactions) for PETC than PETT. These activation energies are also found to decrease due to physical aging.

Overall this study provides a possible tool for predicting the effect of physical aging on viscoelastic behaviours in polyesters. Furthermore, it adds to the understanding of physical aging as a redistribution of free volume and highlights the complexity in the effects of chemical structure.

Materials Today Communications 37 (2023) 107241

Contents lists available at ScienceDirect

Materials Today Communications

journal homepage: www.elsevier.com/locate/mtcomm

The effect of physical aging on the viscoelastoplastic response of glycol modified poly(ethylene terephthalate)

Anne Therese Husth Weyhe [a,b], Aleksey D. Drozdov [c,*], Jesper de Claville Christiansen [c], Emil Andersen [b], Donghong Yu [a,*]

[a] Department of Chemistry and Bioscience, Aalborg University, Fredrik Bajers Vej 7H, DK-9220 Aalborg East, Denmark
[b] LEGO System A/S, Åstvej 1, DK-7190 Billund, Denmark
[c] Department of Materials and Production, Aalborg University, Fibigerstræde 14, DK-9220 Aalborg East, Denmark

ARTICLE INFO

Keywords:
Polyesters
Viscoelasticity
Viscoplasticity
Stress relaxation
Physical aging

ABSTRACT

For most amorphous polymers, their long term viscoelastic behaviour is greatly affected by physical aging, referring to the transition of their non-equilibrium structure towards equilibrium. This, in turn, affects their thermomechanical properties. In this study, we successfully applied a constitutive model, originally developed for semi-crystalline polyesters to assess the impact of physical aging on stress relaxation and creep in two glycol modified poly(ethylene terephthalate) grades, (poly(ethylene-co-1,4-cyclohexylenedimethylene terephthalate) (PECT) and poly(ethylene-co-2,2,4,4-tetramethyl-1,3-cyclobutanediol terephthalate) (PETT). Both copolyesters are subject to annealing at T_g-20 °C for up to 504 h and subsequent uniaxial stress relaxation tests and, for PECT, creep tests. The results show that the annealing time has a significant influence on the viscoelastic behaviour increasing the resistance to creep and stress relaxation. The effect of physical aging on model parameters is described and analysed while it is found that the concentration of active polymer junctions decreases exponentially with annealing time. Generally, PETT and PECT showed almost identical viscoelastic behaviours at 30 °C, suggesting that the chemical structure of the glycol unit (2,2,4,4-tetramethyl-1,3-cyclobutanediol and 1,4-cyclohexylenedimethanol) does not have significant effect on their viscoelasticity. However, when stress relaxation is tested at increased temperatures, the structural effects are more apparent, demonstrating higher activation energies for PECT than those for PETT, describing the rate of the rearrangement of interchain interactions. Physical aging is also found to decrease these activation energies from 326.6 to 128.1 kJ mol^{-1} for PECT and from 262.7 to 78.5 kJ mol^{-1} for PETT.

1. Introduction

Polyesters are one of the most important classes of plastics [1], especially driven by the commodity plastic poly(ethylene terephthalate) (PET) [2–4], which has been extensively used in various industrial applications, including food packaging, textiles, and medical devices, due to its excellent mechanical and physical properties. However, the low impact strength of polyesters [5,6] and poor resistance to stress cracking and creep [7] have limited their use in engineering applications. To overcome these limitations, researchers have developed glycol-modified PET (PETG) by replacing part of the ethylene glycol (EG) with other glycol moieties, leading to higher impact strengths, better optical transparency [8], improved barrier properties [9] and higher chemical resistance than native PET [10]. The most frequently used glycol modification is the incorporation of 1,4-cyclohexylenedimethanol (CHDM) into PET backbone [10–12] (Fig. 1a), leading to ternary copolyesters with low crystallization rates, and hence enabling production of amorphous polyester with improved optical transparency (92% transmittance) [8]. Generally, when CHDM is copolymerized with aliphatic diols such as ethylene glycol and common diacids such as terephthalic acid, the glass transition temperature (T_g) is increased [13] and the backbone is rendered more resistant to hydrolysis [14] with respect to PET. Furthermore, the flexible nature of the CHDM unit increases the toughness of the polyester compared to a diol such as EG. PET modified with CHDM (PECT) is a promising polyester for high-end consumer products and applications where PET is not suitable due to poorer mechanical and thermal properties. Another promising diol, 2,2,4,4-tetramethyl-1,3-cyclobutanediol (TMCD), has more recently been

* Corresponding authors.
E-mail addresses: aleksey@mp.aau.dk (A.D. Drozdov), yu@bio.aau.dk (D. Yu).

https://doi.org/10.1016/j.mtcomm.2023.107241
Received 27 June 2023; Received in revised form 9 September 2023; Accepted 3 October 2023
Available online 5 October 2023

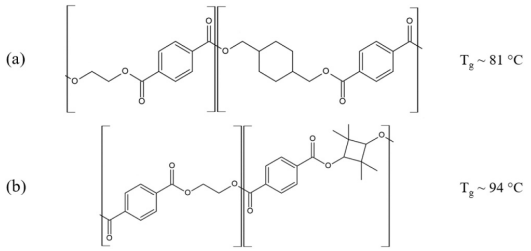

Fig. 1. Chemical structure of (a) poly(ethylene-co-1,4-cyclohexylenedimethylene terephthalate) (PECT) and (b) poly(ethylene-co-2,2,4,4-tetramethyl-1,3-cyclobutanediol terephthalate) (PETT) along with their corresponding T_g's.

used to modify PET (Fig. 1b) [15–17]. Due to the more sterically hindered structure of the substituted cyclobutyl ring, the incorporation of TMCD into the PET backbone increases the T_g even further [18] in respect to both PET and PECT, enabling higher application temperatures. Similar to PECT, PETT crystallizes very slowly compared to PET, and thus amorphous and optical transparent parts are easily produced [8].

Despite many advantages of PETGs, their long-term viscoelastic behaviour remains difficult to predict, especially due to the influence of physical aging on their viscoelasticity. Physical aging is a phenomenon occurring in amorphous polymers due to the molecular structure being frozen in a non-equilibrium state with a high potential energy [19,20], at temperatures below their T_g's. As a result, their molecular structure continuously approach thermodynamic equilibrium or move from one local energy minimum to another by gradual molecular rearrangements [21–23]. These structural changes significantly affect their mechanical and physical properties over time, including changes in stiffness, tensile strength, ductility [24,25] and viscoelastic behaviour [26], which affects the long-term performance and reliability of the material. During physical aging, the viscoelastic material becomes stiffer and hence the compliance decreases compared to the unaged one [27]. This effect has previously been explained by free volume theory [26,28], as a decrease in free volume towards its equilibrium value leading to hindered mobility of chain segments and thereby a higher E-modulus [26]. The effect of aging on creep behaviour can be seen as shifts on creep compliance versus time curves, where increased physical aging leads to shifting of the timescale towards longer time and thus increased resistance to creep.

Apart from physical aging, crystallization might also occur in some polyesters when temperature is increased. This is especially seen in PET and polyesters with linear and highly regular backbones, allowing formation of crystalline domains with closely packed chains and repeating structures. Often, in injection moulded samples with fast cooling, the polymer is not allowed to crystallize fully or the formed crystallites may be of poor quality. Depending on the timescale and storage-/application temperature, recrystallization or refinement of crystalline domains may occur, which would change many of the same properties as physical aging such as increase in tensile strength and stiffness along with embrittlement [29]. However, the incorporation of CHDM or TMCD in specific levels is known to reduce the crystallization rate significantly compared to PET. Polyesters with CHDM/EG and TMCD/EG composition of 30/70 have previously been found to show no crystalline peaks when scanned with DSC before and after aging at T_g-20 for 24 h [30]. Therefore no formation of crystallites are expected at these temperatures. However, it is important to mention, that small spherulites and nuclei can be difficult to detect with DSC.

Poor resistance to creep is a general challenge in polyesters, especially in applications at increased temperatures and long periods of use where design flexibility and durability of products are compromised. Similarly, stress relaxation can become an issue in strained designs, where stress is essential to maintain a given functionality in e.g. press- or snap fits. A possible way to enhance creep and stress relaxation properties of polyesters can be to accelerate physical aging through thermal treatment. In so doing, the long term viscoelastic behaviour can be tailored to fit certain product requirements. However, to predict the necessary aging time and temperature to obtain a polyester with the desired viscoelastic properties, suitable models are needed.

A classic way to describe the effect of physical aging on creep is by the double-logarithmic shift rate, μ, described by Eq. (1) [27].

$$\mu = -\frac{d\log(a_{t_e})}{d\log(t_e)} \tag{1}$$

where a_{t_e} denotes aging time shift factors and t_e describes the aging time at a given temperature. Another common way to shift creep and stress relaxation curves is by the time-temperature superposition principle. The response function in stress relaxation experiments is often represented by the stretched exponential of Kohlrausch-Williams-Watts (KWW) equation in Eq. (2).

$$S(t) = S_0 e^{-(t/\tau_0)^{\beta}} \tag{2}$$

where $S(t)$ is the stress response (or creep compliance), S_0 is the initial response, τ_0 is the characteristic relaxation time and β is the shape parameter. Changes in temperature from T_o to T leads to a change in relaxation time, and the resulting shift is described by $a_t = \tau_{T_0}/\tau_T$. Since physical aging causes a change in timescale for the viscoelastic response, time-aging time shift factors can also be described within the context of the KWW function as $a_t = \tau_{0,t_{e0}}/\tau_{0,t_e}$. These superposition methods can be powerful in predicting long term responses from short term tests, but they do not bring much further understanding of influence of chemistry and morphology. Furthermore the methods can be challenged in describing long term results accurately. J.L. Sullivan demonstrated that prediction of long term creep from short term creep data using a simple shift method led to large overestimations near and below T_g [31]. He explained this observation by the fact that long term creep proceeds much slower relative to short term creep in glassy polymer due to physical aging over time, which alters the properties during long tests [31]. Hutchinson et al. showed the effect of physical aging of PMMA at 125 °C (T_g-20 °C) for up to 120 h on low strain creep response and found that excellent superposition could be achieved by horizontal and vertical shifts [32]. They also found that shift rates for creep did not correspond to the ones found from DSC analysis of enthalpy relaxation, suggesting a more complicated relationship between the two types of relaxation governed by more than change in free volume. A more recent study by Nunes et al., investigating the effect of physical aging on the viscoelastic behaviour of epoxy resins, also employed a time-temperature superposition method and found that the shift rate does not depend on aging temperature at times up to 700 min, whereas the shift rate increases with temperature at longer aging times [33]. They found, that additional aging dependent functions were needed in the viscoelastic model to describe the divergences. This study further demonstrates the complexity of physical aging in polymers. Histova et al. tested the effect of a mineral filler on the creep response of a polyester before and after physical aging was induced [34]. They interpreted experimental results using a generalised Maxwell equation (Maxwell-Gourevich equation) and found that physical aging especially influenced the model parameter related to rubberlike elastic deformation. By assuming the physical sense of the model, they conclude, that physical aging causes significant changes in the structural elements that determine the rubberlike response.

In 2008 a constitutive model was presented, which was able to correctly describe observations in relaxation tests of high density polyethylene at various temperatures and to distinguish effects of constraints on polymer chains imposed by crystallites from effects of temperature on E-modulus [35]. This model was derived for semi crystalline polymers

Table 1
Moulding parameters for tensile bars of PETT and PECT.

	Moisture content [%]	Drying temp. [°C]	Drying time [h]	Melt temp. [°C]	Injection pressure [bar]	Mould temp. [°C]	Cooling time [s]
PETT	0.03	80	8	295	1150	80	20
PECT	0.02	80	8	272	800	60	26

and we believe it offers the possibility to describe the effect of physical aging on viscoelastic behaviour and to isolate the effects on the polymer network related to network homogeneity (distribution of crystallites and/or free volume) and chain interactions.

Even though several studies prove successful modelling of the effect of physical aging on stress relaxation and creep in amorphous polymers [26,34,36], the effect of chemical structure is not fully established. A recent study of star-shaped polystyrene showed that the aging rate decreases with increasing molecular stiffness [37]. Furthermore, an early study of linear polymers (cellulose acetate butyrate ester and polyimide Kapton-H) suggested, that physical aging is slowed down by rigidity of the main chain but not hampered [38]. The structural relaxation also depends on the amount and nature of intermolecular interactions between chains, and thus making the effect of chemical structure a complex subject. The main focus of this work is the effects of physical aging on viscoelastic properties in polyesters with different backbone rigidity.

The objectives of this work are: a) to investigate the effect of chemical structure of glycol modified PET on physical aging behaviour; b) to evaluate the effect of physical aging on stress relaxation and creep in amorphous glycol modified PET, c) to utilise a constitutive model to describe changes in the polyesters caused by physical aging. In this work, PETT and PECT (both with 30% glycol modification and similar molecular weights) are thermally treated to accelerate their physical aging. The constitutive models previously presented [35,39] will be used to characterize stress relaxation and creep behaviour in the two copolyesters and evaluate the effect of annealing time. The laws and methodology for determination of the model parameters are given as well in [35,39].

2. Materials and methods

2.1 Materials

Granulate of poly(ethylene-co-2,2,4,4-tetramethyl-1,3-cyclobutanediol terephthalate) (PETT) (GMX201, Eastman, USA), and poly(ethylene-co-1,4-cyclohexylenedimethylene terephthalate) (PECT) (GN007, Eastman, USA) were injection moulded (Arburg 470E 600–290 Arburg, GER) to tensile test specimens (1BA, ISO 527–2:2012) under conditions listed in Table 1.

Chemical structures and glycol ratios have previously been confirmed by hydrogen- and carbon nuclear magnetic resonance spectroscopy and infrared spectroscopy [30]. Average molecular weights were estimated from gel permeation chromatography as 14.0 and 14.8 kDa for PETT and PECT [30], respectively. Both injection moulded materials were found to be amorphous by DSC, showing neither melting nor crystalline peaks (Fig. S8 and S9).

2.2 Tensile test

Tensile test specimens were fixed with the inlet in the lower pneumatic grip in a universal testing machine (Z005, ZwickRoall, GER) with a 25 mm gauge length extensometer (180102/2008, ZwickRoell, GER) controlled by testXpert II (Zwick, GER). E-modulus and yield strength were evaluated with speed of 1 mm/min until evaluation of E is completed, and an increased speed of 100 mm/min after that, respectively, at 23 ± 2 °C (Fig. S2 and S3, Table S1 and S2).

2.3 Thermal treatment

Tensile specimens were annealed in an oven at T_g-20 °C (61 and 74 °C for PECT and PETT, respectively) for 0.5, 1, 2, 4, 8, 16, 24, and 504 h. After thermal treatment, all samples were stored at room temperature for a least 24 h before testing.

2.4 Creep tests

A series of creep tests were performed on samples of PECT annealed for 0–24 h at T_g-20 °C in a Kappa Multistation (ZwickRoall, GER) with a non-contact strain measurement (videoXtens) and external temperature unit controlled and monitored by testXpert III (ZwickRoall, GER). The samples were subject to an applied stress of 28.6 MPa corresponding to an initial strain of 1.5% for 24 h at 30 °C. A loading speed of 1 mm/min was used.

2.5 Stress relaxation tests

Uniaxial stress relaxation tests were performed on samples in a Kappa Multistation (ZwickRoall, GER) with a non-contact strain measurement (videoXtens) controlled and monitored by testXpert III (ZwickRoall, GER). One series of relaxation tests was performed at 30 ± 3 °C (samples aged 0.5–24 h). Another series of tests was performed at 30, 40, 60, and 70 ± 3 °C (samples aged 0 and 504 h). All tests were performed with loading speed of 1 mm/min and samples were strained at $\epsilon = 1.5\%$ for 24 h.

2.6 Theoretical model

The physical relationships implied in the constitutive model is based on arbitrary three dimensional deformations with small strains (with straight forward extension to finite deformations). The strain tensor for macro-deformation at time $t \geq 0$ is denoted $\widehat{\epsilon}(t)$ and is given by:

$$\widehat{\epsilon}(t) = \widehat{\epsilon}_s(t) + \widehat{\epsilon}_e(t) \tag{3}$$

Where $\widehat{\epsilon}_s(t)$ describes the strain tensor for sliding of junctions and $\widehat{\epsilon}_e(t)$ is the strain tensor for elastic deformation. For the plastic flow in the polymer network, it is assumed that the rate of strain tensor for sliding junctions is linearly related with the rate of strain tensor for macro deformation according to Eq. (4), where ϕ describes the phenomenological relation described in Eq. (5).

$$\frac{d\widehat{\epsilon}_s(t)}{dt} = \phi \frac{d\widehat{\epsilon}(t)}{dt} \tag{4}$$

$$\phi = 1 - \exp(-\alpha \epsilon_e^{\beta}) \tag{5}$$

where, α and β are constants. A homogenization concept is used to account for local density fluctuations and inhomogeneous distribution of crystallites (for semi-crystalline polymers as PET). According to this concept the polymer is modelled as an inhomogeneous network of strands bridged by entanglements between chains, so-called junctions. The network is non-affine, which means, that junctions slide under deformation with respect to their reference position. To determine the inhomogeneity, Σ, of the equivalent network by fitting experimental observations, Eq. (6) is assumed [40].

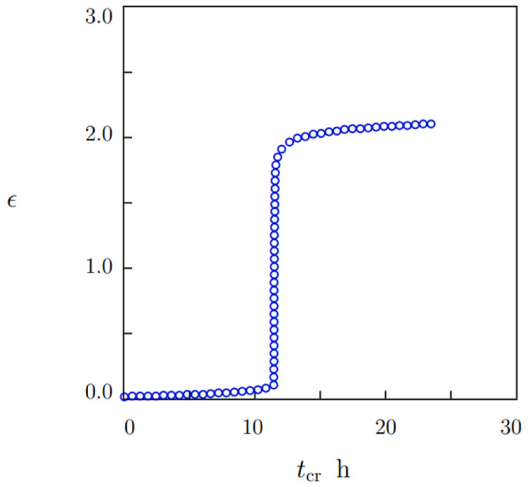

Fig. 2. Tensile strain ϵ versus creep time t_{cr}. Circles: experimental data in creep test with stress $\sigma = 28.6$ MPa at T = 30 °C on non-aged PECT.

$$f(\nu) = f_0 \exp\left(-\frac{\nu^2}{2\Sigma^2}\right) \quad (\nu \geq 0), f(\nu) = 0 (\nu < 0) \tag{6}$$

where ν describes the dimensionless energy of inter-chain interaction at a reference temperature. For a given temperature, the energy of inter-chain interactions, V, is given by:

$$V = a\nu \tag{7}$$

where $a(T)$ describes the effect of temperature on V. The rate of activation of polymer chains, which due to e.g. crystallinity did not take part in the rearrangement, Γ, is related to V by the Eyring equation [41]:

$$\Gamma = \gamma \exp(-V) \tag{8}$$

where γ is the attempt rate, which is independent of deformation and whose temperature dependency can be described by the Arrhenius equation, Eq. (9).

$$\gamma = \bar{\gamma} \exp\left(-\frac{E_a}{RT}\right) \tag{9}$$

Where $\bar{\gamma}$ is a constant, E_a is the apparent activation energy, and R is the universal gas constant. The Eqs. (3)–(9) offer a set of stress-strain relationships to allow modelling with the seven adjustable parameters with the following physical meaning:

E is the modulus describing the linear elastic response.
κ describes the concentration of temporary active junctions
Σ indicates the inhomogeneity of the polymer network
α and β reflects the plastic flow of junctions
γ is the attempt rate of separation of polymer chains
a describes thermally-induced changes in the energy of interactions between chains.

For a more detailed derivation and description of the modelling, we refer to the two previous works [35,39].

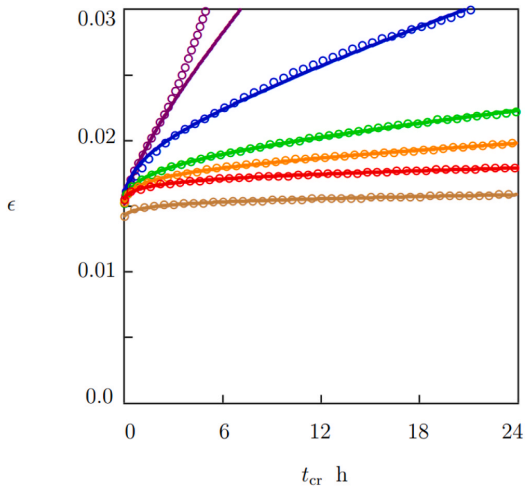

Fig. 3. Tensile strain ϵ versus creep time t_{cr}. Circles: experimental data in creep test with stress $\sigma = 28.6$ MPa at T = 30 °C on PECT samples aged at T = 61 °C for various times t_a: violet - $t_a = 0$, blue - $t_a = 1$, green - $t_a = 4$, orange - $t_a = 24$, red - $t_a = 168$, brown - $t_a = 504$ h. Solid lines: results of numerical analysis.

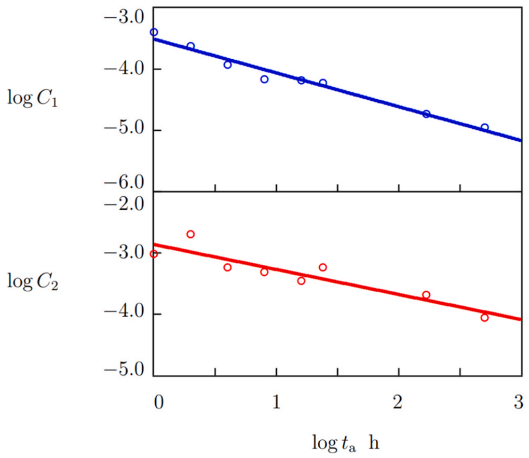

Fig. 4. Parameters C_1 and C_2 versus annealing time t_a. Circles: treatment of observations in creep test with stress $\sigma = 28.6$ MPa at T = 30 °C on PECT samples aged at T = 61 °C. Solid lines: results of numerical analysis.

3. Results and discussion

3.1 Effect of aging on creep resistance of PECT

A set of creep experiments have been performed to investigate the creep resistance in PECT. A relatively high stress of 28.6 MPa is applied to achieve an initial strain of 0.015, corresponding to the strain used in stress relaxation tests. The resulting creep curve of unaged PECT is shown in Fig. 2, where prominent creep is observed in both the primary and secondary creep range. Following, it is seen that tertiary creep leads to pronounced necking, which results in development of a new equilibrium state, while rupture is avoided in the 24 h test time. This phenomena could be caused by chain alignment causing strain hardening in

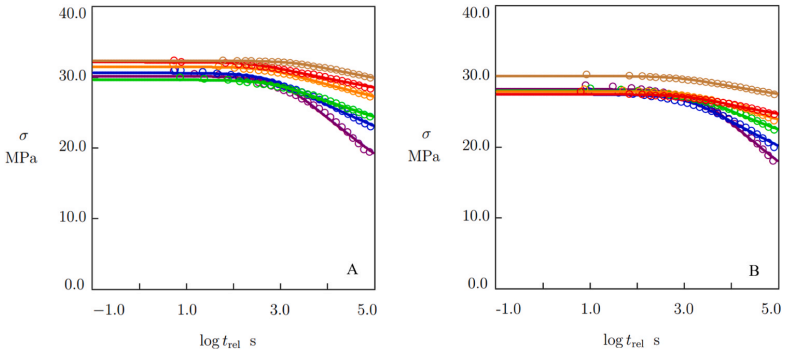

Fig. 5. Tensile stress σ versus relaxation time t_{rel}. Circles: experimental data in stress relaxation test with strain $\epsilon = 0.015$ at T = 30 °C on (A) PETT and (B) PECT samples annealed at T_g–20 °C for various times t_a: violet - $t_a = 0$, blue - $t_a = 1$, green - $t_a = 4$, orange - $t_a = 24$, red - $t_a = 168$, brown - $t_a = 504$ h. Solid lines: results of numerical analysis.

the final stage. However, the geometry of the sample might also influence the measurement, as the neck reaches a thicker part of the sample at very high strains, allowing the cross sectional area to increase (see Fig. S11). These hypotheses need further confirmation leaving the observation yet unexplained.

To assess how the creep resistance of PECT changes with time, accelerated physical aging (annealing sub-T_g for various amounts of time t_a) is conducted, and creep curves of unaged and annealed samples are compared in Fig. 3. To fit the experimental data in these creep curves, the material parameter responsible for the viscoelastic response is firstly found from stress relaxation experiments. The viscoplasticity can then be evaluated from creep data, since the latter reflects both viscoelasticity and –plasticity, whereas stress relaxation only reflects viscoelasticity.

From the experimental curves presented in Fig. 3, it is clear, that aging has a large effect on creep resistance. Each creep curve is fitted separately with two parameters C_1 and C_2 and the effect of annealing time on these coefficients is presented in Fig. 4. The effect is described by linear dependencies in double logarithmic coordinates, where the observations and the simulated results coincide. The resulting modelled creep curves, describe the experimental data well, especially for highly aged samples, while it underestimates the strain in the unaged sample.

It has previously been hypothesised, that creep in PET involves the weakening and rearrangement of interactions between polymer chains rather than stretching of the backbone and thus is governed by the strength of secondary bonds [42]. As the strength of interchain interactions rely on Van der Waals forces it is plausible, that it increases during physical aging, causing greater creep resistance even if the macroscopic density remain the same, Table S3.

3.2 Stress relaxation in PETT and PECT with different annealing time

Fig. 5 shows the experimental and simulated stress response of PETT and PECT annealed at T_g-20 °C for different times. It is evident that preliminary annealing significantly decreases stress relaxation in both polyesters, which is also captured by the theoretical model. From the results shown in Fig. 5, the effect of annealing for PECT is similar to that for PETT.

Each of the curves in Fig. 5 is characterized by three parameters, since the parameter describing inhomogeneity, Σ, of the polymer network is independent of annealing time. This independency could arise from the hypothesis, that physical aging does not increase/induce ordered regions in the amorphous phase, which causes large density fluctuations, as in the case of (re)crystallization. However, physical aging could cause redistribution of free volume and thereby change the local fluctuations on a small scale. Fig. 6 shows E-modulus and the parameter γ (attempt rate of separation of strands) as function of annealing time. The simulations of both parameters, also illustrated in Fig. 6, is able to describe the values determined from fitting experimental data. The E-modulus increases weakly (logarithmically) with annealing time, which correspond well to results from tensile tests presented in Figs. S3–4 and from previous studies of the same polyesters

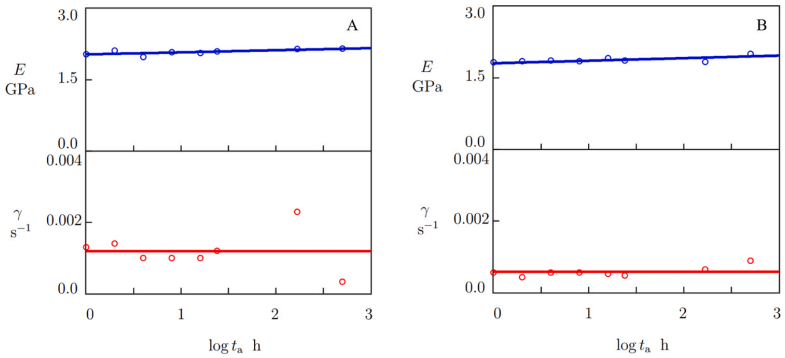

Fig. 6. Parameter E and γ versus annealing time t_a. Circles: treatment of observations in relaxation tests with strain $\epsilon = 0.015$ at T = 30 °C on (A) PETT and (B) PECT samples annealed at T_g–20 °C for various times t_a. Solid lines: results of numerical analysis.

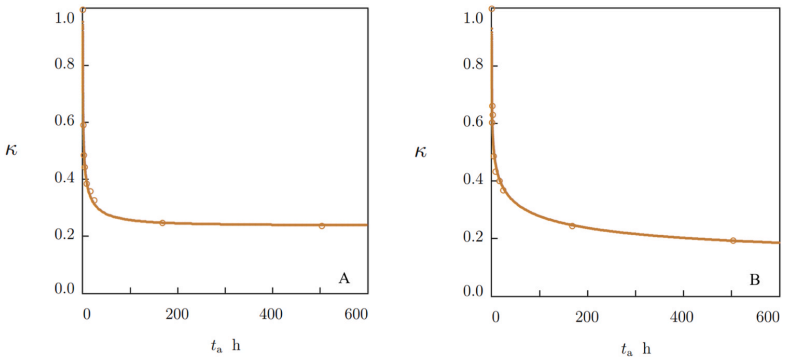

Fig. 7. Parameter κ versus annealing time t_a. Circles: treatment of observations in relaxation tests with strain $\epsilon = 0.015$ at T = 30 °C on (A) PETT and (B) PECT samples annealed at T_g–20 °C for various times t_a. Solid lines: results of numerical analysis.

[30]. The moduli of PETT and PECT differ only slightly showing that PETT is stiffer than PECT. This also consists with results from tensile tests, showing that E-modulus is 2.2 and 1.9 GPa for unaged PETT and PECT, respectively (Figs. S1–2, Table S1–2). The rate of rearrangement of interchain interaction and attempt rate of separation of strands, γ, is independent on annealing time and is twice as high for PETT as compared to PECT. Both observations are rather unexpected. The first suggests that the rate of rearrangements of chain interactions during stress relaxation is not influenced by physical aging, which contradicts the assumption, that molecular movement is prohibited in aged samples, since less free volume is available compared to that in unaged samples. This could suggest that physical aging redistributes free volume and changes the density on a scale that is much smaller compared to the mechanical response. Secondly, the chemical structure of PETT is more rigid compared to PECT, specifically with less flexibility in the TMCD unit of PETT compared to CHDM in PECT, which is manifested in the T_g difference between the two, where that of PETT is ~10 °C higher. The T_g difference implies that more energy is needed to initiate molecular mobility in PETT compared to PECT, and therefore it is notable, that the rate of interaction-rearrangement is found to be highest in PETT at the same temperature (30 °C). Our previous studies of physical aging rates, measured as enthalpy loss at T_g-20 °C, also suggested, that the enthalpy

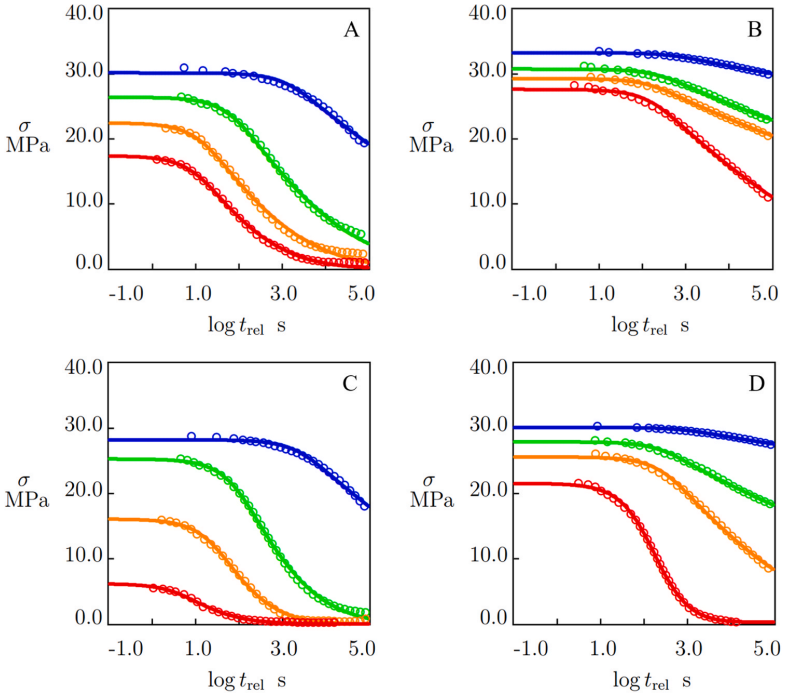

Fig. 8. Tensile stress σ versus relaxation time t_{rel}. Circles: experimental data on (A) non-aged PETT (B) PETT aged for 504 h at T_g–20 °C (C) non-aged PECT and (D) PECT aged for 504 h at T_g–20 °C in stress relaxation test with strain $\epsilon = 0.015$ at temperatures T = 30 (blue), T = 50 (green), T = 60 (orange) and T = 70 (red) °C. Solid lines: results of simulations.

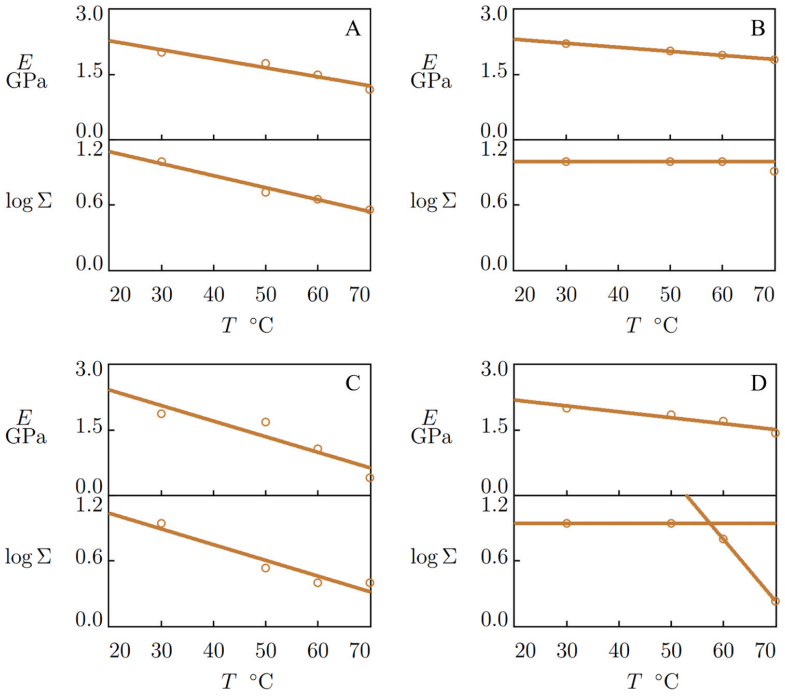

Fig. 9. Parameter E and Σ versus temperature T. Circles: treatment of observations on (A) non-aged PETT (B) PETT aged for 504 h at T_g–20 °C (C) non-aged PECT and (D) PECT aged for 504 h at T_g–20 °C in stress relaxation test with strain $\epsilon = 0.015$. Solid lines: results of simulations.

relaxation occurs faster in PECT than in PETT at the same temperature relative to T_g, suggesting that structural relaxation should occur faster in PECT [30]. However, even when the backbone of PETT is more sterically hindered, the nature of the intermolecular forces in the two polyesters is the same. Therefore, the fitted/simulated values of γ, could imply that the mechanism taking place during stress relaxation of these polyesters does not involve steric crowding and might be predominantly governed by Van der Waals forces and hydrogen bonding.

The effect of annealing on the third model parameter κ is shown in Fig. 7. As E-modulus and γ are almost unaffected by physical aging, much of the explanation, provided by the model, for the decreased stress relaxation in annealed samples, seem to be found in this coefficient. κ decreases strongly with annealing time described by the stretched exponential function $\kappa = \exp(-(t_a/t_{a0})^m)$ with m = 0.33 for PETT and m = 0.23 for PECT. Describing the concentration of temporary active junctions, κ is 1 in unaged samples of both PETT and PECT and hence all junctions are active and able to slide during the stress relaxation experiment on unaged samples. After annealing for 24 h, κ decreases to roughly 0.2 in both polyesters, meaning that ~80% of the junctions have become locked and resists sliding as stress is applied. This observation implies, that the strength and/or amount of secondary bonds increases during physical aging adding to the hypothesis, that these interactions governs the stress relaxation. This agrees with the idea of physical aging as a densification process or a rearrangement of the polymeric segments into a structure with stronger intermolecular interactions, where free volume is decreased and molecular movements inhibited. However, based on the observations of γ, which is unaffected by annealing, the rate of breakage and formation of interchain interactions during stress relaxation is maintained in spite of physical aging. This could suggest, that physical aging causes local densifications, where the entanglements are strongly locked not allowing them to slide, while the rate of rearrangement of bonds remain the same without separating the chains. κ seems do decrease slightly faster in PETT compared to PECT, suggesting that the rigid nature of TMCD causes faster formation of locked junctions in the matrix compared to CHDM.

3.3 Thermal effects

Experimental data obtained at temperatures up to T_g for non-aged samples and samples aged for 504 h at T_g-20 °C are presented in Fig. 8. The stress drops faster the higher the temperature, but is maintained to a significantly higher degree in aged samples compared to the unaged. At increased temperatures, especially at 70 °C, the stress is relaxed much faster in PECT than in PETT. This is because, the temperature is in close proximity to T_g of PECT (81 °C from DSC, Fig. S8 66 °C from dynamic mechanical analysis, Fig. S6). At T_g the storage modulus drops significantly as the material starts to soften leading to fast stress relaxation. Furthermore, a sample is rejuvenated, when kept above T_g for a period of time, since the material is able to obtain an equilibrium state. However, to completely rejuvenate a sample, it is necessary to reach the equilibrium in a liquid-like state, and thus the temperature would need to reach at least the offset of the T_g. This might explain why the initial stress at 70 °C is still three times as high for the aged PECT as for the unaged, suggesting an effect of physical aging, at least on a short timescale.

The effect of temperature on the obtained model parameters are presented in Figs. 9–11. E-modulus decreases linearly with temperature in both copolyesters, where the rate of decay is higher in unaged samples compared to the aged by twice. The decay rate is similar in both materials but is slightly steeper for PECT in both unaged and aged samples. The decrease in E-modulus with increasing temperature is expected, as higher temperature means that the molecules have more kinetic energy,

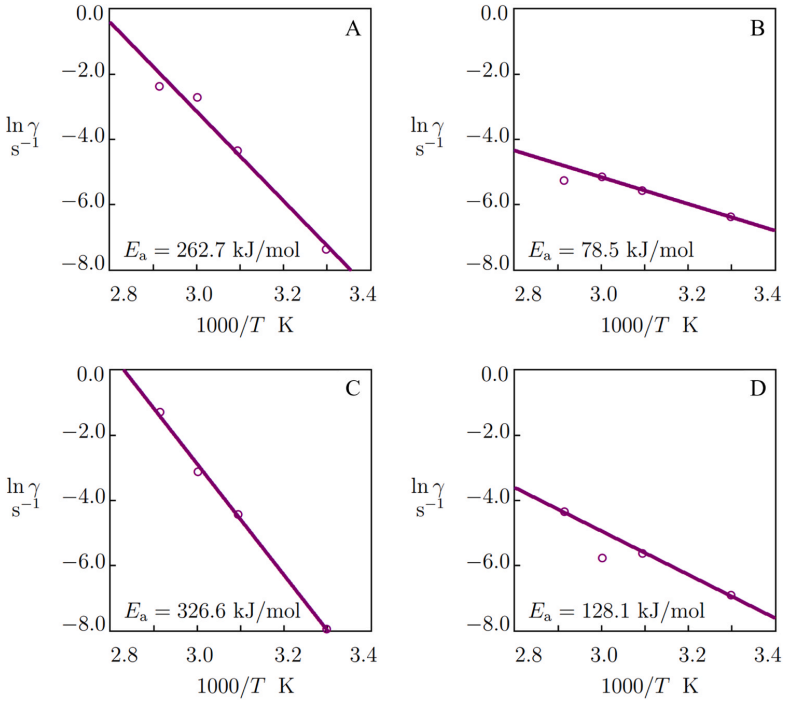

Fig. 10. Parameter γ versus temperature T. Circles: treatment of observations on (A) non-aged PETT (B) PETT aged for 504 h at T_g–20 °C (C) non-aged PECT and (D) PECT aged for 504 h at T_g–20 °C in stress relaxation test with strain $\epsilon = 0.015$. Solid lines: results of simulations.

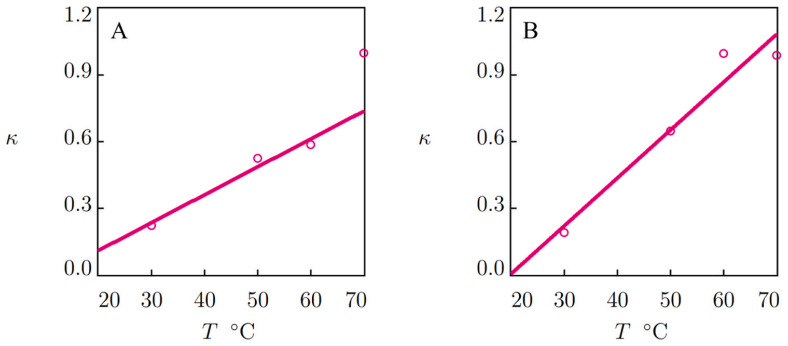

Fig. 11. Parameter κ versus temperature T. Circles: treatment of observations in stress relaxation test with strain $\epsilon = 0.01$ on samples of (A) PETT and (B) PECT aged for 504 h at T_g – 20 °C. Solid lines: results of simulations.

hence the secondary bonds have less effect. The network heterogeneity decreases linearly with temperature in unaged samples, suggesting that higher temperatures allow rearrangement of polymeric segments yielding a more homogenous network. However, for aged samples of both PETT and PECT, the inhomogeneity is unaffected by temperature until T_g is approached (seen for PECT around 60–70 °C in Fig. 9) where it suddenly starts dropping. The reason for the constant inhomogeneity in aged samples might be due to stronger molecular interactions in the aged samples compared to the unaged, and thus more energy is needed to allow further rearrangement of the polymer segments. As T_g is approached, enough thermal energy is provided to break/rearrange the intermolecular interactions and form a more homogeneous network. This consist well with previous observations in the model parameters, suggesting that physical aging forms locked junctions that are strong enough to resist sliding when the sample is strained. These junctions would most likely keep the polymer network fixed until the temperature approaches T_g and enough energy is provided to break the interactions.

The rate of rearrangement of temporary interactions can be described by an Arrhenius dependency (Eq. (9) Section 2.6) with activation energy as indicated in the figure. Aging causes a large decrease in activation energy in both copolyesters, but generally the values are higher for PECT than PETT suggesting a larger effect of temperature in

PECT, which also fits well with the experimental data. This observation also agrees with previous studies of enthalpy relaxation in PECT and PETT, where activation energies of 218–224 and 134–159 kJ mol^{-1} where found, respectively [30]. However, from the data shown in Fig. 6, it is seen, that the rate of secondary bond rearrangement is independent of annealing time, which questions the direct connection to the data presented here, where a difference in γ is clearly seen between unaged and aged samples.

Fig. 11 depicts κ as function of temperature. As κ describes the concentration of active junctions, a value of 1 means that all interactions between chains are temporary and can be broken easily during stress relaxation compared to locked junctions. In unaged samples all values for κ were 1 at any temperatures, and hence all junctions are active. In aged samples of both PETT and PECT, locked interactions are formed, probably due to rearrangement of polymer segments into conformations with stronger/more secondary bonds as previously discussed. However, when temperature is raised up to T_g, the locked junctions disappear, as seen for PECT, where κ reaches 1 at 70 °C.

Generally, observations of κ (concentration of active junctions), which strongly decreases with annealing time, and Σ (inhomogeneity of the polymer network), which is independent of temperature in annealed samples but significantly affected by temperature in unaged samples, suggest that stronger intermolecular interactions are formed during physical aging. The model also suggest that the secondary bonds have a larger effect on stress relaxation than stiffness of the polymer backbone, since the viscoelastic behaviour is almost identical in the two copolyesters but is greatly affected by annealing. Based on κ, the model suggests that the rate of physical aging is higher in PETT than PECT, as the decay in κ with annealing time is greatest for PETT. Furthermore, the model implies, that the attempt rate of separation of polymer chains is twice as high in PETT compared to PECT, suggesting more secondary bond rearrangement, which could enable faster structural changes. In our previous work, physical aging, especially manifested as enthalpy relaxation, occurred faster in copolyesters containing CHDM compared to TMCD. These earlier results combined with the results presented here imply, that the effect of physical aging cannot be explained by free volume theory alone, and that chemical structure also has an influence, which yet needs to be fully understood.

4. Conclusion

In this work we apply a constitutive model to describe the mechanical response in two glycol modified PET polymers, namely PETT and PECT, with different thermal history. The model uses a homogenization concept, which account for local density fluctuations in the polymer network, enabling the model to capture the structural development during physical aging. The results show that the model can predict the stress relaxation of PETT and PECT annealed for different durations with satisfactory precision. Furthermore, the model can describe creep in annealed PECT but underestimates the resulting strain in the unaged samples. The effect of physical aging on model parameters has been described, where κ is most strongly affected by aging. The concentration of active junctions decreases exponentially with annealing time, indicating that molecular configurations with stronger interchain interactions are formed during physical aging rendering the entanglements immobile when strained. Generally, PETT and PECT showed similar behaviours at 30 °C, suggesting that the chemical structure of the glycol unit (TMCD and CHDM) does not have significant effect on stress relaxation in the tested compositions. This also implies that PETT and PECT age with similar rates at T_g-20 °C, which contradicts previous work. When stress relaxation is tested at increased temperatures, the structural effects are more visible, demonstrating higher activation energies for PECT than PETT. The work presented here provides insights into how physical aging affects the viscoelastic response of polyesters, which is merely a small contribution to the future work of describing the complex non-equilibrium behaviour of amorphous polymers.

CRediT authorship contribution statement

Anne Therese Husth Weyhe: Conceptualization, Methodology, Investigation, Writing – original draft, Writing – review & editing. **Aleksey D. Drozdov:** Conceptualization, Methodology, Formal analysis, Writing – review & editing. **Jesper de Claville Christiansen:** Conceptualization, Supervision, Writing – review & editing. **Emil Andersen:** Conceptualization, Writing – review & editing. **Donghong Yu:** Conceptualization, Supervision, Writing – review & editing.

Declaration of Competing Interest

The authors declare that they have no known competing financial interests or personal relationships that could have appeared to influence the work reported in this paper.

Data availability

Data will be made available on request.

Acknowledgements

Innovation Fund Denmark has partly funded this work under file number 0153–00105B. The authors would like to give special thanks to Klaudia Chruslinska for extraordinary help with material testing.

Appendix A. Supporting information

Supplementary data associated with this article can be found in the online version at doi:10.1016/j.mtcomm.2023.107241.

References

[1] C. Vilela, et al., The quest for sustainable polyesters – insights into the future, Polym. Chem. vol. 5 (9) (2014) 3119–3141, https://doi.org/10.1039/C3PY01213A.
[2] A.M. Al-Sabagh, F.Z. Yehia, Gh Eshaq, A.M. Rabie, A.E. ElMetwally, Greener routes for recycling of polyethylene terephthalate, Egypt. J. Pet. vol. 25 (1) (2016) 53–64, https://doi.org/10.1016/j.ejpe.2015.03.001.
[3] P. Benyathiar, P. Kumar, G. Carpenter, J. Brace, D.K. Mishra, Polyethylene terephthalate (PET) bottle-to-bottle recycling for the beverage industry: a review, Polymers vol. 14 (12) (2022) 2366, https://doi.org/10.3390/polym14122366.
[4] M.K. Eriksen, J.D. Christiansen, A.E. Daugaard, T.F. Astrup, Closing the loop for PET, PE and PP waste from households: influence of material properties and product design for plastic recycling, Waste Manag vol. 96 (2019) 75–85, https://doi.org/10.1016/j.wasman.2019.07.005.
[5] W. Loyens, Ultimate mechanical properties of rubber toughened semicrystalline PET at room temperature, Polymer vol. 43 (21) (2002) 5679–5691, https://doi.org/10.1016/S0032-3861(02)00472-X.
[6] N. Chapleau, M.A. Huneault, Impact modification of poly(ethylene terephthalate), J. Appl. Polym. Sci. vol. 90 (11) (2003) 2919–2932, https://doi.org/10.1002/app.13016.
[7] T.H. Zhou, W.H. Ruan, J.L. Yang, M.Z. Rong, M.Q. Zhang, Z. Zhang, A novel route for improving creep resistance of polymers using nanoparticles, Compos. Sci. Technol. vol. 67 (11–12) (2007) 2297–2302, https://doi.org/10.1016/j.compscitech.2007.01.015.
[8] H.C.A. Lim, Thermoplastic Polyesters. Brydson's Plastics Materials, Elsevier, 2017, pp. 527–543, https://doi.org/10.1016/B978-0-323-35824-8.00020-7.
[9] J. Wang, X. Liu, Z. Jia, L. Sun, Y. Zhang, J. Zhu, Modification of poly(ethylene 2,5-furandicarboxylate) (PEF) with 1, 4-cyclohexanedimethanol: influence of stereochemistry of 1,4-cyclohexylene units, Polymer vol. 137 (2018) 173–185, https://doi.org/10.1016/j.polymer.2018.01.021.
[10] S.R. Turner, Development of amorphous copolyesters based on 1,4-cyclohexanedimethanol, J. Polym. Sci. Part Polym. Chem. vol. 42 (23) (2004) 5847–5852, https://doi.org/10.1002/pola.20460.
[11] C.J. Kibler, A. Bell, and J.G. Smith, Linear polyesters and polyester-amides from 1,4-cyclohexanedimethanol, 2901466, Aug. 25, 1959.
[12] S.R. Turner, R.W. Seymour, T.W. Smith, Cyclohexanedimethanol polyesters, USA: John Wiley & Sons, Inc.. Encyclopedia of Polymer Science and Technology, John Wiley & Sons, Inc.,, Hoboken, NJ, 2001, p. pst257, https://doi.org/10.1002/0471440264.pst257. USA: John Wiley & Sons, Inc.
[13] T. Chen, G. Jiang, G. Li, Z. Wu, J. Zhang, Poly(ethylene glycol-co-1,4-cyclohexanedimethanol terephthalate) random copolymers: effect of copolymer

composition and microstructure on the thermal properties and crystallization behavior, RSC Adv. vol. 5 (74) (2015) 60570–60580, https://doi.org/10.1039/C5RA09252C.
[14] T. Chen, W. Zhang, J. Zhang, Alkali resistance of poly(ethylene terephthalate) (PET) and poly(ethylene glycol-co-1,4-cyclohexanedimethanol terephthalate) (PETG) copolyesters: The role of composition, Polym. Degrad. Stab. vol. 120 (2015) 232–243, https://doi.org/10.1016/j.polymdegradstab.2015.07.008.
[15] A.V. Cugini, A.J. Lesser, Aspects of physical aging, mechanical rejuvenation, and thermal annealing in a new copolyester, Polym. Eng. Sci. vol. 55 (8) (2015) 1941–1950, https://doi.org/10.1002/pen.24035.
[16] E. Andersen, R. Mikkelsen, S. Kristiansen, M. Hinge, Real-time ageing of polyesters with varying diols, Mater. Chem. Phys. vol. 261 (2021), 124240, https://doi.org/10.1016/j.matchemphys.2021.124240.
[17] K.A. Iyer, Chain mobility, secondary relaxation, and oxygen transport in terephthalate copolyesters with rigid and flexible cyclic diols, Polymer vol. 129 (2017) 117–126, https://doi.org/10.1016/j.polymer.2017.09.049.
[18] D.R. Kelsey, B.M. Scardino, J.S. Grebowicz, H.H. Chuah, High impact, amorphous terephthalate copolyesters of rigid 2,2,4,4-tetramethyl-1,3-cyclobutanediol with flexible diols, Macromolecules vol. 33 (16) (2000) 5810–5818, https://doi.org/10.1021/ma000223.
[19] M. Goldstein, Viscous liquids and the glass transition: a potential energy barrier picture, J. Chem. Phys. vol. 51 (9) (1969) 3728–3739, https://doi.org/10.1063/1.1672587.
[20] N. Mousseau, G.T. Barkema, Traveling through potential energy landscapes of disordered materials: the activation-relaxation technique, Phys. Rev. E vol. 57 (2) (1998) 2419–2424, https://doi.org/10.1103/PhysRevE.57.2419.
[21] I.M. Hodge, A.R. Berens, Effects of annealing and prior history on enthalpy relaxation in glassy polymers. 2, Math. Model., *Macromol.* vol. 15 (3) (1982) 762–770, https://doi.org/10.1021/ma00231a016.
[22] N. Doulache, M.W. Khemici, A. Gourari, M. Bendaoud, DSC study of polyethylene terephtalate's physical ageing. 2010 10th IEEE International Conference on Solid Dielectrics, IEEE, Jul,, Potsdam, 2010, pp. 1–4, https://doi.org/10.1109/ICSD.2010.5568072.
[23] I.M. Hodge, Physical aging in polymer glasses, Science vol. 267 (5206) (1995) 1945–1947, https://doi.org/10.1126/science.267.5206.1945.
[24] K. Chen, C. Zhou, H. Liu, Y. Wang, Physical aging-induced embrittlement of PLA/PBAT blends probed by tensile test and AFM nanomechanical mapping, Mater. Lett. vol. 326 (2022), 132938, https://doi.org/10.1016/j.matlet.2022.132938.
[25] B.-W. Wang, H. Liu, J. Ying, C.-T. Liu, C.-Y. Shen, Y.-M. Wang, Effect of physical aging on heterogeneity of poly(ε-caprolactone) toughening poly(lactic acid) probed by nanomechanical mapping, Chin. J. Polym. Sci. vol. 41 (1) (2023) 143–152, https://doi.org/10.1007/s10118-022-2806-1.
[26] L.C.E. Struik, Physical aging in plastics and other glassy materials, Polym. Eng. Sci. vol. 17 (3) (1977) 165–173, https://doi.org/10.1002/pen.760170305.
[27] E. Gruber, 'L.G.E. Struik: Physical Aging in Amorphous Polymers and Other Materials. Elsevier Sci. Publ. Comp., Amsterdam-Oxford-New York 1978. 229 Seiten, 141 Abbildungen, Holl. Gulden 97,50., *Berichte Bunsenges. Für Phys. Chem.*, vol. 82, no. 9, pp. 1019–1019, 1978, ⟨doi:10.1002/bbpc.19780820975⟩.
[28] D.M. Bigg, A review of positron annihilation lifetime spectroscopy as applied to the physical aging of polymers, Polym. Eng. Sci. vol. 36 (6) (1996) 737–743, https://doi.org/10.1002/pen.10461.
[29] E. Andersen, R. Mikkelsen, S. Kristiansen, M. Hinge, Accelerated physical ageing of poly(1,4-cyclohexylenedimethylene- *co* -2,2,4,4-tetramethyl-1,3-cyclobutanediol terephthalate), RSC Adv. vol. 9 (25) (2019) 14209–14219, https://doi.org/10.1039/C9RA00925F.
[30] A.T. Weyhe, E. Andersen, R. Mikkelsen, D. Yu, Accelerated physical aging of four PET copolyesters: enthalpy relaxation and yield behaviour, Polymer vol. 278 (2023), 125987, https://doi.org/10.1016/j.polymer.2023.125987.
[31] J.L. Sullivan, Creep and physical aging of composites, Compos. Sci. Technol. vol. 39 (3) (1990) 207–232, https://doi.org/10.1016/0266-3538(90)90042-4.
[32] J.M. Hutchinson, S. Smith, B. Horne, G.M. Gourlay, Physical aging of polycarbonate: enthalpy relaxation, creep response, and yielding behavior, Macromolecules vol. 32 (15) (1999) 5046–5061, https://doi.org/10.1021/ma981391t.
[33] S.G. Nunes, et al., Physical aging effect on viscoelastic behavior of polymers, Compos. Part C. Open Access vol. 7 (2022), 100223, https://doi.org/10.1016/j.jcomc.2021.100223.
[34] J. Hristova, V. Valeva, J. Ivanova, Aging and filler effects on the creep model parameters of thermoset composites, Compos. Sci. Technol. vol. 62 (7–8) (2002) 1097–1103, https://doi.org/10.1016/S0266-3538(02)00055-6.
[35] A.D. Drozdov, J. deC. Christiansen, Thermo-viscoelastic and viscoplastic behavior of high-density polyethylene, Int. J. Solids Struct. vol. 45 (14–15) (2008) 4274–4288, https://doi.org/10.1016/j.ijsolstr.2008.03.008.
[36] J. Guo, Z. Li, J. Long, R. Xiao, Modeling the effect of physical aging on the stress response of amorphous polymers based on a two-temperature continuum theory, Mech. Mater. vol. 143 (2020), 103335, https://doi.org/10.1016/j.mechmat.2020.103335.
[37] B.R. Frieberg, E. Glynos, G. Sakellariou, M. Tyagi, P.F. Green, Effect of molecular stiffness on the physical aging of polymers, Macromolecules vol. 53 (18) (2020) 7684–7690, https://doi.org/10.1021/acs.macromol.0c01331.
[38] G. Levita, L.C.E. Struik, Physical ageing in rigid chain polymers, Polymer vol. 24 (8) (1983) 1071–1074, https://doi.org/10.1016/0032-3861(83)90162-3.
[39] A.D. Drozdov, J. deC. Christiansen, Creep failure of polypropylene: experiments and constitutive modeling, Int. J. Fract. vol. 159 (1) (2009) 63–79, https://doi.org/10.1007/s10704-009-9384-x.
[40] B. Derrida, Random-energy model: limit of a family of disordered models, Phys. Rev. Lett. vol. 45 (2) (1980) 79–82, https://doi.org/10.1103/PhysRevLett.45.79.
[41] A.S. Krausz, H. Eyring, and others, *Deformation kinetics*. Wiley, 1975.
[42] C. Lechat, A.R. Bunsell, P. Davies, Tensile and creep behaviour of polyethylene terephthalate and polyethylene naphthalate fibres, J. Mater. Sci. vol. 46 (2) (2011) 528–533, https://doi.org/10.1007/s10853-010-4999-x.

The Effect of Physical Aging on the Viscoelastoplastic Response of Glycol Modified Poly(ethylene terephthalate)

Anne Therese Weyhe [a,b], Aleksey D. Drozdov [c,*], Jesper de Claville Christiansen [c], Emil Andersen [b], Donghong Yu [a,*,]

[a] *Department of Chemistry and Bioscience, Aalborg University, Fredrik Bajers Vej 7H, DK-9220 Aalborg East, Denmark*

[b] *LEGO System A/S, Åstvej 1, DK-7190 Billund, Denmark*

[c] *Department of Materials and Production, Aalborg University, Fibigerstræde 14, DK-9220 Aalborg East, Denmark*

Supporting information

Methods

1. Differential Scanning Calorimetry

5-10 mg samples were cut from tensile test specimens, placed in pans (Tzero hermetic pan 901683.901, TA Instruments, USA) with lids (Tzero hermetic lid 901683.901, TA Instruments, USA). All samples were heated twice from 20 to 300 °C at 10 °C/min with in-between cooling to 20 °C at 10 °C/min in a DSC (Q2000, TA Instruments, USA) with nitrogen flow (50 mL/min). Samples were tested in triplicates and T_g evaluated using the 'inflection point' methodology.

2. Dynamic Mechanical Analysis

Samples were cut from the middle of tensile bars (See Fig. S1) and tested in bending mode using a dual cantilever in dynamic mechanical analyser (Discovery DMA 850, TA Instruments, USA). The temperature ranged from -70 to 120 °C, the frequency was 1 Hz, and the oscillation strain was 1 %.

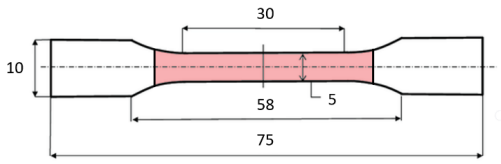

Figure S1. Illustration of a 1BA tensile bar with dimensions in mm. Red indicates the part used for DMA.

3. Density measurements

Density of tensile bars was measured according to Archimedes principle using an analytical balance (Quintix 124-1S, Sartorius, GER) and density determination kit (YDK03, Sartorius, GER).

Results

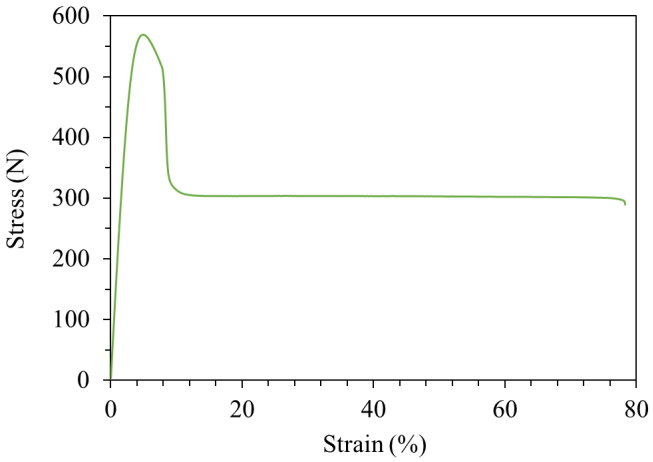

Figure S2. Stress strain curve from tensile test of unaged poly(ethylene-co-1,4-cyclohexylenedimethylene terephthalate) (PECT).

Table S1. E-modulus, yield strength (σ_Y), maximum strength (σ_M), strength at break (σ_B), elongation at yield (ε_Y), elongation at max stress (ε_M), elongation at break (ε_B), of unaged poly(ethylene-co-1,4-cyclohexylenedimethylene terephthalate) (PECT). Test was done in triplicate.

	E (N/mm^2)	σ_Y (N/mm^2)	σ_M (N/mm^2)	σ_B (N/mm^2)	ε_Y (%)	ε_M (%)	ε_B (%)
Avg.	2223.17	61.34	61.34	33.41	5.06	5.06	32.01
Std.	11.058	0.092	0.092	0.84	0.031	0.031	10.03
v (%)	0.50	0.15	0.15	2.51	0.61	0.61	31.35

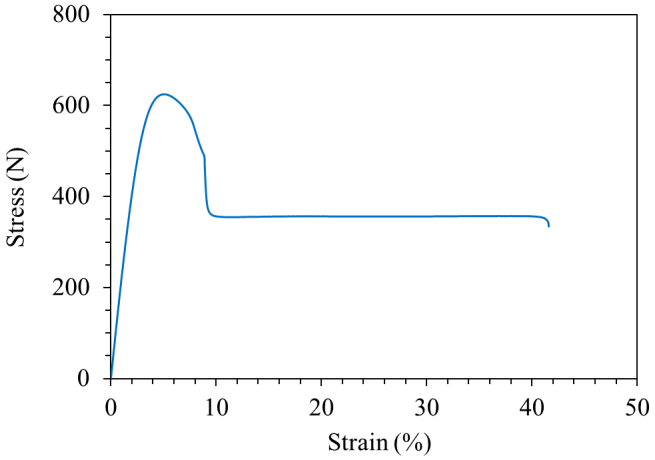

Figure S3. Stress strain curve from tensile test of unaged poly(ethylene-co-2,2,4,4-tetramethyl-1,3-cyclobutanediol terephthalate) (PETT).

Table S2. E-modulus, yield strength (σ_Y), maximum strength (σ_M), strength at break (σ_B), elongation at yield (ε_Y), elongation at max stress (ε_M), elongation at break (ε_B), of unaged poly(ethylene-co-2,2,4,4-tetramethyl-1,3-cyclobutanediol terephthalate) (PETT). Test was done in triplicate.

	E (N/mm^2)	σ_Y (N/mm^2)	σ_M (N/mm^2)	σ_B (N/mm^2)	ε_Y (%)	ε_M (%)	ε_B (%)
Avg.	1934.92	54.60	54.60	27.34	4.88	4.88	77.37
Std.	10.93	0.18	0.18	0.50	0.065	0.065	15.26
v (%)	0.56	0.32	0.32	1.84	1.33	1.33	19.73

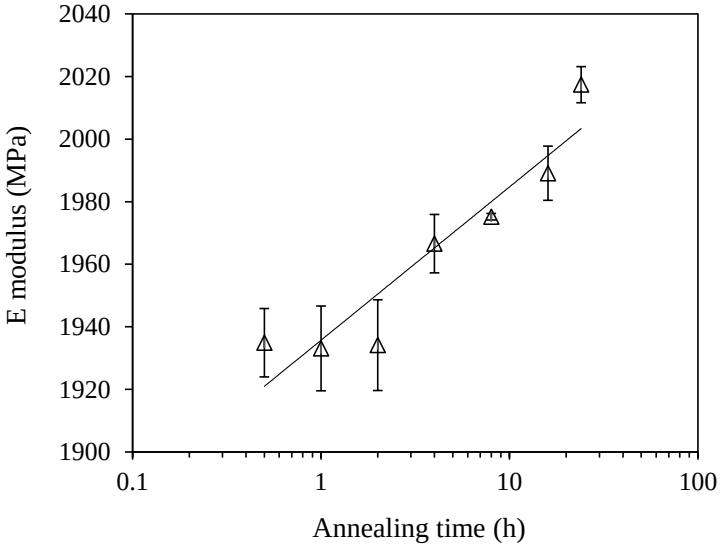

Figure S4. E-modulus of poly(ethylene-co-1,4-cyclohexylenedimethylene terephthalate) (PECT) with different annealing time at T_g-20 °C.

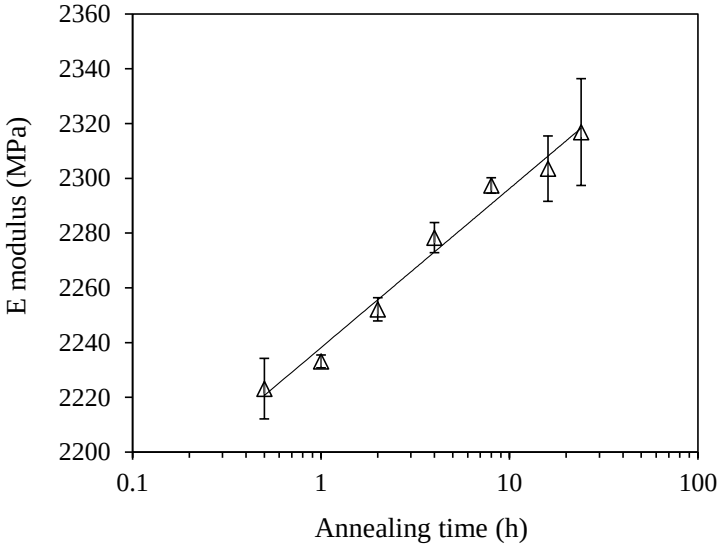

Figure S5. E-modulus of poly(ethylene-co-2,2,4,4-tetramethyl-1,3-cyclobutanediol terephthalate) (PETT) with different annealing time at T_g-20 °C.

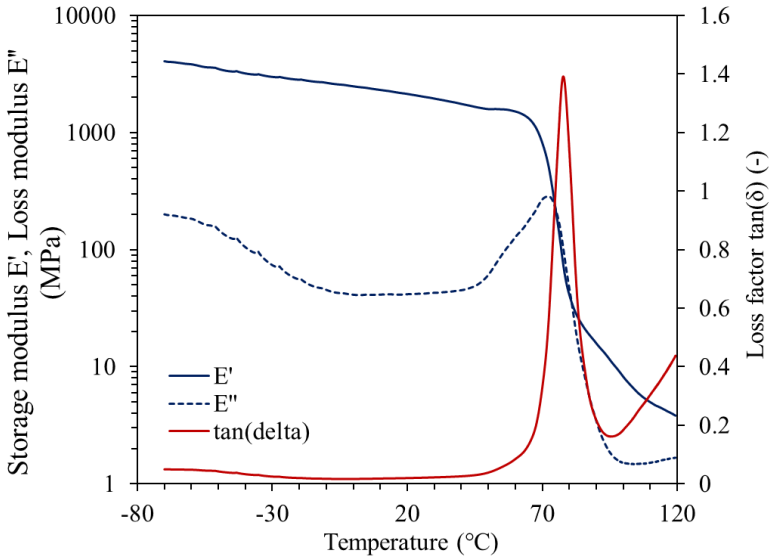

Figure S6. Dynamic mechanical properties of poly(ethylene-co-1,4-cyclohexylenedimethylene terephthalate) (PECT).

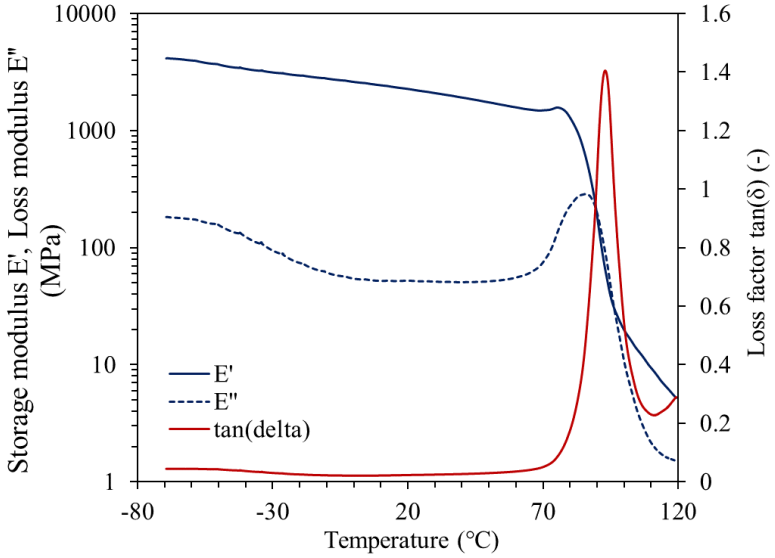

Figure S7. Dynamic mechanical properties of poly(ethylene-co-2,2,4,4-tetramethyl-1,3-cyclobutanediol terephthalate) (PETT)

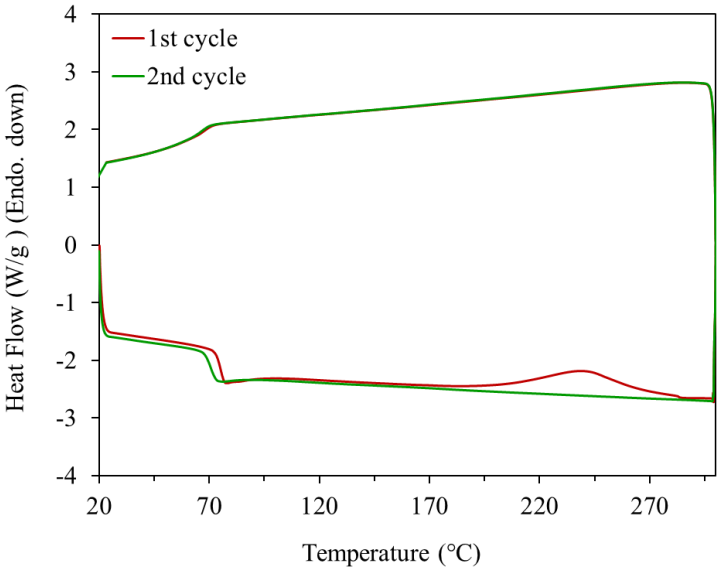

Figure S8. Sequential DSC traces of unaged poly(ethylene-co-1,4-cyclohexylenedimethylene terephthalate) (PECT) showing glass transition (T_g ~ 81 ºC) and no crystalline peaks or significant enthalpic overshoot around T_g.

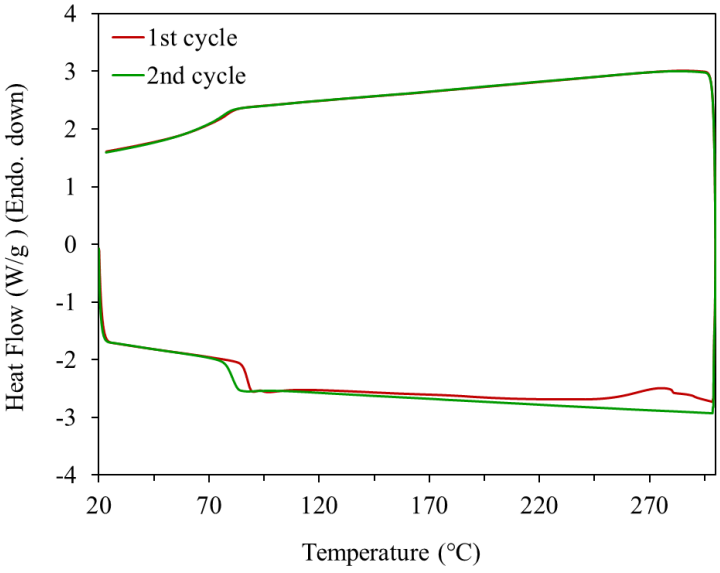

Figure S9. Sequential DSC traces of poly(ethylene-co-2,2,4,4-tetramethyl-1,3-cyclobutanediol terephthalate) (PETT) showing glass transition (T_g ~ 94 ºC) and no crystalline peaks or significant enthalpic overshoot around T_g.

Table S3. Density of unaged and aged poly(ethylene-co-2,2,4,4-tetramethyl-1,3-cyclobutanediol terephthalate) (PETT) and poly(ethylene-co-1,4-cyclohexylenedimethylene terephthalate) (PECT).

	Density [g/cm^3]	
	Unaged	Aged 24 h (T_g-20 °C)
PETT	1.273	1.275
PECT	1.279	1.278

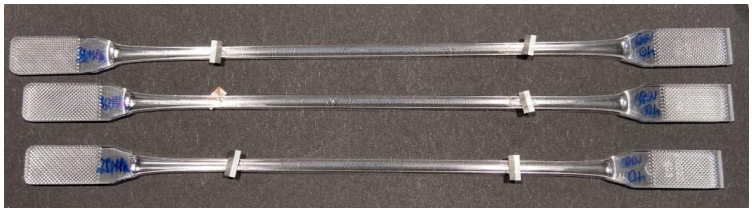

Figure S10. Photos of unaged poly(ethylene-co-1,4-cyclohexylenedimethylene terephthalate) (PECT) samples after creep tests at 30 ºC with applied stress of 28.6 MPa for 24 h.

Figure S11. Photo-zoom of Figure S10 showing the neck reaching the thicker part of the tensile bar with a larger cross sectional area.

CHAPTER 5. PHYSICAL AGING IN IMPACT MODIFIED POLYETHYLENE TEREPHTHALATE

PET is well-known for its exceptional mechanical properties, thermal stability, and clarity, making it a preferred material for various industrial and consumer applications. However, to meet the diverse demands of different applications, modifications are often employed to tailor material properties further. One of the key development areas is impact modification, where various additives are utilized to enhance toughness and impact resistance. Impact modification of PET can be of great importance, especially in applications where the material may be subjected to mechanical stresses, dynamic loading, or potential impact events. Incorporating impact modifiers into PET matrices allows manufacturers to expand its applications into areas that require higher resilience and durability. However, there are certain challenges and potential drawbacks associated with impact modification, such as potential trade-offs between enhanced toughness and viscoelastic behaviour. Furthermore, understanding the interplay between these modifications and the material's physical aging behaviour is essential to ensure the long-term performance and reliability of PET-based products.

In this chapter, the effect of accelerated physical aging on impact-modified PET will be investigated and discussed. The main focus is the effects on viscoelastic properties, since these are crucial in the development of durable products e.g. snap and press fits. Furthermore, the enthalpic response and yielding behaviour have been investigated. The findings have resulted in a patent application, which will be presented by the patent abstract, concluding the chapter.

5.1. INTRODUCTION

Generally, impact modifiers are rubbery phases which dissipates the fracture energy by inducing an overall deformation instead of a local one. Polyethylene (PE) has been found to increase toughness, but since PE is immiscible in the PET matrix, poor interfacial adhesion between the two phases causes the effectiveness of impact modification to decrease [94]. Therefore, reactive elastomers are used, achieving compatibilisation through implementation of polar and functional moieties to the impact modifier [95].

A reactive impact modifier suitable for PET is the ternary polymer ethylene-butyl acrylate-glycidyl methacrylate (E-BA-GMA) (T_g = -55 °C) [31], whose chemical structure is illustrated in Figure 5.1. The main component is PE, thus inducing an

aliphatic backbone with high flexibility. Butyl acrylate is an acrylic ester, which both induce flexibility and polarity, thereby working as an emulsifier. Glycidyl methacrylate allows grafting of the impact modifier onto PET through ring opening of the epoxy group, as shown in Figure 5.2.

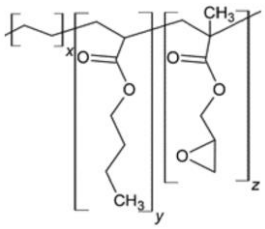

Figure 5.1 Chemical structure of E-BA-GMA

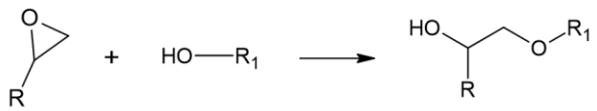

Figure 5.2 Schematic representation of the reaction between epoxide and PET end-group

No general rules exist regarding the effect of impact modifiers on physical aging behaviour, since different impact modifiers interacts differently with the structure of the matrix. Some studies have explored the effect of crosslinking and found that while crosslinking impede physical aging in some materials it does not have a significant influence in others [96-98]. Crosslinking generally makes an interconnected network, locking the structure compared to one that is non-crosslinked, which would intuitively prevent molecular movement. However, that segmental motions involved in physical aging might be on a much smaller scale compared to what is prevented by crosslinking. Fewer studies have been concerned with physical aging in two-phase systems. One study investigated PLA blended with immiscible poly(ε-caprolactone) (PCL) and found that physical aging enhanced the heterogeneity of the PLA matrix. It was furthermore concluded, that the introduction of PCL did not inhibit physical aging [99].

While the primary goal of impact modification is to improve the impact toughness, other mechanical properties including stress relaxation can be influenced. Stress relaxation, being the phenomenon in which a material gradually reduces internal stresses when subject to constant strain over time, can be affected in several ways, depending on the type of impact modifier. Enhanced crosslinking would for example increase the overall strength and dimensional stability thus decreasing stress relaxation. On the other hand, some impact modifiers might not be fully compatible with the polymer matrix, forming separate phases, which can create localized

concentrations of stress and have poor interface adhesion consequently increasing stress relaxation. In the case of E-BA-GMA, both partial crosslinking and phase separation can occur, even though crosslinking is not very likely. Furthermore, 90 % of the impact modifier consists of PE (molar ratio: E:BA:GMA = 90.3:8.3:1.4 [100]), creating rubbery phases with low E-modulus that might act as a plasticizer easing the movement of polymer chains and increasing the ability to reduce stress. This effect is undesirable in press-fit functions such as the LEGO clutch function, where stress is needed to maintain a durable connectivity. Therefore, it is crucial to strike a balance between impact improvement and preserving the material's long-term performance, especially in applications where prolonged service life is paramount. In this work, the effects of accelerated aging on E-BA-GMA modified PET will be investigated to explore the possible improvements on stress relaxation behaviour.

5.2. MATERIALS AND METHODS

5.2.1. MATERIALS

Poly(ethylene terephthalate) (PET, PQB15-089E, PolyQuest, USA) and reactive impact modifier (Elvaloy PTW™, DuPont, USA) (E-BA-GMA with weight ratio 66.75:28:5.25), was compounded using a twin screw extruder yielding granulates with 0, 2.5, 5.0 and 8.0 wt% impact modifier. Tensile test specimens (1BA, ISO 527-2:2012) were injection moulded (Arburg 470E 600-290, Arburg, GER) with moulding conditions shown in Table 5.1.

Table 5.1. Injection moulding parameters

Impact modifier wt% [%]	Moisture content [%]	Drying temp. [°C]	Drying time [h]	Injection pressure [bar]	Mould temp. [°C]	Cooling time [s]
0.0	0.013	155	8	796	20	16
2.5	0.013	140	6	648	20	20
5.0	0.007	140	6	725	20	15
8.0	0.006	140	6	494	20	20

5.2.2. ACCELERATED AGING

Samples for DSC measurements were thermally aged in pans (Tzero hermetic pan 901683.901, TA Instruments, USA) with lids (Tzero hermetic lid 901683.901, TA Instruments, USA). The samples were placed in ovens along with tensile bars. Samples for DSC and tensile tests were aged at 50 ºC for 0.5, 1, 2, 4, 8, 16 and 24 h. Samples for stress relaxation tests were aged at 50 ºC for 216 h.

5.2.3. ENTHALPY RELAXATION

5-10 mg samples (cut from tensile bars) were measured in a DSC (Q2000, TA Instruments, USA) with nitrogen flow (50 mL/min). Both aged and unaged samples were tested in pans as described above. All samples were heated twice from 20 to 300 °C at 10 °C/min with their cooling to 20 °C at 10 °C/min in between and tested in triplicates.

The enthalpy lost upon aging ($\Delta H(T_g)$), was determined from an endotherm peak at T_g, as the integral between each of the aged samples and an unaged reference sample.

5.2.4. TENSILE TESTS

Tensile test specimens were fixed with the inlet in the lower pneumatic grip in a universal testing machine (Z005, ZwickRoall, GER) with a 25 mm gauge length extensometer (180102/2008, ZwickRoell, GER) controlled by testXpert II (Zwick, GER). E-modulus and yield strength were evaluated with speed of 1 and 100 mm/min, respectively, at 23 ± 2 °C.

5.2.5. STRESS RELAXATION TEST

Uniaxial stress relaxation tests were performed on tensile bars in a universal testing machine (Z005, ZwickRoall, GER) with a 25 mm gauge length extensometer (180102/2008, ZwickRoell, GER) controlled by testXpert II (Zwick, GER). Tests were performed on unaged samples and samples thermally aged for 216 h at 50 °C in an oven with loading speed of 1 mm/min. Samples were strained at ϵ = 2 % for 60 min at 23 ± 2 °C.

5.3. RESULTS AND DISCUSSION

5.3.1. ENTHALPY RELAXATION

The recoverable enthalpy, shown in Figure 5.3, increases linearly with the logarithm of aging time from 2 to 24 hours regardless of impact modifier content. For aging times shorter than 2 hours, no enthalpic overshoot is observed, and hence no physical aging occurs, or the initial structural changes does not result in significant enthalpy loss. There is no evident effect of E-BA-GMA content up to 8 wt% on the physical aging rate of PET measured with DSC. This suggests, that the structural relaxation in form of interchain interactions is not influenced much by the introduction of PE to the matrix.

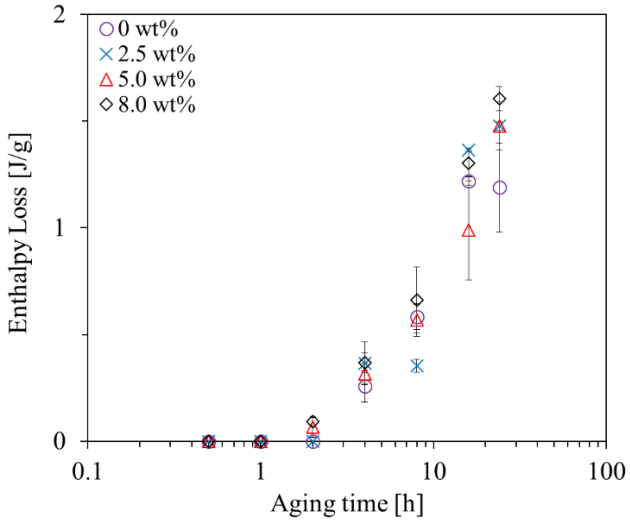

Figure 5.3 Enthalpy loss as function of aging time for samples aged at 50 °C for up to 24 h. Legends indicate the weight percent of E-BA-GMA in the samples

5.3.2. TENSILE TESTS

The yield strength as function of aging time is illustrated in Figure 5.4. The first notable thing is, that the yield strength decreases linearly with E-BA-GMA wt%. It is expected to decrease, due to the fundamental trade off that often exists between yield strength and toughness. Materials that are more ductile and capable of absorbing impact energy tend to have lower yield strengths compared to brittle materials that break upon smaller deformation. This is because impact modifiers, such as E-BA-GMA has a plasticizing effect that allows the polymer to undergo more deformation before breaking. While this is advantageous for impact resistance, it leads to a reduction in yield strength, because the material is less resistant to permanent deformation. As seen in Figure 5.4, the yield strength increases logarithmically with aging time for all grades. This increase is also expected due to the decrease/redistribution of free volume caused by physical aging. After 24 hours of aging, the largest yield strength increase is 2.6 MPa in native PET samples, whereas the lowest increase is 0.9 MPa in samples with 8 wt% E-BA-GMA corresponding to 4.0 and 1.9 % increase, respectively. This could suggest that the introduction of E-BA-GMA slightly decelerates physical aging.

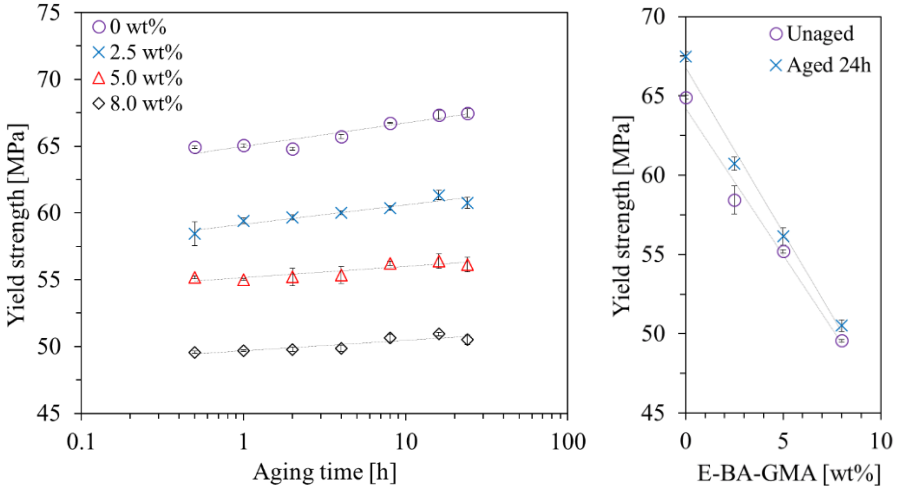

Figure 5.4 (Left) Yield strength versus aging time for samples aged at 50 °C for up to 24 h. Legends indicate the weight percent of E-BA-GMA in the samples. (Right) Yield strength as function of E-BA-GMA content for unaged samples and samples aged for 24 h

From tensile tests, the E-moduli are also determined and shown in Figure 5.5. The stiffness of PET decreases with increasing E-BA-GMA content. This is also an effect of the incorporated elastomer, which induces flexibility to the polymer network, hence less stress is needed to strain the samples. Furthermore, the E-modulus increases with aging time, which is expected from amorphous and semi crystalline polymers. During physical aging, the material becomes stiffer due to stronger interchain interactions, which is observed as an increase in E-modulus. Another study showed only small increases in E-modulus of virgin PET during 24 hour aging at T_g-20 °C (~79 MPa) (Paper III supporting information), and it could therefore be hypothesized that the temperature used for aging in this study (~T_g-30 °C) would have less effect on the E-modulus. However, the E-moduli reported here increase between 94 and 119 MPa, which is a similar scale. The increase in stiffness is not affected significantly by the E-BA-GMA content (4.0 % for 0 wt% and 5.3 % for 8 wt%) suggesting that E-BA-GMA does not influence the physical aging rate in the tested concentrations.

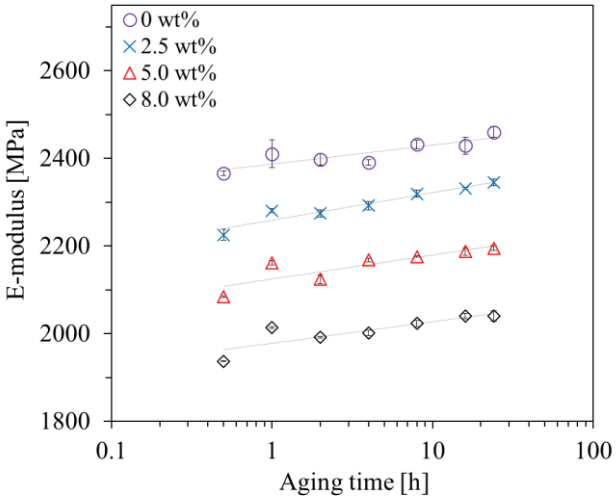

Figure 5.5 E-modulus as function of aging time for samples aged at 50 °C for up to 24 h. Legends indicate the weight percent of E-BA-GMA in the samples

5.3.3. STRESS RELAXATION

The stress as function of relaxation time under 2 % strain is shown in Figure 5.6. The stress is generally lowered with the higher content of E-BA-GMA (wt%) in the sample. Especially the difference in initial stress between the PET grades reflects the difference in stiffness which is lowered by E-BA-GMA content, thus higher E-BA-GMA wt% gives lower initial stress. The percentage of stress relaxation over 60 min increases linearly with E-BA-GMA content from 14.7 % in virgin PET to 16.7, 18.1, and 20.4 % in samples with 2.5, 5.0 and 8.0 wt%, respectively (unaged samples). This is quite expectable since impact modification with E-BA-GMA introduces flexibility and mobility to the polymer chains. The increased chain mobility both allows the polymer to absorb and dissipate more energy but also increases its ability to reduce the internal stresses when strained.

After aging for 216 h at 50 °C the initial stress increases in all grades, proving an increase in stiffness. This observation confirms the results from tensile tests, where an increase in stiffness was found in the first 24 hours of aging. The stress relaxation is decreased by physical aging in all samples. After 60 min the stress is reduced by 5.4, 7.0, 7.9 and 9.4 % for 0, 2.5, 5.0 and 8.0 wt%, respectively, suggesting the formation of stronger or more interchain interactions locking the structure and thereby resisting mobility to a higher degree. These results are important in relation to products, such as LEGO bricks, where high impact strength and functional durability is needed simultaneously. The results demonstrate that stress relaxation can be repressed by accelerating physical aging in impact modified PET. Furthermore, they show that the

degree of stress relaxation inhibition is independent of E-BA-GMA content in the tested range. This enables tuning of the strain dependent function in e.g. LEGO bricks.

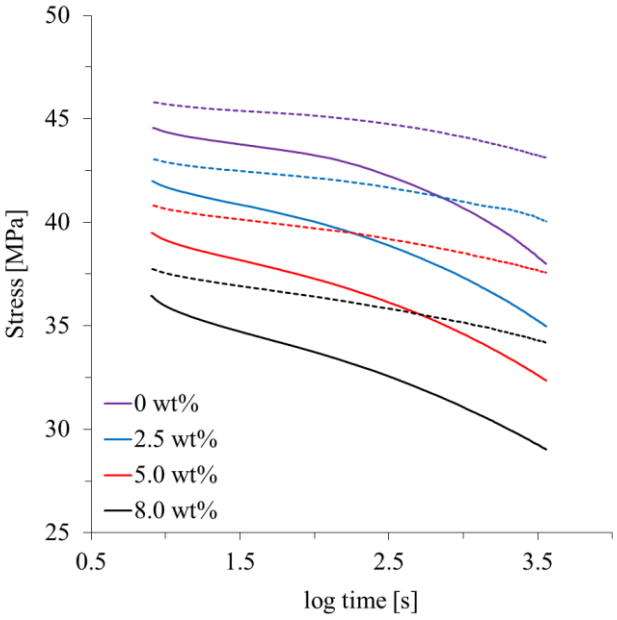

Figure 5.6 Tensile stress versus relaxation time. Legends indicate the weight percent of E-BA-GMA in the samples. Solid lines indicate unaged samples and dashed lines indicates samples aged for 216 h at 50 °C

5.4. CONCLUSION

Different methods have been used to investigate physical aging in PET impact modified with E-BA-GMA, i.e. DSC, tensile and stress relaxation tests. All experiments show that the introduction of E-BA-GMA to PET does not prevent physical aging from happening and thus enthalpy loss, yield strength and E-modulus increase, whereas stress relaxation is reduced after thermal treatment below T_g. This means that while improving impact properties at the cost of decreased stiffness and increased stress relaxation, these can be improved through accelerated physical aging. Hence both impact strength and function can be maintained over time in PET products with press fits.

PATENT APPLICATION ABSTRACT:

"The present invention relates to a method for the manufacture of a toy building element with improved functional durability made of an impact modified amorphous material having an enthalpic relaxation of at least 0.3 J/g, such as in the range of 0.3 to 4 J/g and a shrinkage of maximum 0.2%. The present invention also relates to a toy building element with improved functional durability made of an impact modified amorphous material having an enthalpic relaxation of at least 0.3 J/g, such as in the range of 0.3 to 4 J/g and a shrinkage of maximum 0.2%."

CHAPTER 6. PHYSICAL AGING IN HIGH GLASS TRANSITION TEMPERATURE POLYESTERS

Recently, there has been a significant interest in the development of polyesters with high T_g's and high impact strengths. These properties are highly desirable in products where durability is demanded and where service temperatures may lead to physical aging of common polyesters, such as PET.

Having both high T_g and high impact strength in a polymer can be challenging because these two properties are often inversely related. T_g is a measure of a polymer's ability to resist deformation under heat, while impact strength is a measure of a polymer's ability to absorb energy without breaking under an impact load. Polymers with high T_g tend to have a more rigid and ordered molecular structure, which makes them less likely to deform under heat. However, this rigid structure can also make them brittle and more susceptible to failure under an impact load. In contrast, polymers with high impact strength typically have a more flexible and disordered molecular structure, which enables them to absorb energy and deform without breaking under an impact load. However, this flexible structure can also make them more susceptible to deformation under heat, leading to a lower T_g. To be a possible ABS replacement, polyesters have to offer sufficient impact strength, and at the same time have a certain resistance to physical aging, which might be offered by a high T_g.

This chapter presents the study of three polyesters containing isosorbide (1,4:3,6-dianhydroxitol) with high T_g and high impact strength compared to PET. The study focusses on the effect of physical aging on these polyesters compared to the effect in PET and PCTT. Furthermore, the study aims so investigate the relationship between T_g and aging rate.

6.1. PAPER III

This study presents the physical aging behaviour of three isosorbide polyesters with varying diol composition: poly(isosorbide-co-1,4-butanediol terephthalate) (PIBT), poly(isosorbide-co-diethylene glycol terephthalate) (PIDT) and poly(isosorbide-co-1,4-cyclohexanedimethanol terephthalate) (PICT) (all with ~50 mol% isosorbide) compared to PET and PCTT.

The results showed that physical aging, measured as recoverable enthalpy, occurred faster in PIBT than in PCTT at 60 and 70 °C despite both having a T_g of 108-9 °C. This suggests that T_g alone does not control the aging rate. The increase in recoverable

enthalpy follow Arrhenius behaviour in all tested polyesters with activation energies from 161.8 to 202.3 kJ/mol. A similar Arrhenius behaviour was found for increasing tensile strength in PICT, PET and PCTT with activation energies of 225.6-260.1 kJ/mol, suggesting that the increase in tensile strength is generally more affected by temperature compared to enthalpy loss.

Stress relaxation experiments of unaged samples revealed greater resistance to stress reduction in PICT and PCTT compared to the other polyesters, suggesting a retaining effect of CHDM. An influence of aging was found in all polyesters, reducing the stress relaxation significantly after 168 h of thermal treatment. This suggests, that the viscoelastic properties of the three isosorbide polyesters can be enhanced to ensure function over time in product designs such as LEGO bricks.

Physical Aging of Aromatic Copolyesters with High Isosorbide Content and High Glass Transition Temperatures

Anne Therese Weyhe [a,b], Bruno Bottega Pergher [c,d], Gert-Jan M. Gruter [c,d], Donghong Yu [a,*]

[a] *Department of Chemistry and Bioscience, Aalborg University, Fredrik Bajers Vej 7H, DK-9220 Aalborg East, Denmark*

[b] *LEGO System A/S, Åstvej 1, DK-7190 Billund, Denmark*

[c] *Van't Hoff Institute of Molecular Science, University of Amsterdam, P.O. Box 94720, 1090GS Amsterdam, The Netherlands*

[d] *Avantium Chemicals BV, Zekeringstraat 29, 1014BV Amsterdam, The Netherlands*

Abstract

In the pursuit of more sustainable and durable polymers, polyesters containing isosorbide (1,4:3,6-dianhydroxitol) emerge as promising candidates. This work elucidates the physical aging behaviour of three isosorbide polyesters with varying diol composition: poly(isosorbide-*co*-1,4-butanediol terephthalate) (PIBT), poly(isosorbide-*co*-diethylene glycol terephthalate) (PIDT) and poly(isosorbide-*co*-1,4-cyclohexanedimethanol terephthalate) (PICT) (all with ~50 % (mol%) isosorbide) compared to the common poly(ethylene terephthalate) (PET) and the state-of-the-art high T_g polyester poly(1,4-cyclohexylenedimethylene-co-2,2,4,4-tetramethyl-1,3-cyclobutanediol terephthalate) (PCTT). The polyesters underwent thermal treatment at temperatures below and close to their respective glass transition temperatures (T_g) for up to 504 h to accelerate physical aging. Enthalpy relaxation was measured as recoverable enthalpy by differential scanning calorimetry and compared to mechanical changes expressed as an increase in tensile strength and alterations in stress relaxation behaviour. Generally, the observed increase in recoverable enthalpy and yield strength follows Arrhenius behaviour in all tested polyesters with activation energies ranging from 161.8 to 260.1 kJ/mol, demonstrating higher values for yield strength than recoverable enthalpy. Physical aging occurred more rapidly in PIBT than in PCTT at 60 and 70 °C despite both having a T_g of 108-9 °C. This observation implies that T_g cannot solely indicate the physical aging rate, and other factors, such as chemical structure also has an influence.

Keywords: Polyester, Isosorbide, Physical Aging, Enthalpy relaxation, Tensile strength

1. Introduction

One of the most important challenges in the global plastic industry is reducing its dependence on fossil-based resources, from which most plastics are currently derived [1-3]. To achieve this goal, the substitution of polymers from petroleum-based feedstock must be replaced by materials made from renewable sources such as recycled materials, biomass or CO_2 conversion [4]. Polyesters as a class of polymers, hold potential for this substitution, offering both renewable sourcing and possibilities for chemical and mechanical recycling [5]. Chemical recycling becomes feasible due to the easily cleavable ester bond allowing for monomer recovery at relatively low process temperatures in the presence of solvents like methanol [6]. This method facilitates the obtaining of (modified) starting monomers and hence production of virgin-quality materials, which is not achievable through traditional (mechanical) recycling [7]. Additionally, numerous polyester monomers from renewable sources can be combined to produce materials with tunable properties, allowing production of engineering grade polymers.

Polyesters are already widely used in various fields today due to their excellent properties such as good tensile strength, barrier properties and thermal stability. Especially the commodity plastic poly(ethylene terephthalate) (PET) is extensively used in products such as beverage bottles, food packaging and textiles. However, the application of polyesters in high temperature environments is often limited by their relatively low glass transition temperatures (T_g) (~80 °C for PET [8]). Furthermore, polyesters face challenges in durable products due to their physical aging behavior leading to changes in their mechanical properties over time, especially a decrease in impact toughness [9] and an increase in stiffness [10]. Physical aging is a phenomenon occurring in polymers when kept below their T_g for a period of time. When a polymer is cooled rapidly from a molten state to a temperature below its T_g (e.g. during injection moulding), it retains a disordered configuration. Over time, the polymer chains gradually reorganize themselves to a more stable configuration, causing a decrease in internal free volume [11]. During this structural relaxation process the internal energy of the system decreases and enthalpy is lost. This amount of enthalpy lost can be measured with differential scanning calorimetry (DSC) as recoverable enthalpy during the glass transition, providing a method for determination of aging rates [12]. Previous research has shown that the Arrhenius equation (Eq. 1) can describe how the rate of physical aging changes as a function of temperature below T_g, even though physical aging in polymers involves a distribution of relaxation times [13-15]. Using the Arrhenius equation for predicting aging rates can be a useful tool for estimating the long-term behavior of materials in various applications, and for comparing the temperature effects in different polymers. The two equations Eq. 1 and 2, where k is the rate constant, A is the Arrhenius factor, E_a is the activation energy, R is the gas constant, T is the exposed temperature, T_{ref} is a reference temperature and a_T is

the shift factor, provides the possibility to estimate the activation energies from observed changes in properties accelerated by temperature.

(1) $$k = A \exp\left[\frac{E_a}{RT}\right]$$

(2) $$a_T = \exp\left[\frac{E_a}{R}\left(\frac{1}{T_{ref}} - \frac{1}{T}\right)\right]$$

A way to retard a material's physical aging and mitigate the resulting negative effects, is to increase its T_g, which also broadens its range of applications. Thermoplastics composed of aromatic units, such as symmetrical aryl groups, are usually good candidates for high T_g and thermal stability, as these moieties impart molecular rigidity. Rigid and symmetrical aliphatic molecules suitable for polyesters are rare. One molecule belonging to that class is 2,2,4,4-tetramethyl-1,3-cyclobutanediol (TMCD), which has been used in terephthalate copolyesters with other diols such as 1,4-cyclohexanedimethanol (CHDM), 1,3-propanediol and 1,4-butanediol, yielding T_g values ranging from 105-168 °C [16]. In particular, poly(1,4-cyclohexylenedimethylene-co-2,2,4,4-tetramethyl-1,3-cyclobutanediol terephthalate) (PCTT), with its structure illustrated in Figure 1, has gained interest, since it has become commercially available and exhibits not only high T_g but also high impact resistance [13,17,18].

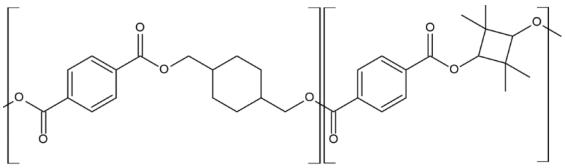

Figure 1. Chemical structure of poly(1,4-cyclohexylenedimethylene-co-2,2,4,4-tetramethyl-1,3-cyclobutanediol terephthalate) (PCTT).

Another sustainable co-monomer, used to increase T_g in polyesters and other plastics, is isosorbide (1,4:3,6-dianhydroxitol) [19], which is made from glucose-derived sorbitol, a naturally occurring sugar [20]. This makes isosorbide polyesters more renewable compared to traditional petroleum based diols. In addition, isosorbide-containing polyesters can exhibit enhanced mechanical properties, such as higher tensile modulus [21], making them suitable for a wide range of applications where durability and strength are essential e.g. toys, automotive components and biomedical devices. However, incorporating isosorbide in significant amounts into polyesters poses challenges due to the unreactive secondary alcohol groups. Most previous work have used catalysts tailored for PET synthesis to

overcome the low reactivity of these alcohols [21-23], whereas recent studies demonstrate the effectiveness of reactive aryl solvents in facilitating the synthesis of certain isosorbide containing polyesters [24,25]. The addition of an aryl alcohol to diol monomers was observed to generate reactive aryl esters during esterification. This occurrence greatly aided the chain growth process during polycondensation, ultimately yielding high molecular weight polyesters (up to M_n = 42.8 kDa for poly(isosorbide succinate) [24]). Further exploration of this method has proven successful in producing aromatic polyesters such as poly(isosorbide-*co*-1,4-cyclohexanedimethanol), PICT, (see Figure 2 for chemical structure) with M_n = 41.9 kDa and polymer composition of ~50.1 % isosorbide (mol%) [14]. For the current study, we made use of this synthesis strategy to produce polyesters with a high isosorbide content, previously described by Bottega Pergher *et al.* [25], in order to characterize their long-term behaviour.

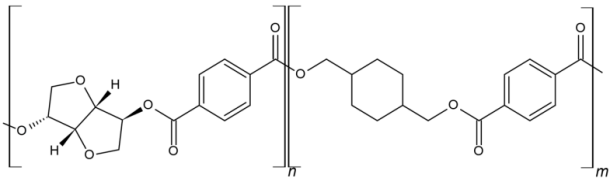

Figure 2. Chemical structure of poly(isosorbide-*co*-1,4-cyclohexanedimethanol terephthalate) (PICT).

In this work we aim to enhance the understanding of the physical aging behaviour in polyesters with high isosorbide content. To simulate long-term changes, we subject the polyesters to thermal treatment at temperatures below their T_g's, effectively accelerating the physical aging process. The aging kinetics are evaluated in three polyesters, each containing a different diol in combination with isosorbide and compared to the commodity polyester PET and state-of-the-art high-T_g-polyester PCTT. DSC studies are applied to quantify enthalpy relaxation, while changes in yield- and tensile strength are tracked through tensile testing. These properties are evaluated to investigate whether they exhibit similar time and temperature dependencies, thereby exploring the existence of a simple relationship between them. The Arrhenius equation is used to determine the activation energies for recoverable enthalpy and tensile strength. Furthermore, the effect of aging on stress relaxation is evaluated, to explore the polyesters long term viscoelastic behavior. Ultimately, this work aims to investigate how chemical structure of different diols alters physical aging and whether T_g alone serves as a reliable predictor for physical aging rate in polyesters.

2. **Materials and methods**

2.1 *Materials*

Granulates of poly(ethylene terephthalate) (PET) and poly(1,4-cyclohexylenedimethylene-co-2,2,4,4-tetramethyl-1,3-cyclobutanediol terephthalate) (PCTT) where purchased from (PQB7-080, PolyQuest) and (TX1001, Eastman, USA), respectively. The PCTT used has ~77 mol % CHDM and ~23 mol % TMCD in relation to total diols, analyzed by proton NMR [13].

The following materials were used to synthesize the other studied polyesters. Isosorbide (≥ 99.9%) was obtained from Roquette Frères. Terephthalic acid (TPA, > 99%), 1,4-butanediol (>99%) and the reactive solvent p-methyl phenol (cresol, > 99%) were purchased from Acros Organics. 1,4-Cyclohexanedimethanol was purchased from TCI, with ~70% of trans isomer. Finally, diethylene glycol (99%) and dimethyl terephthalate (≥99%) were purchased from Sigma Aldrich. The catalysts titanium(IV) butoxide (97%) and butyltin hydroxide oxide hydrate (97%) were purchased from Sigma Aldrich.

2.2 *Synthesis of aromatic polyesters with isosorbide*

The terephthalate polyesters were synthesized with the use of reactive phenolic solvents, as described previously by Bottega Pergher *et al.* [25] and Weinland *et al.* [24]. One example is listed below, while the other polyesters were synthesized analogously. More details can be found in a previous work by Bottega Pergher *et al.* [26].

All components for the synthesis of poly(isosorbide butanediol terephthalate), PIBT, were weighed and added from the beginning to a 100-ml 3-neck round bottom flask: 26.00 g of terephthalic acid (0.134 mol, 1.0 equivalent), 10.66 g of isosorbide (0.073 mol, 0.55 eq.) and 6.58 g of 1,4-butanediol (0.073 mol, 0.55 eq.), 22.6 mg of titanium(IV)butoxide (0.05 mol % vs TPA) and 14.3 g of p-cresol (0.133 mol, 1.0 eq.).

After the ingredients were added to the round bottom flask, the vessel was placed in an oil bath and the system was exposed to a nitrogen flow of ~40 mL/min while heating at 230 °C (oil bath temperature). Once the components were melted, the mixture was mechanically stirred at 100 rpm. This first step, referred to as (trans)esterification, was performed for 15-17 hours. Immediately afterwards, the nitrogen flow was halted and vacuum was applied to the system, gradually decreasing from 500 mbar to <1 mbar within ~1.7 to 2 hours. Once the mixture displayed higher viscosity, due to an increase in molecular

weight and the removal of the reactive solvent cresol, the temperature was raised to 280 °C. Once full vacuum was applied, with pressures below 1 mbar, the system was then kept for 3.0-3.5 hours at 280 °C. The polymer was subsequently removed from the reaction flask under nitrogen flow.

2.3 *Nuclear magnetic resonance spectroscopy*

The analysis of the structural composition of the copolyesters was performed via nuclear magnetic resonance spectroscopy (^{1}H-NMR), using a Bruker AMX 400 (400 MHz), with chloroform-d as a solvent. The molar proportions are displayed in relation to the integration of the diacid peak. Detailed spectra of all synthesized material are found in Figure S1-3.

2.4 *Gel Permeation Chromatography*

The molecular weights of the polyesters were determined by gel permeation chromatography (GPC), in a column from Agilent, under the specifications Poroshell 120 EC-C18, 4.6 x 100 mm, 2.7 µm. Dichloromethane was utilized as an eluent at 35 °C, and the analysis was made in relation to polystyrene standards, using a refractive index detector 1260 Infinity II.

2.5 *Injection moulding*

Samples of PET and PCTT were injection moulded (Arburg 470E 600-290 Arburg, GER) to tensile bars (1BA, ISO 527-2:2012) under the conditions listed in Table 1.

Table 1. Moulding parameters for tensile bars of PET and PCTT.

	Moisture content [%]	Drying temp. [°C]	Drying time [h]	Processing temp. [°C]	Injection pressure [bar]	Mould temp. [°C]	Cooling time [s]
PET	0.02	155	8	290	796	20	16
PCTT	0.03	85	6	285	936	80	18

Samples of PIBT, PIDT and PICT were injection moulded using a HAAKE MiniJet II, from Thermo Fisher Scientific. The tensile bars were produced according to ISO 527-2, sample type 5A. PIDT and PIBT were molded with the injection temperature of 215-220 °C, while PICT was molded at 260 °C. All samples were injected at 1000 bar, and all materials were dried prior to injection under vacuum at 60 °C for at least 24 hours.

2.6 *Thermal treatment*

Tensile test specimens and DSC samples were aged in the ovens at the temperatures and conditions displayed in Table 2. The temperatures were chosen to be under each specimen's T_g, the highest being close to T_g-20 °C. After their thermal treatment, all samples were stored at room temperature for at least 24 hours before testing.

Table 2. Overview of aging times and temperatures chosen for each material and test type. Displayed T_g values are determined from DSC measurements.

Material	**T_g (°C)**	Aging times (h) = 1, 3, 8, 24, 138, 336, 504		0, 168
		DSC Aging temperatures (°C)	**Tensile test** Aging temperatures (°C)	**Stress relaxation** Aging temperatures (°C)
PET	79	39, 49, 59	39, 49, 59	59
PCTT	108	60, 70, 80, 90	70, 80, 90	88
PICT	140	60, 70, 80, 90, 110, 120	90, 110, 120	120
PIBT	109	60, 70, 80, 90	70, 80, 90	90
PIDT	93	50, 60, 70	50, 60, 70	-

2.7 *Differential scanning calorimetry*

Before and after thermal treatment, 5-10 mg samples were cut from tensile specimens, placed in pans (Tzero hermetic pan 901683.901, TA Instruments, USA) covered with lids (Tzero hermetic lid 901683.901, TA Instruments, USA) and measured in a DSC (Q2000, TA Instruments, USA) using a nitrogen flow (50 mL/min). All samples were tested in triplicates and swept twice from 20 to 300 °C at

10 °C/min with cooling to 20 °C at 10 °C/min in-between. T_g was determined from the midpoint between the extrapolated heat flow baselines. The recoverable enthalpy ($\Delta H(T_g)$) after aging, was determined from an endotherm peak around the T_g, as the integrated area, calculated with the TRIOS software (TA Instruments) with linear baselines (an example can be found in Figure S4).

2.8 *Tensile test*

Tensile specimens were tested in a universal testing machine (Z005, ZwickRoall, GER) with a 25 mm gauge length extensometer (180102/2008, ZwickRoell, GER) controlled by testXpert II (Zwick, GER) fixed with the inlet in the lower pneumatic grip. Elastic (tensile) modulus was evaluated at a speed of 1 mm/min, while yield- and tensile strength were evaluated at 100 mm/min, both at 23 ± 2 °C. The elastic modulus was measured within the strain range of 0.05% to 0.25%. The tensile strength was measured according to ASTM D638-03, as well as the (offset) yield strength, using an offset of 0.2%.

2.9 *Stress relaxation*

Tensile stress relaxation tests were performed on tensile test specimens in a Kappa Multistation (ZwickRoall, GER) equipped with a non-contact strain measuring tool (videoXtens) controlled and monitored by testXpert III (ZwickRoall, GER). Relaxation tests were performed at 30 ± 3 ºC with loading speed of 1 mm/min. All samples were strained at ϵ = 1.5 % for 24 hours.

3. **Results and discussion**

3.1 *Structural analysis*

The synthesis method using reactive solvents allows for the production of polyesters with high isosorbide contents and relatively high molecular weights, as described previously by Bottega Pergher *et al.* [25,26] and Weinland *et al.* [24]. Our work builds upon that method to investigate the long-term performance of some of the high T_g materials of PICT, PIBT and PIDT recently studied by Bottega Pergher *et al*. [26]. The aim was to obtain these polyesters with a composition of 50 mol% (out of the total diol content) for each diol resulting in 50 mol% isosorbide and 50 mol% co-diol 1, 2 or 3 as illustrated in Figure 3. Table 3 presents some of the main characteristics of these synthesized polyesters.

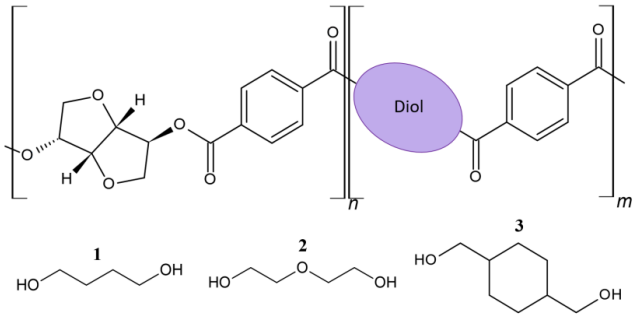

Figure 3. Chemical structure of isosorbide containing polyesters with three different diols: 1,4-butanediol (1), diethylene glycol (2) and 1,4-cyclohexanedimethanol (3), yielding the polyesters PIBT, PIDT and PICT, respectively.

Table 3. Overview of average isosorbide content, M_n, T_g and synthesis details for PICT, PIBT and PIDT.

Polyester	(Average) isosorbide content [st. dev.] by NMR, (mol %)	M_n (range) by GPC [st. dev.] {dispersity, *Đ*}, (kg/mol)	T_g (average) [st. dev.], (°C)	Synthesis details	feed IS/co-diol vs TPA, (mol %)
PICT - Poly(isosorbide-co-1,4-cyclohexanedimethanol terephthalate)	50.1	20.0 {2.0}	139.7	Single batch from 2 l autoclave	53/50
PIBT - Poly(isosorbide-co-butanediol terephthalate)	51.9 [0.5]	19.6 [1.1] {2.1 [0.1]}	109.1 [0.8]	5 batches from 100-ml reactors (mixed)	55/55
PIDT - Poly(isosorbide-co-diethylene glycol terephthalate)	49.7 [0.4]	21.1 [1.4] {2.2 [0.1]}	92.7 [0.9]	5 batches from 100-ml reactors (mixed)	53/50

The synthesized polyesters were found to have isosorbide content ranging from 49.7 to 51.9 mol%, indicating a minor difference in isosorbide/co-diol ratio which is deemed insignificant in relation to altering the studied properties. Furthermore, the similar molecular weights (M_n 19.6-21.1 kg/mol) could indicate that this is not a relevant factor differentiating the studied polyesters. It is therefore believed

that differences between the three synthesized polyesters are attributed primarily to the structure of the co-diol – CHDM, 1,4-butanediol or diethylene glycol.

The PCTT used in this study contains 78 mol% CHDM, 22 mol% TMCD and has a M_n of 13.4 kg/mol [13], which is significantly lower than those containing isosorbide and might be partly responsible for the lower T_g of PCTT (108 °C) compared to PICT (140 °C). PET contains ethylene glycol as the only diol, has a M_n of 17.2 kg/mol and the lowest T_g among the tested polyesters (79 °C). Among the isosorbide containing polyesters, the T_g's vary from 94 to 140 °C depending on the second diol. Diethylene glycol yields the lowest T_g, while 1,4-butanediol gives a T_g approximately 10 °C higher. Both diethylene glycol and 1,4-butanediol introduce flexibility due to the free rotation on the C-O and C-C bonds, where the ether bond in diethylene glycol gives it more mobility when heated. PIDT, however, has an apparently more effective packing at room temperature due to the polarity of the oxygen, which translates into higher elastic modulus and lower impact strength if compared to PIBT. The highest T_g is found in PICT containing the bulky diol CHDM which not only prevents close fitting of the polymer chains but also reduces the chain mobility.

Overall, the factor expected to affect the aging of the polyesters the most, is the T_g, which varies considerably according to the different compositions. Furthermore, in terms of real life applications, lower T_g's, like the one of PET, will not allow for certain procedures such as hot washing or exposure to mildly high temperatures (e.g. ~60 °C) without significant aging, which is a limitation in terms of usage. For a more comprehensive understanding of such materials, the aging results obtained in this paper should be analyzed in combination with the mechanical and thermal properties of such materials, present in a previous publication by Bottega Pergher *et al.* [26].

3.2 *Enthalpy relaxation*

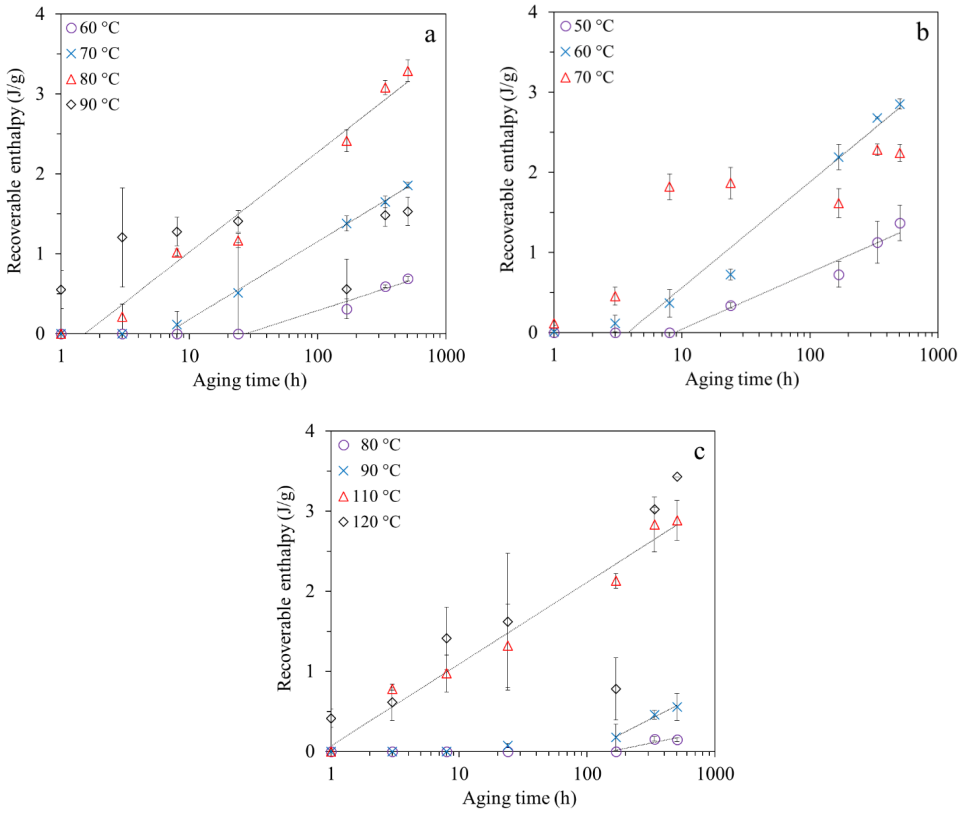

Figure 4. Recoverable enthalpy $\Delta H(T_g)$ calculated from DSC traces of PIBT (a), PIDT (b), and PICT (c) with T_g values of 108, 94 and 140 °C, respectively.

The recoverable enthalpy from PIBT (a), PIDT (b) and PICT (c) is illustrated in Figure 4 as function of aging time. Samples were thermally aged at different temperatures below their respective T_g's as indicated in the figure. For PICT, the results from aging at 60 and 70 °C have been left out, since no enthalpic overshoot was observed in the tested timespan. The enthalpy increases linearly with the logarithm of aging time as expected for amorphous polymers. Furthermore, a temperature-dependent rate increase is observed with exception of PIBT aged at 90 °C. At this temperature the enthalpy changes rapidly in the first three hours but then remains roughly constant. This can possibly be explained by the proximity of the aging temperature to T_g of PIBT (T_g = 109 °C), where the difference between the two is 19 °C. When the temperature approaches T_g from below, the kinetic energy of the polymer chains increases, leading to higher molecular mobility. As the aging temperature gets close to T_g, the polymer

chains become highly mobile, and the material starts to approach the rubbery state. In this rubbery state, the chains are already quite mobile, and the opportunity for further significant chain reorganization decreases. As a result, the aging rate decreases and eventually reaches a minimum value. Previous studies of amorphous polymers, including glycol modified PET, have demonstrated thermal aging at T_g-20 °C without reaching a decrease in aging rate [13,27]. This could suggest that the distance from the T_g to the temperature with the maximum aging rate depends on the chemical structure. For PICT, the rate of aging at 120 °C (correspond to T_g-20 °C) is very similar to that at 110 °C, suggesting that the maximum rate is achieved between or close to these two temperatures.

Figure 5 shows a comparison of recoverable enthalpy in the isosorbide containing polyesters along with PET and PCTT aged at 60 and 70 °C. PET, having the lowest T_g, also exhibit the highest amount of recoverable enthalpy at 60 °C and hence the highest physical aging rate at this temperature. However, at 70 °C, PET shows recoverable enthalpy in the range 0.17-0.55 J/g with no increase as a function of aging time. This behavior suggests that the aging temperature is too close to the T_g of PET, and might approach a temperature range in which the polymer chains are not packing more closely together as during aging, but instead are moving more freely and disorderly in a similar manner as when the polymer is melting. Apart from PET, the other polyesters follow the same order of aging rates at 60 and 70 °C (PIDT > PIBT > PCTT > PICT).

Although, PCTT and PIBT both have T_g of 108-9 °C, it is evident from Figure 5, that more enthalpy is recoverable from PIBT than from PCTT aged at both 60 and 70 °C, suggesting that physical aging occurs faster in PIBT. This observation implies that the T_g of a polyester is not the only factor that determines the physical aging rate, and other aspects such as chemical structure also have an influence. The structure of 1,4-butanediol is likely more capable of packing closely than the other diols CHDM and TMCBD, due to its less bulky and more linear aspect. This can also be deduced from analyzing PICT's mechanical properties versus those of PIBT [26], which shows that CHDM (PICT) performs much better in terms of impact strength but with a lower value of elastic modulus.

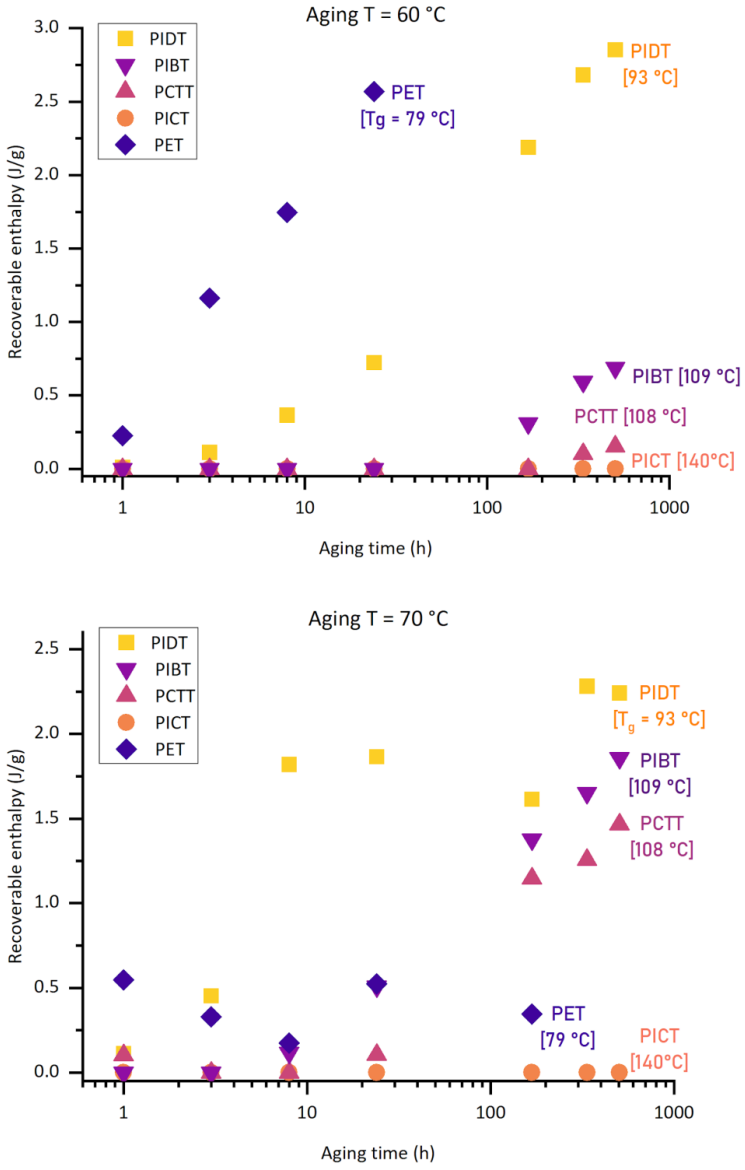

Figure 5. Comparison of recoverable enthalpy in PET and PCTT aged at 60 (top) and 70 °C (bottom). T_g's are displayed in square brackets for each material.

PICT shows no change in recoverable enthalpy at 60-70 °C during the tested timespan. These two aging temperatures are 50-60 °C below the T_g of PICT and thus more energy is needed to cause rearrangements of the polymer segments in this polyester. The Arrhenius activation energies (E_a),

displayed in Table 4, range from 162-202 kJ/mol, which correspond well with previous findings in polyesters [13,28]. PICT has the lowest E_a, indicating that temperature has lower effect on the enthalpy relaxation in this polyester compared to the others.

Table 4. Arrhenius activation energies, E_a, achieved from horizontal shift of recoverable enthalpy as function of aging time and fitting the shift factors as function of temperature. See Figure S5-9 for plots.

Polyester	E_a (kJ/mol)
PICT	161.8
PIBT	170.1
PIDT	175.6
PCTT	198.3
PET	202.3

3.3 *Tensile strength*

The yield strength of amorphous polymers is known to increase due to physical aging [13,17,27,29], owing to stronger intermolecular interactions in the polymer network caused by the redistribution of free volume [30]. While an increase in yield strength is also observed in this study (see Table S1), a much clearer trend was found between tensile strength and aging time for the isosorbide-containing polyesters, as shown in Figure 6. This could be linked to the semi-brittle nature of the polyesters in this study, causing continuous shear yielding until break [31,32]. Consequently, the difference between yield strength and tensile strength observed here is larger and less consistent compared to other studies of more ductile polyesters [13,27]. Tensile strength in both PIBT, PICT, PCTT and PET increases logarithmically with aging time. Furthermore, an acceleration caused by temperature is observed as a shift towards higher tensile strength with increased aging temperature in all polyesters. However, for PIBT aged at 80 °C, a larger increase in tensile strength is observed, than aging at 90 °C. This effect is similar to that seen for recoverable enthalpy in PIBT, where 90 °C is too close to its T_g to achieve the maximum aging rate and hence the aging rate decreases compared to slightly lower temperatures. Similarly, aging of PCTT at 80 and 90 °C results in indistinguishable aging rates. For PICT, a more straightforward time and temperature dependence is found, hence the highest aging temperature (120 °C) gives the highest aging rate. PIDT is excluded from Figure 6, since it became brittle after thermal treatment, causing samples to break in tensile tests before reaching a tensile strength (data can be found in Table S1).

Due to the abovementioned complications with results from PIBT (no clear time-temperature relationship) and PIDT (embrittlement) it has only been possible to obtain Arrhenius activation energies

for PICT, PCTT and PET, as displayed in Table 5. Generally, the E_a's for tensile strength are higher than for recoverable enthalpy, suggesting that the aging of tensile strength is more sensitive to aging temperature variations. The largest discrepancy is found for PICT, where E_a for tensile strength is 38 % higher than that for enthalpy. It is also noteworthy, that PICT shows the lowest temperature acceleration of recoverable enthalpy among the tested polyesters, while it shows the highest acceleration of tensile strength. This emphasizes the need to evaluate the aging rate of each property separately. A contradictory relationship between E_a's for yield strength and those for recoverable enthalpy has previously been found in other glycol modified PET grades containing TMCD and/or CHDM [13], where enthalpy relaxation exhibited slightly higher E_a than yield strength in most of the tested polyesters. It should, however, be noted, that the trend in the mentioned study was not unanimous and the standard deviations could suggest an insignificant difference between aging of the two properties.

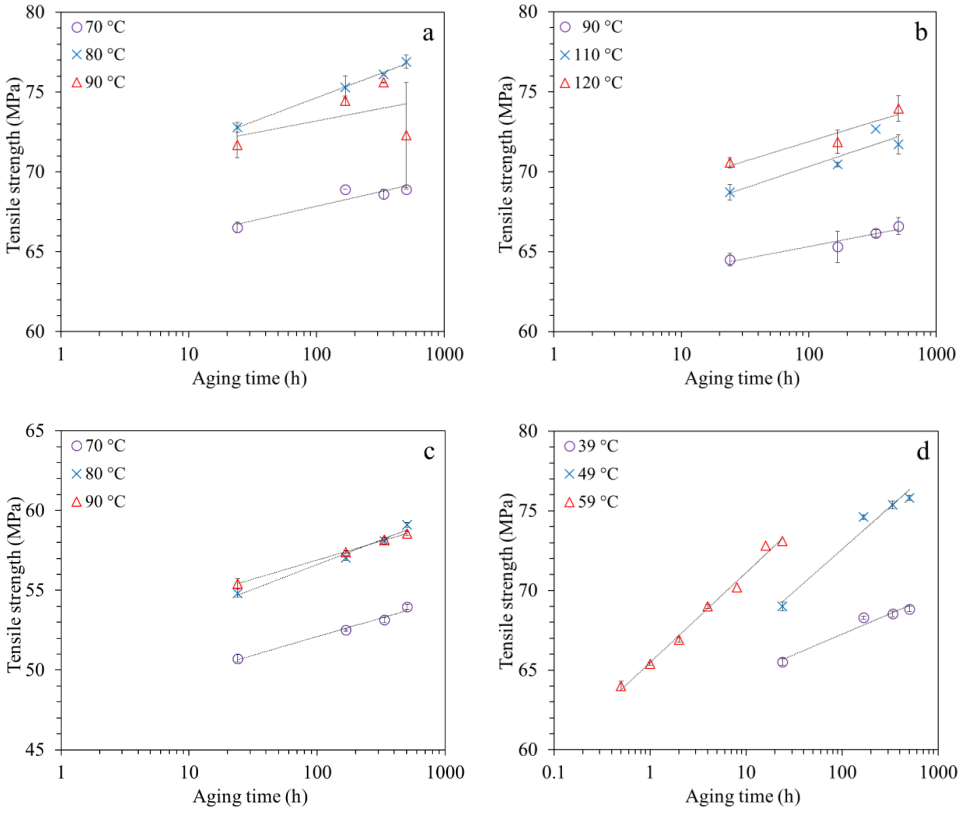

Figure 6. Tensile strength of PIBT (a), PICT (b), PCTT (c) and PET (d) after aging. Measurements of PIDT are left out, as all samples turned brittle after aging and no tensile strength could be determined.

Table 5. Arrhenius activation energies, E_a, achieved from horizontal shift of tensile strength as function of aging time and fitting the shift factors as function of temperature. See Figure S10-12 for plots.

Polyester	E_a (kJ/mol)
PET	225.6
PCTT	244.7
PICT	260.1

3.4 *Stress relaxation*

Stress relaxation tests were performed in order to compare the viscoelastic response of the different polyesters. Figure 7 shows the resulting stress relaxation curves for all unaged polyesters subjected to 1.5 % strain for 24 h. Firstly, the initial stress levels corresponding to 1.5 % strain differs significantly, showing PET as the stiffest polyester among those tested. The initial stress for PET is 37.2 MPa, while the lowest value is 22.8 MPa for PCTT, demonstrating the effect of the flexible CHDM unit on the stiffness, significantly reducing it in PCTT. The initial stress for the isosorbide containing polyesters ranges from 34.8 (for PIDT) to 26.1 MPa (for PICT), again indicating the effect of the CHDM unit on the elastic modulus. PIDT shows higher stiffness than PIBT, implying more effective packing of the chains induced by the polar oxygen atoms.

After the 24 hours of accelerated aging, PIDT reveals the most extreme decrease in stress, followed by PIBT and PET. After 24 h, PIDT also shows the overall lowest stress level of 16.7 MPa, resulting in a stress reduction of 52 %. This could suggest that the close packing induced by the oxygen atom is not capable of withstanding significant strain, leading to higher chain mobility. PIBT, PET and PICT exhibit reductions of 39, 32 and 31 %, respectively, while PCTT performs better showing the smallest stress reduction of 17 %. However, its final stress value is close to those of the isosorbide containing polyester, ranging between 17 and 19 MPa. These observations could indicate that polyesters containing bulky monomers such as CHDM and TMCD are less prone to stress relaxation.

After aging, the stiffness generally increased in the isosorbide containing polyesters (1.1-3.4 MPa increase in initial stress level), while it remained almost unaffected in PET and PCTT. The stress relaxation curves for aged PIBT, PICT, PET and PCTT are presented in Figure 8, in which no cross over points exists between PIBT, PICT and PCTT showing more similar behaviours. After aging, PIDT

became too brittle to strain 1.5 % without breaking, why there is no comparable results for PIDT. Compared to the unaged polyesters, all show reduced stress relaxation after aging. Especially, PIBT and PICT, showing 13 and 6 % stress relaxation after 24 h, leading to improvements (reductions) of 66 and 80 %, respectively. PET showed 19 % stress relaxation, which is highest among the tested polyesters, but still achieving 42 % improvement compared to unaged PET. PCTT show 8 % stress relaxation, which is similar to PICT (6 %), demonstrating that PICT can be elevated to the same level of stress retainment as PCTT after accelerated aging. Low stress relaxation over time is an important feature in terms of maintaining shape stability of materials that are kept under strain, as demanded by some applications.

When comparing the effect of aging on stress relaxation to the recoverable enthalpy, the chosen aging temperature for PIBT might not be optimal. 90 °C seems too close to its T_g (109 °C) to provide the same level of aging as e.g. 80 °C. However, the effect on stress relaxation suggests that significant aging has occurred in PIBT, increasing the strength of its interchain interactions. For PCTT and PICT the aging temperatures are in the same proximity to their T_g's, approximately T_g-20 °C, but the effect on stress relaxation is much more pronounced in PICT than in PCTT, suggesting that other factors could be involved in the effect on stress relaxation.

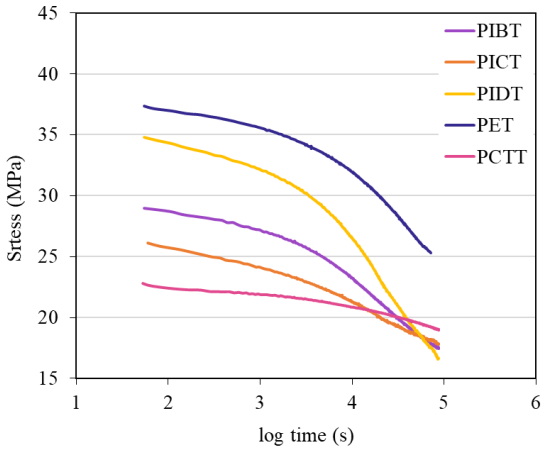

Figure 7. Tensile stress versus relaxation time at ϵ = 1.5 % for 24 hours in unaged PIBT, PICT, PIDT, PET and PCTT.

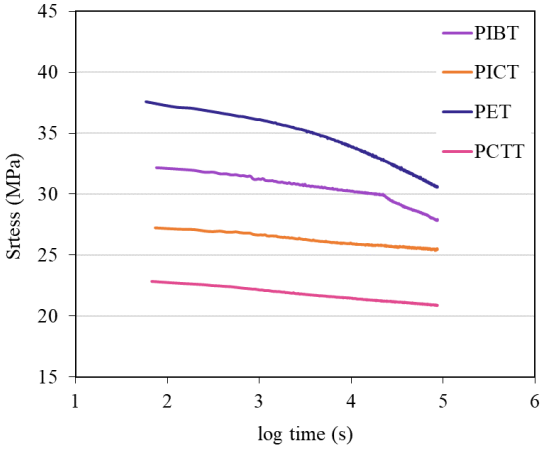

Figure 8. Tensile stress versus relaxation time at ϵ = 1.5 % for 24 hours in unaged PIBT, PICT, PET and PCTT after aging for 168 h at temperatures approximately T_g-20 °C.

Overall, the materials that performed the best in terms of stress relaxation were PCTT and PICT. The observations presented here could suggest that polyesters containing bulky monomers such as CHDM and TMCD undergo less stress relaxation, though PICT had to undergo aging for that to occur, and otherwise performed similarly to PET. Besides the reduction in tensile stress in percentual terms, it is important to evaluate the final values of the stress retained by each polymer. Although PET shows significant stress relaxation, it still maintains higher final values of stress, 25-30 MPa, when compared to PICT and PCTT in both unaged (17-19 MPa) and aged (21-25 MPa) scenarios. These final values of stress should be taken into account when considering specific applications for such materials.

4. **Conclusion**

From analyzing the physical aging in the studied polyesters, it is evident that recoverable enthalpy and tensile strength increase logarithmically in all polyesters when treated below T_g. At temperatures close to T_g ($T > T_g$-20 °C), an overall retarded aging was observed in the recoverable enthalpy of PIBT and PIDT, deviating from the logarithmic trend. In the initial aging interval (up to 3-8 hours) the aging rate was faster near T_g. However, beyond this point, the aging slowed down and was exceeded by lower aging temperatures. The increase in recoverable enthalpy follow Arrhenius behaviour in all tested polyesters with activation energies from 161.8 to 202.3 kJ/mol. The same Arrhenius behaviour was found for increasing tensile strength in PICT, PET and PCTT with activation energies of 225.6-260.1 kJ/mol, suggesting that the increase in tensile strength is generally more sensitive to temperature.

Stress relaxation experiments showed greater resistance to stress reduction in PICT and PCTT compared to the other polyesters, suggesting a retaining effect of CHDM. A significant influence of aging was found in all polyesters reducing the stress relaxation over time. However, the relationship between the effect on stress relaxation and recoverable enthalpy seem complex and need further investigations.

Physical aging, measured as recoverable enthalpy, occurred faster in PIBT than in PCTT at 60 and 70 °C despite both having a T_g of 108-9 °C. This observation implies that T_g alone cannot fully indicate the physical aging rate, but that other factors, such as chemical structure, which are not "included" in T_g also play a significant role. This observation contribute modestly to the understanding of physical aging in polymers, but it remains important in the screening and application of new polyesters.

Acknowledgements

The authors would like to give special thanks to Borbála Kovacs and Klaudia Chruslinska for great help in sample preparation in the laboratory. This research was partly funded by the Innovation Fund Denmark under grant number 0153-00105B and by Netherlands Organisation for Scientific Research (NWO) under grant number 731.017.203 in the framework of the Innovation Fund for Chemistry and from the Ministry of Economic Affairs in the framework of the "TKI/PPS-Toeslagregeling". Finally the authors would like to thank LEGO System A/S and Avantium for co-funding the project.

References

[1] S. Walker and R. Rothman, 'Life cycle assessment of bio-based and fossil-based plastic: A review', *J. Clean. Prod.*, vol. 261, p. 121158, Jul. 2020, doi: 10.1016/j.jclepro.2020.121158.

[2] J. Zheng and S. Suh, 'Strategies to reduce the global carbon footprint of plastics', *Nat. Clim. Change*, vol. 9, no. 5, pp. 374–378, May 2019, doi: 10.1038/s41558-019-0459-z.

[3] S. Spierling, 'Bio-based plastics - A review of environmental, social and economic impact assessments', *J. Clean. Prod.*, 2018.

[4] X. Sun, M. Xie, L. Mai, and E. Y. Zeng, 'Biobased plastic: A plausible solution toward carbon neutrality in plastic industry?', *J. Hazard. Mater.*, vol. 435, p. 129037, Aug. 2022, doi: 10.1016/j.jhazmat.2022.129037.

[5] A. B. Raheem, Z. Z. Noor, A. Hassan, M. K. Abd Hamid, S. A. Samsudin, and A. H. Sabeen, 'Current developments in chemical recycling of post-consumer polyethylene terephthalate wastes

for new materials production: A review', *J. Clean. Prod.*, vol. 225, pp. 1052–1064, Jul. 2019, doi: 10.1016/j.jclepro.2019.04.019.

[6] D. Paszun and T. Spychaj, 'Chemical Recycling of Poly(ethylene terephthalate)'.

[7] P. Huang, J. Pitcher, A. Mushing, F. Lourenço, and M. P. Shaver, 'Chemical recycling of multi-materials from glycol-modified poly(ethylene terephthalate)', *Resour. Conserv. Recycl.*, vol. 190, p. 106854, Mar. 2023, doi: 10.1016/j.resconrec.2022.106854.

[8] N. Doulache, M. W. Khemici, A. Gourari, and M. Bendaoud, 'DSC study of polyethylene terephtalate's physical ageing', in *2010 10th IEEE International Conference on Solid Dielectrics*, Potsdam: IEEE, Jul. 2010, pp. 1–4. doi: 10.1109/ICSD.2010.5568072.

[9] A. J. Hill, K. J. Heater, and C. M. Agrawal, 'The effects of physical aging in polycarbonate', *J. Polym. Sci. Part B Polym. Phys.*, vol. 28, no. 3, pp. 387–405, Feb. 1990, doi: 10.1002/polb.1990.090280310.

[10] L. C. E. Struik, 'Physical Aging in Plastics and Other Glassy Materials', *Polym. Eng. Sci.*, vol. 17, no. 3, pp. 165–173, Mar. 1977, doi: 10.1002/pen.760170305.

[11] A. J. Kovacs, 'Glass transition in amorphous polymers: a phenomenological study', *Adv Polym Sci*, vol. 3, no. 3, pp. 394–507, 1963.

[12] A. Ohara and H. Kodama, 'Correlation between enthalpy relaxation and mechanical response on physical aging of polycarbonate in relation to the effect of molecular weight on ductile-brittle transition', *Polymer*, vol. 181, p. 121720, Oct. 2019, doi: 10.1016/j.polymer.2019.121720.

[13] A. T. Weyhe, E. Andersen, R. Mikkelsen, and D. Yu, 'Accelerated physical aging of four PET copolyesters: Enthalpy relaxation and yield behaviour', *Polymer*, vol. 278, p. 125987, Jun. 2023, doi: 10.1016/j.polymer.2023.125987.

[14] K. T. Gillen, R. Bernstein, and D. K. Derzon, 'Evidence of non-Arrhenius behaviour from laboratory aging and 24-year field aging of polychloroprene rubber materials', *Polym. Degrad. Stab.*, vol. 87, no. 1, pp. 57–67, Jan. 2005, doi: 10.1016/j.polymdegradstab.2004.06.010.

[15] E. Andersen, R. Mikkelsen, S. Kristiansen, and M. Hinge, 'Real-time ageing of polyesters with varying diols', *Mater. Chem. Phys.*, vol. 261, p. 124240, Mar. 2021, doi: 10.1016/j.matchemphys.2021.124240.

[16] D. R. Kelsey, B. M. Scardino, J. S. Grebowicz, and H. H. Chuah, 'High Impact, Amorphous Terephthalate Copolyesters of Rigid 2,2,4,4-Tetramethyl-1,3-cyclobutanediol with Flexible Diols', *Macromolecules*, vol. 33, no. 16, pp. 5810–5818, Aug. 2000, doi: 10.1021/ma000223+.

[17] E. Andersen, R. Mikkelsen, S. Kristiansen, and M. Hinge, 'Accelerated physical ageing of poly(1,4-cyclohexylenedimethylene- *co* -2,2,4,4-tetramethyl-1,3-cyclobutanediol terephthalate)', *RSC Adv.*, vol. 9, no. 25, pp. 14209–14219, 2019, doi: 10.1039/C9RA00925F.

[18] A. V. Cugini and A. J. Lesser, ‘Aspects of physical aging, mechanical rejuvenation, and thermal annealing in a new copolyester’, *Polym. Eng. Sci.*, vol. 55, no. 8, pp. 1941–1950, Aug. 2015, doi: 10.1002/pen.24035.

[19] S. Legrand *et al.*, ‘Isosorbide and Tricyclodecanedimethanol for the Synthesis of Amorphous and High T_g Partially Biobased Copolyesters’, *ACS Sustain. Chem. Eng.*, vol. 8, no. 40, pp. 15199–15208, Oct. 2020, doi: 10.1021/acssuschemeng.0c04679.

[20] C. Dussenne, T. Delaunay, V. Wiatz, H. Wyart, I. Suisse, and M. Sauthier, ‘Synthesis of isosorbide: an overview of challenging reactions’, *Green Chem.*, vol. 19, no. 22, pp. 5332–5344, 2017, doi: 10.1039/C7GC01912B.

[21] D. H. Weinland, R.-J. Van Putten, and G.-J. M. Gruter, ‘Evaluating the commercial application potential of polyesters with 1,4:3,6-dianhydrohexitols (isosorbide, isomannide and isoidide) by reviewing the synthetic challenges in step growth polymerization’, *Eur. Polym. J.*, vol. 164, p. 110964, Feb. 2022, doi: 10.1016/j.eurpolymj.2021.110964.

[22] J. C. Bersot *et al.*, ‘Efficiency Increase of Poly(ethyleneterephthalate-co-isosorbide terephthalate)Synthesis using Bimetallic Catalytic Systems’, *Macromol. Chem. Phys.*, vol. 212, no. 19, pp. 2067–2180, 2011, doi: 10.1002/macp.201100146.

[23] S. Legrand *et al.*, ‘Synthesis and properties of poly(1,4-cyclohexanedimethylene-co-isosorbide terephthalate), a biobased copolyester with high performances’, *Eur. Polym. J.*, vol. 115, pp. 22–29, Jun. 2019, doi: 10.1016/j.eurpolymj.2019.03.018.

[24] D. H. Weinland *et al.*, ‘Overcoming the low reactivity of biobased, secondary diols in polyester synthesis’, *Nat. Commun.*, vol. 13, no. 1, p. 7370, Nov. 2022, doi: 10.1038/s41467-022-34840-2.

[25] B. Bottega Pergher *et al.*, ‘Reactive phenolic solvents applied to the synthesis of renewable aromatic polyesters with high isosorbide content’, *Polym. Chem.*, vol. 14, no. 27, pp. 3225–3238, 2023, doi: 10.1039/D2PY01578A.

[26] B. Bottega Pergher, R.-J. Van Putten, and G.-J. M. Gruter, ‘Renewable aromatic polyesters with high isosorbide content - the search for high impact rigid polyesters with high Tg’, *unpublished*, 2024.

[27] J. M. Hutchinson, S. Smith, B. Horne, and G. M. Gourlay, ‘Physical Aging of Polycarbonate: Enthalpy Relaxation, Creep Response, and Yielding Behavior’, *Macromolecules*, vol. 32, no. 15, pp. 5046–5061, Jul. 1999, doi: 10.1021/ma981391t.

[28] A. T. H. Weyhe, A. D. Drozdov, J. De Claville Christiansen, E. Andersen, and D. Yu, ‘The effect of physical aging on the viscoelastoplastic response of glycol modified poly(ethylene terephthalate)’, *Mater. Today Commun.*, vol. 37, p. 107241, Dec. 2023, doi: 10.1016/j.mtcomm.2023.107241.

[29] V. Ramakrishnan, S. Harsiny, J. G. P. Goossens, T. L. Hoeks, and G. W. M. Peters, 'Physical aging in polycarbonate nanocomposites containing grafted nanosilica particles: A comparison between enthalpy and yield stress evolution', *J. Polym. Sci. Part B Polym. Phys.*, vol. 54, no. 20, pp. 2069–2081, Oct. 2016, doi: 10.1002/polb.24125.

[30] E.-A. McGonigle, J. H. Daly, S. D. Jenkins, J. J. Liggat, and R. A. Pethrick, 'Influence of Physical Aging on the Molecular Motion and Structural Relaxation in Poly(ethylene terephthalate) and Related Polyesters', *Macromolecules*, vol. 33, no. 2, pp. 480–489, Jan. 2000, doi: 10.1021/ma9909197.

[31] R. A. C. Deblieck, D. J. M. Van Beek, K. Remerie, and I. M. Ward, 'Failure mechanisms in polyolefines: The role of crazing, shear yielding and the entanglement network', *Polymer*, vol. 52, no. 14, pp. 2979–2990, Jun. 2011, doi: 10.1016/j.polymer.2011.03.055.

[32] D. G. Legrand, 'Crazing, yielding, and fracture of polymers. I. Ductile brittle transition in polycarbonate', *J. Appl. Polym. Sci.*, vol. 13, no. 10, pp. 2129–2147, Oct. 1969, doi: 10.1002/app.1969.070131010.

Physical Aging of Aromatic Copolyesters with High Isosorbide Content and High Glass Transition Temperatures

Anne Therese Weyhe [a,b], Bruno Bottega Pergher [c,d], Gert-Jan M. Gruter [c,d], Donghong Yu [a,*]

[a] *Department of Chemistry and Bioscience, Aalborg University, Fredrik Bajers Vej 7H, DK-9220 Aalborg East, Denmark*

[b] *LEGO System A/S, Åstvej 1, DK-7190 Billund, Denmark*

[c] *Van't Hoff Institute of Molecular Science, University of Amsterdam, P.O. Box 94720, 1090GS Amsterdam, The Netherlands*

[d] *Avantium Chemicals BV, Zekeringstraat 29, 1014BV Amsterdam, The Netherlands*

Supporting information

1. ^{1}H-NMR spectra

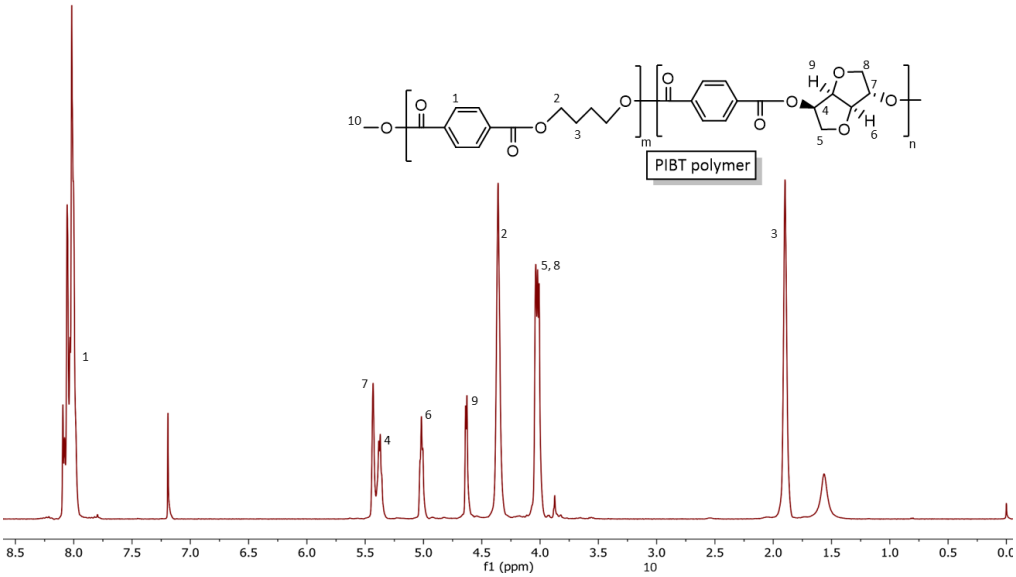

Figure S1. ^{1}H-NMR spectrum of synthesized of poly(isosorbide-*co*-1,4-butanediol terephthalate) (PIBT).

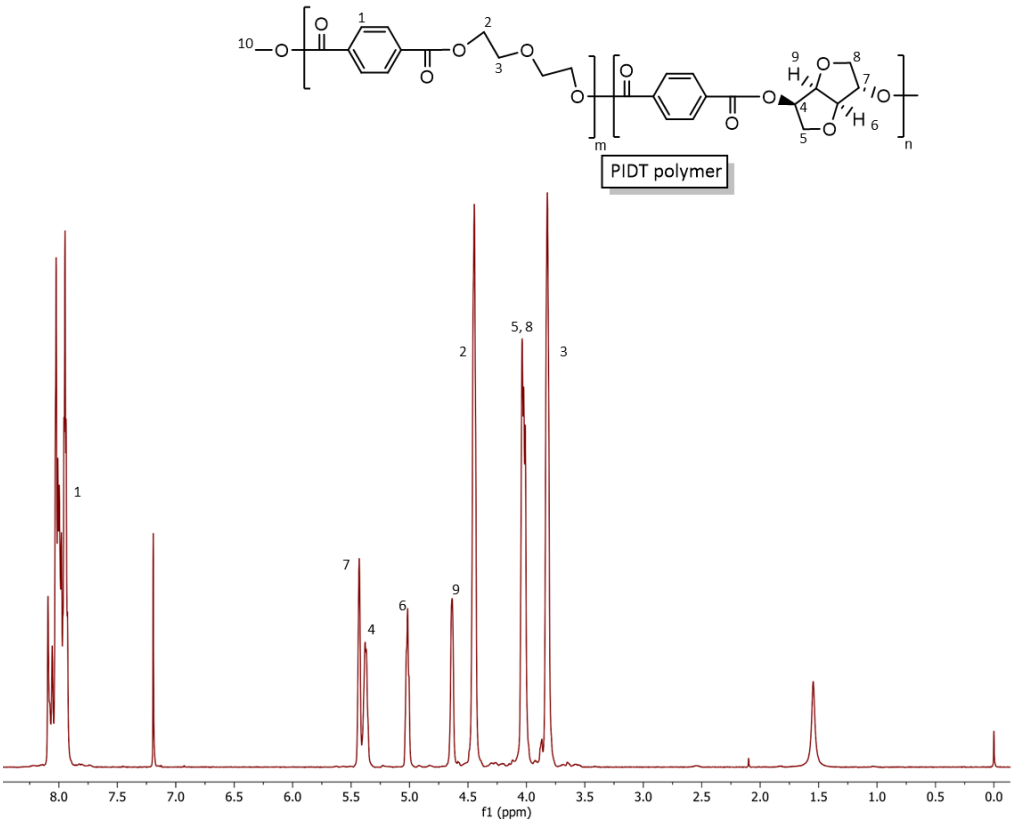

Figure S2. ^{1}H-NMR spectrum of synthesized of poly(isosorbide-*co*-diethylene glycol terephthalate) (PIDT).

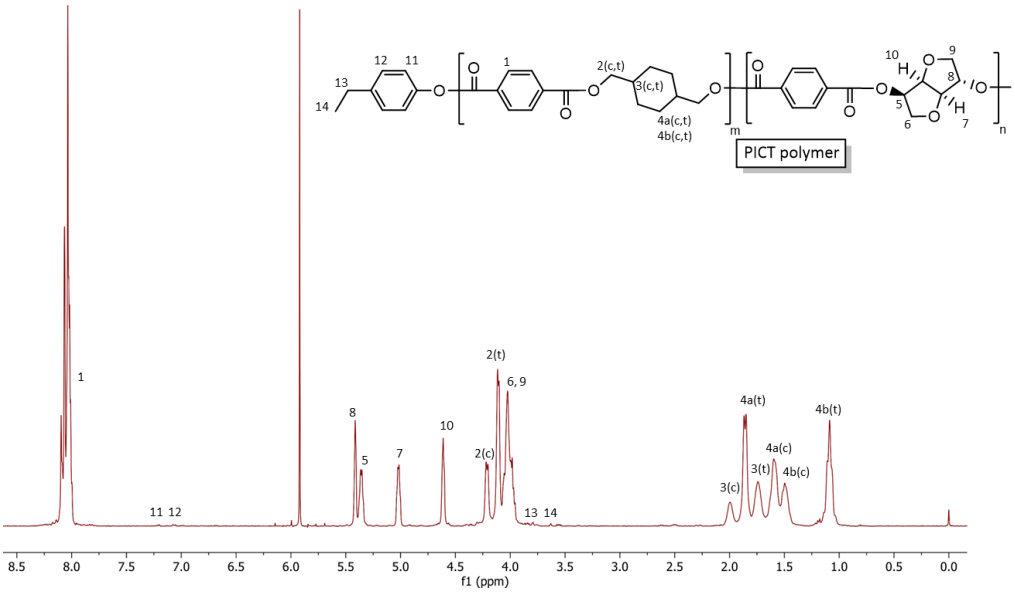

Figure S3. [1]H-NMR spectrum of synthesized of poly(isosorbide-*co*-1,4-cyclohexanedimethanol terephthalate) (PICT).

2. Differential scanning calorimetry

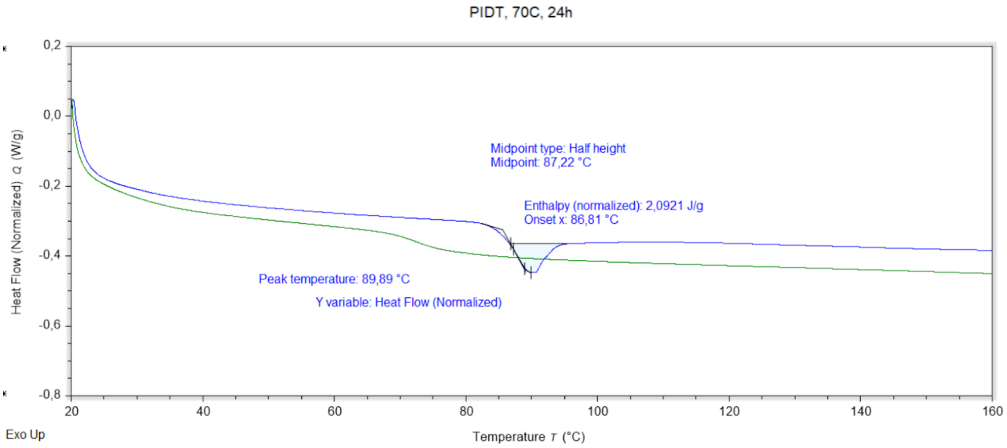

Figure S4. Example of DSC traces of PIDT, aged for 24h at 70 °C. Integration performed with TRIOS software. Normalized by the sample's mass. The integration is made using the first heating cycle at 10 °C/min, by drawing a line which is parallel to the baseline around the region of the T_g. The area between the line and the curve is the recoverable enthalpy in J/g.

3. Tensile tests (aged samples)

Table S1. Data obtained from tensile tests.

Aging time (h)	Avg. yield strength (MPa)	SD	Avg. tensile strength (MPa)	SD	Avg. E-modulus (MPa)	SD
PIBT T_a = 70 °C						
24	26.93	1.4	66.5	0.3	2166.2	32.0
168	42.82	2.8	68.9	-	2200.0	7.4
336	42.19	1.2	68.6	0.3	2157.1	16.1
504	43.58	1.6	68.9	-	2213.9	111.9
PIBT T_a = 80 °C						
24	42.35	0.7	72.8	0.3	2239.6	21.2
168	46.33	0.5	75.3	0.7	2185.5	33.8
336	44.12	1.5	76.1	0.1	2207.6	34.2
504	47.34	5.3	76.9	0.4	2233.5	10.6
PIBT T_a = 90 °C						
24	29.31	3.4	71.7	0.8	2166.4	22.6
168	49.34	3.0	74.5	0.3	2156.0	28.7
336	46.63	1.4	75.6	0.1	2162.1	18.6
504	44.82	0.7	72.3	3.3	2170.3	16.2
PIDT T_a = 60 °C						
24	-	-	-	-	-	-
168	49.77	0.6	Brittle	-	2566.6	72.0
336	51.30	2.0	Brittle	-	2572.0	43.0
504	48.50	-	Brittle	-	2602.0	29.0
PIDT T_a = 70 °C						
24	31.57	2.2	Brittle	-	2551.0	19.6
168	50.00	4.4	Brittle	-	2505.0	5.9
336	50.17	2.6	79.8	-	2506.3	38.0
504	50.40	-	Brittle	-	2511.0	27.0
PIDT T_a = 80 °C						
24	Brittle	-	Brittle	-	Brittle	-
168	Brittle	-	Brittle	-	Brittle	-
336	Brittle	-	Brittle	-	Brittle	-
504	Brittle	-	Brittle	-	Brittle	-
PICT T_a = 90 °C						
24	29.72	2.8	64.5	0.4	1931.7	5.2
168	38.45	4.1	65.3	1.0	1883.3	14.7
336	34.84	0.4	66.2	0.2	1933.7	23.0
504	35.59	0.9	66.6	0.5	1939.2	10.1

PICT T_a = 110 °C						
24	37.3	4.2	68.7	0.5	1961.9	12.0
168	38.0	1.8	70.5	0.1	1980.1	11.4
336	39.7	2.5	72.7	-	1975.6	5.7
504	37.2	2.6	72.0	1.0	1948.9	25.5
PICT T_a = 120 °C						
24	32.8	2.0	70.6	0.3	1937.9	10.6
168	38.7	1.0	71.9	0.7	1955.9	21.6
336	35.6	0.7	-	-	1945.8	35.9
504	39.2	1.4	74.0	0.8	1940.6	7.6
PCTT T_a = 70 °C						
24	31.6	2.0	50.7	0.2	1593.3	17.9
168	39.3	0.5	52.5	0.1	1618.5	9.1
336	40.0	0.9	53.1	0.2	1618.7	12.4
504	41.2	1.3	54.0	0.2	1633.4	11.4
PCTT T_a = 80 °C						
24	40.1	0.5	54.8	0.3	1654.9	18.0
168	42.5	1.6	57.0	0.1	1616.6	10.4
336	42.8	0.7	58.1	0.2	1628.5	5.8
504	42.1	0.4	59.1	0.2	1660.5	7.6
PCTT T_a = 90 °C						
24	34.6	2.6	55.4	0.3	1572.8	8.2
168	42.1	0.5	57.4	0.1	1589.8	5.2
336	42.7	1.4	58.2	0.2	1619.6	9.5
504	43.1	1.5	58.6	0.1	1627.6	7.4
PET T_a = 39 °C						
0.5	-	-	63.7	0.1	2504.5	9.9
1	-	-	64.3	0.3	2518.7	9.7
2	-	-	64.9	0.2	2509.3	6.2
4	-	-	65.2	0.3	2512.3	14.8
8	-	-	65.3	0.1	2520.5	7.9
16	-	-	65.4	0.4	2492.4	4.2
24	-	-	65.5	0.2	2495.8	13.3
168	-	-	68.3	1.2	2515.9	16.5
336	-	-	68.5	0.1	2525.2	9.8
504	-	-	68.8	0.1	2515.7	17.3
PET T_a = 49 °C						
0.5	-	-	63.2	0.3	2218.2	60.6
1	-	-	64.0	0.1	2244.9	43.6
2	-	-	64.4	0.1	2169.2	31.2
4	-	-	64.4	0.4	2135.5	8.9
8	-	-	66.6	0.2	2442.1	8.0
16	-	-	67.9	0.1	2436.9	12.3
24	-	-	69.0	0.5	2432.6	4.1
168	-	-	74.6	0.1	2460.0	6.8
336	-	-	75.4	0.1	2525.3	1.2
504	-	-	75.8	0.1	2531.6	11.4

PET T_a = 49 °C						
0.5	-	-	64.0	0.2	2328.4	19.6
1	-	-	65.4	0.1	2333.7	3.5
2	-	-	66.9	0.3	2343.1	10.8
4	-	-	69.0	0.3	2355.0	8.4
8	-	-	70.2	0.1	2361.0	18.3
16	-	-	72.8	0.2	2399.1	17.4
24	-	-	73.1	0.1	2407.4	15.6

4. Arrhenius fits

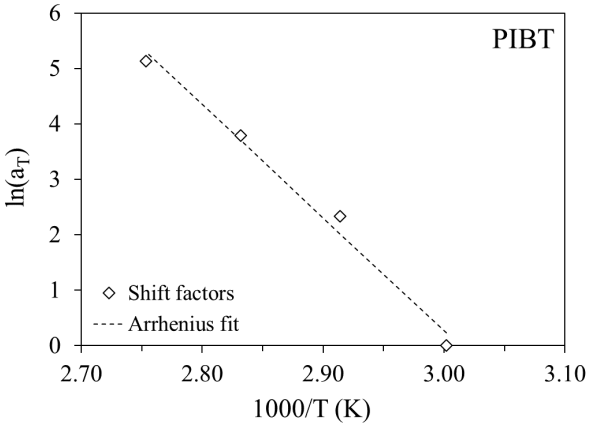

Figure S5. Shift factors versus 1000/T for enthalpy relaxation of poly(isosorbide-*co*-1,4-butanediol terephthalate) (PIBT) obtained from data in Figure 4.

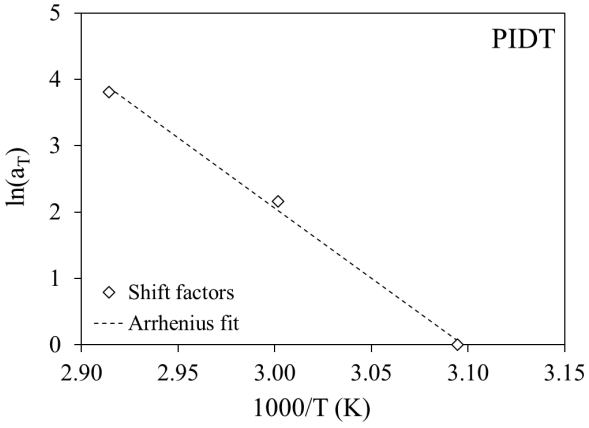

Figure S6. Shift factors versus 1000/T for enthalpy relaxation of poly(isosorbide-*co*-diethylene glycol terephthalate) (PIDT) obtained from data in Figure 4.

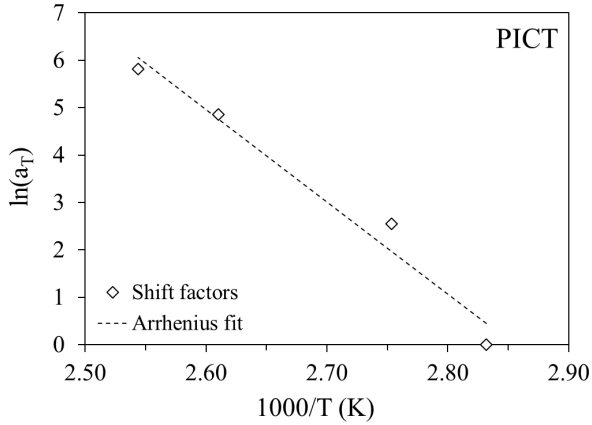

Figure S7. Shift factors versus 1000/T for enthalpy relaxation of poly(isosorbide-*co*-1,4-cyclohexanedimethanol terephthalate) (PICT) obtained from data in Figure 4.

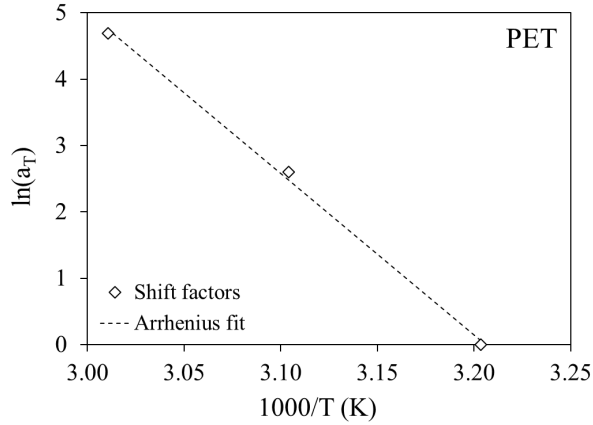

Figure S8. Shift factors versus 1000/T for enthalpy relaxation of poly(ethylene terephthalate) (PET) obtained from data in Table S2.

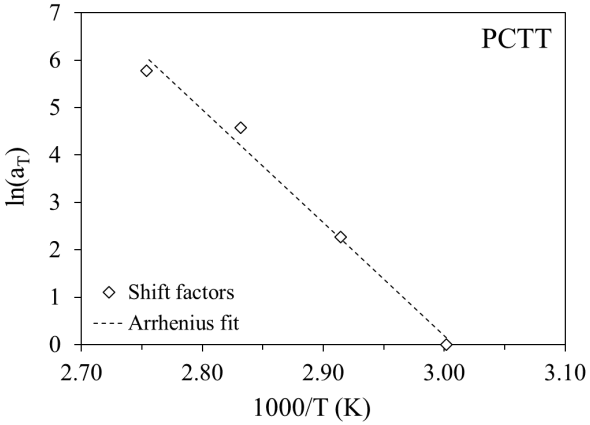

Figure S9. Shift factors versus 1000/T for enthalpy relaxation of poly(1,4-cyclohexylenedimethylene-co-2,2,4,4-tetramethyl-1,3-cyclobutanediol terephthalate) (PCTT) obtained from data in Table S3.

Table S2. Recoverable enthalpy of poly(ethylene terephthalate) (PET) determined according to the method described in Section 2.7 and Figure S4.

Aging time (h)	Avg. recoverable enthalpy (J/g) (T_a = 39 °C)	SD	Avg. recoverable enthalpy (J/g) (T_a = 49 °C)	SD	Avg. recoverable enthalpy (J/g) (T_a = 59 °C)	SD
1	0	0	0	0	0.225	0.13
3	0	0	0.098	0.05	1.161	0.03
8	0	0	0.487	0.03	1.746	0.13
24	0	0	1.037	0.13	2.568	0.15
168	0.418	0.15	2.567	0.12	-	-
336	0.342	0.17	3.668	0.19	-	-
504	0.922	0.19	3.765	0.16	-	-

Table S3. Recoverable enthalpy of poly(1,4-cyclohexylenedimethylene-co-2,2,4,4-tetramethyl-1,3-cyclobutanediol terephthalate) (PCTT) determined according to the method described in Section 2.7 and Figure S4.

Aging time (h)	Avg. recoverable enthalpy (J/g) (T_a = 60 °C)	SD	Avg. recoverable enthalpy (J/g) (T_a = 70 °C)	SD	Avg. recoverable enthalpy (J/g) (T_a = 80 °C)	SD	Avg. recoverable enthalpy (J/g) (T_a = 90 °C)	SD
1	0	0	0.102	0	0	0	0.433	0.16
3	0	0	0	0	0.106	0.12	0.884	0.03
8	0	0	0	0	0.474	0.18	1.139	0.05
24	0	0	0.105	0.02	1.498	0.19	1.994	0.02
168	0	0	1.147	0.17	2.486	0.03	2.925	0.17
336	0.101	0.02	1.257	0.26	2.708	0.02	2.917	0.28
504	0.154	0.01	1.467	0.05	2.907	0.11	2.832	0.05

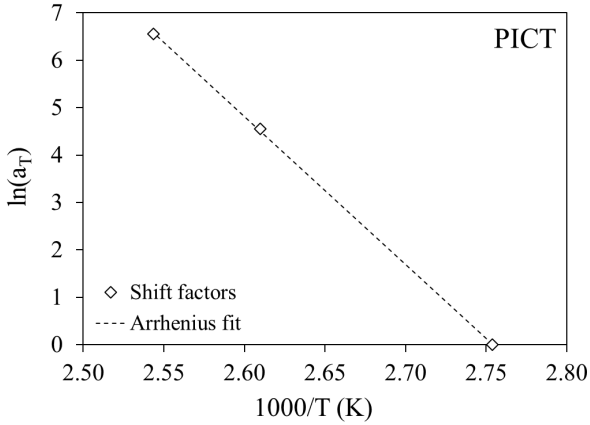

Figure S10. Shift factors versus 1000/T for tensile strength increase of poly(isosorbide-*co*-1,4-cyclohexanedimethanol terephthalate) (PICT) obtained from data in Figure 6.

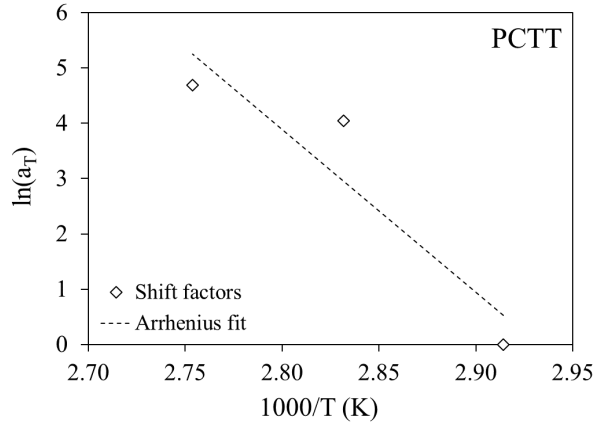

Figure S11. Shift factors versus 1000/T for tensile strength increase of poly(1,4-cyclohexylenedimethylene-co-2,2,4,4-tetramethyl-1,3-cyclobutanediol terephthalate) (PCTT) obtained from data in Figure 6.

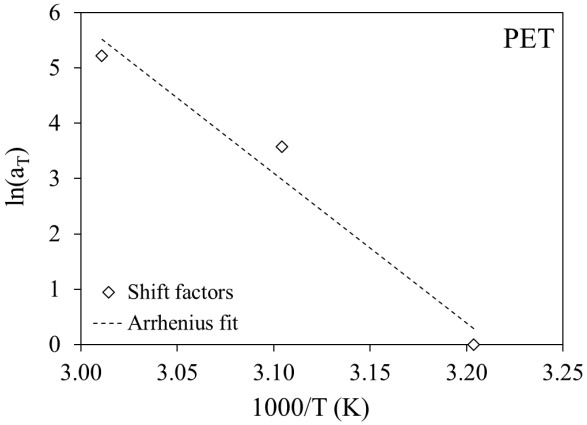

Figure S12. Shift factors versus 1000/T for tensile strength increase of poly(ethylene terephthalate) (PET) obtained from data in Figure 6.

CHAPTER 7. CONCLUSION AND PERSPECTIVES

The title of this thesis is “Physical Aging of Sustainable Polyester Materials towards High-End Consumer Products”. In that context, this thesis provides insights into the behaviours of polyesters as more sustainable alternatives to ABS in durable products such as LEGO bricks. The thesis especially focusses on the phenomenon, physical aging, which is unavoidable in amorphous and semi crystalline polymers, including polyesters.

The current state-of-the-art regarding physical aging of polymers is difficult to translate directly to engineering applications, where thermal history is not as easily controlled as in more ideal modelling systems. Furthermore, engineering plastics often contain different additives, making their behaviour difficult to predict. Knowing how physical aging affects thermodynamic- and mechanical properties plays a vital role in prediction of long term material behaviours in engineering materials. The enthalpy loss, seen as an overshoot near T_g is theoretically linked directly to a decrease in volume, affecting mechanical and viscoelastic properties. However, exactly how one way of observing physical aging, such as enthalpy loss, correlate to another proved to be highly complex. Monomers inducing stiffness to the polymer chains such as the rigid TMCD impede physical aging in some cases (enthalpy loss and yield strength). However, TMCD does not hamper the effect on stress relaxation compared to a flexible diol like CHDM. Furthermore, isosorbide, also being a rigid diol, does not slow down physical aging significantly in copolyesters with 50/50 (mol%) compositions with other diols (CHDM, diethylene glycol and butanediol), measured as enthalpy loss. Generally, this thesis highlights the importance of treating physical aging of each property individually in polyester materials suggesting that each has its own dependence on the structural changes.

Additionally, the effect of chemical structure on physical aging rate cannot be expressed through T_g alone. This is most clear for PCTT and PIBT, both having T_g = 108-9 °C, while aging with different rates at 60 and 70 °C. A similar conclusion can be drawn from looking at aging rates of PETT, PECT and PCTT when aging at the same temperature relative to their respective T_g’s.

The Arrhenius model might not capture the non-linearity associated with the presence of several relaxation times. Nonetheless, it offers a simple application in screening and comparing the effects of aging in different materials, holding high value in an industrial context. From superposition of enthalpy loss and yield strength the VFT model does not provide a better fit than the Arrhenius equation in the tested time and temperature ranges.

In addition, this thesis demonstrates a possible tool for predicting the effect of physical aging on stress relaxation in polyesters. A proposed constitutive model was successful in describing the effects of physical aging on both stress relaxation and creep. Analysis of the model parameters suggests that the concentration of active strands decreases exponentially with annealing time, indicating that molecular clusters are formed during physical aging, rendering the strands immobile when strained. PETT and PECT showed almost identical behaviours at 30 °C, suggesting that the chemical structure of the glycol unit (TMCD and CHDM) does not have significant effects on stress relaxation in the tested compositions.

The study of PET impact modified with E-BA-GMA is a minor contribution to the elucidation of physical aging in polyesters. However, it provides valuable knowledge in relation to improving safety and function simultaneously over time in LEGO bricks of PET and possibly other polyesters. It is evident, that modification with E-BA-GMA up to 8 wt% in PET does not hamper the effect of physical aging on stress relaxation, and thus a more durable function can be achieved through accelerated aging.

The overall findings of this thesis can be summarized into the following: Physical aging rates depend essentially on the observation method. A simple relationship between aging rates in thermodynamic-, mechanical- and viscoelastic properties does not exist, hence one cannot be used to predict another. T_g is a good measure of effective temperature range for physical aging, however, it is not solely determining the aging rates of the mentioned properties. From all studies in this thesis, it is evident, that chemical structure cannot be ignored when evaluating the influence of physical aging on the mentioned variables, why each polyester should be tested using the appropriate observation methods to detect aging.

However, several aspects such as thermal history makes the investigation into the effect of structure highly challenging. In many cases, specimens have to be moulded under slightly different conditions depending on the material and the shape of the specimens. This leads to different T_f's and "starting points" for aging making accurate comparisons difficult. Furthermore, a complex thermal history must be expected, during the real life time of products as LEGO bricks. The effect of this could prove valuable to investigate.

Better understanding of volume relaxation in polyesters would also be valuable. Through the methods used during this thesis, no changes in volume were detected after aging. However, connecting enthalpy and volume relaxation to changes in other properties could further strengthen the understanding of the interplay between them.

Further validation of the models' ability to predict long term effect of aging is also critically important, since no real time data has been collected to compare with accelerated aging.

Finally, in relation to clutch force in LEGO bricks, it is crucial to gain further understanding of the influence of friction and tribology in general. Unfortunately, these subjects are too broad for the scope of this thesis, and thus further studies are needed to map the possibilities of tuning the function over time in LEGO bricks.

LITERATURE LIST

[1] E. Andersen, 'Feasibility of sustainable polyester materials in high-end consumer products', Ph.D. dissertation, Aarhus University, 2020.

[2] T. E. Long and J. Scheirs, *Modern polyesters: chemistry and technology of polyesters and copolyesters*. John Wiley & Sons, 2005.

[3] K. Pang, R. Kotek, and A. Tonelli, 'Review of conventional and novel polymerization processes for polyesters', *Prog. Polym. Sci.*, vol. 31, no. 11, pp. 1009–1037, Nov. 2006, doi: 10.1016/j.progpolymsci.2006.08.008.

[4] F. Awaja and D. Pavel, 'Recycling of PET', *Eur. Polym. J.*, vol. 41, no. 7, pp. 1453–1477, Jul. 2005, doi: 10.1016/j.eurpolymj.2005.02.005.

[5] L. Shen, E. Worrell, and M. K. Patel, 'Open-loop recycling: A LCA case study of PET bottle-to-fibre recycling', *Resour. Conserv. Recycl.*, vol. 55, no. 1, pp. 34–52, Nov. 2010, doi: 10.1016/j.resconrec.2010.06.014.

[6] B. Shojaei, M. Abtahi, and M. Najafi, 'Chemical recycling of PET: A stepping-stone toward sustainability', *Polym. Adv. Technol.*, vol. 31, no. 12, pp. 2912–2938, 2020.

[7] A. Bohre, P. R. Jadhao, K. Tripathi, K. K. Pant, B. Likozar, and B. Saha, 'Chemical Recycling Processes of Waste Polyethylene Terephthalate Using Solid Catalysts', *ChemSusChem*, vol. 16, no. 14, p. e202300142, Jul. 2023, doi: 10.1002/cssc.202300142.

[8] A. B. Raheem, Z. Z. Noor, A. Hassan, M. K. Abd Hamid, S. A. Samsudin, and A. H. Sabeen, 'Current developments in chemical recycling of post-consumer polyethylene terephthalate wastes for new materials production: A review', *J. Clean. Prod.*, vol. 225, pp. 1052–1064, Jul. 2019, doi: 10.1016/j.jclepro.2019.04.019.

[9] X. Fei, J. Wang, J. Zhu, X. Wang, and X. Liu, 'Biobased Poly(ethylene 2,5-furancoate): No Longer an Alternative, but an Irreplaceable Polyester in the Polymer Industry', *ACS Sustain. Chem. Eng.*, vol. 8, no. 23, pp. 8471–8485, Jun. 2020, doi: 10.1021/acssuschemeng.0c01862.

[10] J. Louw, S. Farzad, and J. F. Görgens, 'Polyethylene furanoate: technoeconomic analysis of biobased production', *Biofuels Bioprod. Biorefining*, vol. 17, no. 1, pp. 135–152, Jan. 2023, doi: 10.1002/bbb.2430.

[11] S. Zhao, J. Zhang, X. Wang, L. Wang, J. Wang, and C. Pang, 'Semiaromatic Polyesters from a Rigid Diphenyl-Terephthalic Acid: From Synthesis to Properties', *ACS Appl. Polym. Mater.*, vol. 5, no. 4, pp. 2408–2416, Apr. 2023, doi: 10.1021/acsapm.2c02101.

[12] J. Wang, S. Mahmud, X. Zhang, J. Zhu, Z. Shen, and X. Liu, 'Biobased Amorphous Polyesters with High T_g: Trade-Off between Rigid and Flexible Cyclic Diols', *ACS Sustain. Chem. Eng.*, vol. 7, no. 6, pp. 6401–6411, Mar. 2019, doi: 10.1021/acssuschemeng.9b00285.

[13] S. R. Turner, 'Development of amorphous copolyesters based on 1,4-cyclohexanedimethanol', *J. Polym. Sci. Part Polym. Chem.*, vol. 42, no. 23, pp. 5847–5852, Dec. 2004, doi: 10.1002/pola.20460.

[14] C. J. Kibler, A. Bell, and J. G. Smith, 'Linear polyesters and polyester-amides from 1,4-cyclohexanedimethanol', 2901466, Aug. 25, 1959.

[15] E. Andersen, R. Mikkelsen, S. Kristiansen, and M. Hinge, 'Accelerated physical ageing of poly(1,4-cyclohexylenedimethylene- *co* -2,2,4,4-tetramethyl-1,3-cyclobutanediol terephthalate)', *RSC Adv.*, vol. 9, no. 25, pp. 14209–14219, 2019, doi: 10.1039/C9RA00925F.

[16] X.-G. Li *et al.*, 'Cleaner synthesis and systematical characterization of sustainable poly(isosorbide-co-ethylene terephthalate) by environ-benign and highly active catalysts', *J. Clean. Prod.*, vol. 206, pp. 483–497, Jan. 2019, doi: 10.1016/j.jclepro.2018.09.046.

[17] D. H. Weinland, R.-J. Van Putten, and G.-J. M. Gruter, 'Evaluating the commercial application potential of polyesters with 1,4:3,6-dianhydrohexitols (isosorbide, isomannide and isoidide) by reviewing the synthetic challenges in step growth polymerization', *Eur. Polym. J.*, vol. 164, p. 110964, Feb. 2022, doi: 10.1016/j.eurpolymj.2021.110964.

[18] B. Bottega Pergher, R.-J. Van Putten, and G.-J. M. Gruter, 'Renewable aromatic polyesters with high isosorbide content - the search for high impact rigid polyesters with high Tg', *unpublished*, 2024.

[19] S. Legrand *et al.*, 'Isosorbide and Tricyclodecanedimethanol for the Synthesis of Amorphous and High T_g Partially Biobased Copolyesters', *ACS Sustain. Chem. Eng.*, vol. 8, no. 40, pp. 15199–15208, Oct. 2020, doi: 10.1021/acssuschemeng.0c04679.

[20] S. Legrand *et al.*, 'Synthesis and properties of poly(1,4-cyclohexanedimethylene-co-isosorbide terephthalate), a biobased copolyester with high performances',

Eur. Polym. J., vol. 115, pp. 22–29, Jun. 2019, doi: 10.1016/j.eurpolymj.2019.03.018.

[21] Y. Wang, J. Wu, C. E. Koning, and H. Wang, 'Short-process synthetic strategies of sustainable isohexide-based polyesters towards higher molecular weight and commercial applicability', *Green Chem.*, vol. 24, no. 22, pp. 8637–8670, 2022, doi: 10.1039/D2GC02608B.

[22] A. T. Weyhe, E. Andersen, R. Mikkelsen, and D. Yu, 'Accelerated physical aging of four PET copolyesters: Enthalpy relaxation and yield behaviour', *Polymer*, vol. 278, p. 125987, Jun. 2023, doi: 10.1016/j.polymer.2023.125987.

[23] E. Andersen, R. Mikkelsen, S. Kristiansen, and M. Hinge, 'Real-time ageing of polyesters with varying diols', *Mater. Chem. Phys.*, vol. 261, p. 124240, Mar. 2021, doi: 10.1016/j.matchemphys.2021.124240.

[24] M. Monti, M. Scrivani, I. Kociolek, Å. Larsen, K. Olafsen, and V. Lambertini, 'Enhanced Impact Strength of Recycled PET/Glass Fiber Composites', *Polymers*, vol. 13, no. 9, p. 1471, May 2021, doi: 10.3390/polym13091471.

[25] H. Xie, L. Wu, B.-G. Li, and P. Dubois, 'Modification of Poly(ethylene 2,5-furandicarboxylate) with Biobased 1,5-Pentanediol: Significantly Toughened Copolyesters Retaining High Tensile Strength and O_2 Barrier Property', *Biomacromolecules*, vol. 20, no. 1, pp. 353–364, Jan. 2019, doi: 10.1021/acs.biomac.8b01495.

[26] L. P. Chen, A. F. Yee, J. M. Goetz, and J. Schaefer, 'Molecular Structure Effects on the Secondary Relaxation and Impact Strength of a Series of Polyester Copolymer Glasses', *Macromolecules*, vol. 31, no. 16, pp. 5371–5382, Aug. 1998, doi: 10.1021/ma971671t.

[27] T. Sang, C. J. Wallis, G. Hill, and G. J. P. Britovsek, 'Polyethylene terephthalate degradation under natural and accelerated weathering conditions', *Eur. Polym. J.*, vol. 136, p. 109873, Aug. 2020, doi: 10.1016/j.eurpolymj.2020.109873.

[28] P. Pan, B. Zhu, and Y. Inoue, 'Enthalpy Relaxation and Embrittlement of Poly(L-lactide) during Physical Aging', *Macromolecules*, vol. 40, no. 26, pp. 9664–9671, Dec. 2007, doi: 10.1021/ma071737c.

[29] G. M. Odegard and A. Bandyopadhyay, 'Physical aging of epoxy polymers and their composites', *J. Polym. Sci. Part B Polym. Phys.*, vol. 49, no. 24, pp. 1695–1716, Dec. 2011, doi: 10.1002/polb.22384.

[30] C. H. Ho and T. Vu-Khanh, ‘Effects of time and temperature on physical aging of polycarbonate’, *Theor. Appl. Fract. Mech.*, vol. 39, no. 2, pp. 107–116, Mar. 2003, doi: 10.1016/S0167-8442(02)00151-9.

[31] R. Mikkelsen and E. Andersen, ‘Toy building elements made of a polymeric PET material’, WO/2019/106124, Jun. 06, 2019.

[32] C. A. Angell, ‘Formation of Glasses from Liquids and Biopolymers’, *Science*, vol. 267, no. 5206, pp. 1924–1935, Mar. 1995, doi: 10.1126/science.267.5206.1924.

[33] L. C. E. Struik, ‘Physical Aging in Plastics and Other Glassy Materials’, *Polym. Eng. Sci.*, vol. 17, no. 3, pp. 165–173, Mar. 1977, doi: 10.1002/pen.760170305.

[34] M. L. Williams, R. F. Landel, and J. D. Ferry, ‘The Temperature Dependence of Relaxation Mechanisms in Amorphous Polymers and Other Glass-forming Liquids’, *J. Am. Chem. Soc.*, vol. 77, no. 14, pp. 3701–3707, Jul. 1955, doi: 10.1021/ja01619a008.

[35] E.-A. McGonigle, J. H. Daly, S. D. Jenkins, J. J. Liggat, and R. A. Pethrick, ‘Influence of Physical Aging on the Molecular Motion and Structural Relaxation in Poly(ethylene terephthalate) and Related Polyesters’, *Macromolecules*, vol. 33, no. 2, pp. 480–489, Jan. 2000, doi: 10.1021/ma9909197.

[36] A. T. H. Weyhe, A. D. Drozdov, J. De Claville Christiansen, E. Andersen, and D. Yu, ‘The effect of physical aging on the viscoelastoplastic response of glycol modified poly(ethylene terephthalate)’, *Mater. Today Commun.*, vol. 37, p. 107241, Dec. 2023, doi: 10.1016/j.mtcomm.2023.107241.

[37] L. Andreozzi, M. Faetti, M. Giordano, and D. Palazzuoli, ‘Enthalpy relaxation of low molecular weight PMMA: a strategy to evaluate the Tool Narayanaswamy Moynihan model parameters’, *J. Phys. Condens. Matter*, vol. 15, no. 11, pp. S1215–S1226, Mar. 2003, doi: 10.1088/0953-8984/15/11/339.

[38] N. M. Alves, J. L. Gómez Ribelles, and J. F. Mano, ‘Enthalpy relaxation studies in polymethyl methacrylate networks with different crosslinking degrees’, *Polymer*, vol. 46, no. 2, pp. 491–504, Jan. 2005, doi: 10.1016/j.polymer.2004.11.016.

[39] K. Sasaki, M. Takatsuka, R. Kita, N. Shinyashiki, and S. Yagihara, ‘Enthalpy and Dielectric Relaxation of Poly(vinyl methyl ether)’, *Macromolecules*, vol. 51, no. 15, pp. 5806–5811, Aug. 2018, doi: 10.1021/acs.macromol.8b00780.

[40] R. Greiner and F. R. Schwarzl, 'Volume relaxation and physical aging of amorphous polymers I. Theory of volume relaxation after single temperature jumps', *Colloid Polym. Sci.*, vol. 267, no. 1, pp. 39–47, Jan. 1989, doi: 10.1007/BF01410147.

[41] S. L. Simon, J. W. Sobieski, and D. J. Plazek, 'Volume and enthalpy recovery of polystyrene', *Polymer*, vol. 42, no. 6, pp. 2555–2567, Mar. 2001, doi: 10.1016/S0032-3861(00)00623-6.

[42] C. G. Robertson and G. L. Wilkes, 'Refractive index: A probe for monitoring volume relaxation during physical aging of glassy polymers', *Polymer*, vol. 39, no. 11, pp. 2129–2133, Jan. 1998, doi: 10.1016/S0032-3861(97)00508-9.

[43] N. Tanio and T. Nakanishi, 'Physical Aging and Refractive Index of Poly(methyl methacrylate) Glass', *Polym. J.*, vol. 38, no. 8, pp. 814–818, Aug. 2006, doi: 10.1295/polymj.PJ2005192.

[44] V. M. Boucher, D. Cangialosi, A. Alegrìa, J. Colmenero, J. González-Irun, and L. M. Liz-Marzan, 'Physical aging in PMMA/silica nanocomposites: Enthalpy and dielectric relaxation', *J. Non-Cryst. Solids*, vol. 357, no. 2, pp. 605–609, Jan. 2011, doi: 10.1016/j.jnoncrysol.2010.05.091.

[45] M. S. McCaig and D. R. Paul, 'Effect of film thickness on the changes in gas permeability of a glassy polyarylate due to physical agingPart I. Experimental observations', *Polymer*, vol. 41, no. 2, pp. 629–637, Jan. 2000, doi: 10.1016/S0032-3861(99)00172-X.

[46] Y. Huang and D. R. Paul, 'Physical aging of thin glassy polymer films monitored by gas permeability', *Polymer*, vol. 45, no. 25, pp. 8377–8393, Nov. 2004, doi: 10.1016/j.polymer.2004.10.019.

[47] P. Tiemblo, J. Guzmán, E. Riande, C. Mijangos, and H. Reinecke, 'Effect of physical aging on the gas transport properties of PVC and PVC modified with pyridine groups', *Polymer*, vol. 42, no. 11, pp. 4817–4823, May 2001, doi: 10.1016/S0032-3861(00)00922-8.

[48] A. Q. Tool, 'Relation between inelastic deformability and thermal expansion of glass in its annealing range', *J. Am. Ceram. Soc.*, vol. 29, no. 9, pp. 240–253, Sep. 1946, doi: 10.1111/j.1151-2916.1946.tb11592.x.

[49] A. Q. Tool, 'Viscosity and the extraordinary heat effects in glass', *J. Res. Natl. Bur. Stand.*, vol. 37, no. 2, p. 73, Aug. 1946, doi: 10.6028/jres.037.033.

[50] A. Q. Tool, L. W. Tilton, and J. B. Saunders, ‘Changes caused in the refractivity and density of glass by annealing’, *J. Res. Natl. Bur. Stand.*, vol. 38, no. 5, p. 519, May 1947, doi: 10.6028/jres.038.034.

[51] A. Q. Tool and C. G. Eicitlin, ‘Variations caused in the heating curve of glass by heat treatment’, *J. Am. Ceram. Soc.*, vol. 14, no. 4, pp. 276–308, Apr. 1931, doi: 10.1111/j.1151-2916.1931.tb16602.x.

[52] Y. Z. Yue, J. deC. Christiansen, and S. L. Jensen, ‘Determination of the fictive temperature for a hyperquenched glass’, *Chem. Phys. Lett.*, vol. 357, no. 1–2, pp. 20–24, May 2002, doi: 10.1016/S0009-2614(02)00434-7.

[53] C. T. Moynihan, A. J. Easteal, M. A. Bolt, and J. Tucker, ‘Dependence of the Fictive Temperature of Glass on Cooling Rate’, *J. Am. Ceram. Soc.*, vol. 59, no. 1–2, pp. 12–16, Jan. 1976, doi: 10.1111/j.1151-2916.1976.tb09376.x.

[54] A. J. Kovacs, ‘Glass transition in amorphous polymers: a phenomenological study’, *Adv Polym Sci*, vol. 3, no. 3, pp. 394–507, 1963.

[55] B. Riechers *et al.*, ‘Predicting nonlinear physical aging of glasses from equilibrium relaxation via the material time’, *Sci. Adv.*, vol. 8, no. 11, p. eabl9809, Mar. 2022, doi: 10.1126/sciadv.abl9809.

[56] C. R. Schultheisz and G. B. McKenna, ‘Volume recovery and physical aging in glassy polycarbonate following temperature jumps’, in *Polymeric Materials Science and Engineering, Proceedings of the ACS Division of Polymeric Materials Science and Engineering*, 1997, pp. 221–222.

[57] G. B. McKenna, ‘Looking at the glass transition: Challenges of extreme time scales and other interesting problems’, *Rubber Chem. Technol.*, vol. 93, no. 1, pp. 79–120, Jan. 2020, doi: 10.5254/rct.20.80376.

[58] J. C. Dyre, ‘Narayanaswamy’s 1971 aging theory and material time’, *J. Chem. Phys.*, vol. 143, no. 11, p. 114507, Sep. 2015, doi: 10.1063/1.4930551.

[59] D. Cangialosi, V. M. Boucher, A. Alegría, and J. Colmenero, ‘Direct Evidence of Two Equilibration Mechanisms in Glassy Polymers’, *Phys. Rev. Lett.*, vol. 111, no. 9, p. 095701, Aug. 2013, doi: 10.1103/PhysRevLett.111.095701.

[60] X. Monnier, S. Marina, X. Lopez De Pariza, H. Sardón, J. Martin, and D. Cangialosi, ‘Physical Aging Behavior of a Glassy Polyether’, *Polymers*, vol. 13, no. 6, p. 954, Mar. 2021, doi: 10.3390/polym13060954.

[61] D. Cangialosi, V. M. Boucher, A. Alegría, and J. Colmenero, 'Physical aging in polymers and polymer nanocomposites: recent results and open questions', *Soft Matter*, vol. 9, no. 36, p. 8619, 2013, doi: 10.1039/c3sm51077h.

[62] R. A. Pethrick, 'Positron annihilation—A probe for nanoscale voids and free volume?', *Prog. Polym. Sci.*, vol. 22, no. 1, pp. 1–47, Jan. 1997, doi: 10.1016/S0079-6700(96)00023-8.

[63] D. Cangialosi, M. Wübbenhorst, H. Schut, A. Van Veen, and S. J. Picken, 'Dynamics of polycarbonate far below the glass transition temperature: A positron annihilation lifetime study', *Phys. Rev. B*, vol. 69, no. 13, p. 134206, Apr. 2004, doi: 10.1103/PhysRevB.69.134206.

[64] D. Cangialosi, H. Schut, A. Van Veen, and S. J. Picken, 'Positron Annihilation Lifetime Spectroscopy for Measuring Free Volume during Physical Aging of Polycarbonate', *Macromolecules*, vol. 36, no. 1, pp. 142–147, Jan. 2003, doi: 10.1021/ma021214z.

[65] B. W. Rowe, S. J. Pas, A. J. Hill, R. Suzuki, B. D. Freeman, and D. R. Paul, 'A variable energy positron annihilation lifetime spectroscopy study of physical aging in thin glassy polymer films', *Polymer*, vol. 50, no. 25, pp. 6149–6156, Nov. 2009, doi: 10.1016/j.polymer.2009.10.045.

[66] D. M. Bigg, 'A review of positron annihilation lifetime spectroscopy as applied to the physical aging of polymers', *Polym. Eng. Sci.*, vol. 36, no. 6, pp. 737–743, Mar. 1996, doi: 10.1002/pen.10461.

[67] N. Doulache, M. W. Khemici, A. Gourari, and M. Bendaoud, 'DSC study of polyethylene terephtalate's physical ageing', in *2010 10th IEEE International Conference on Solid Dielectrics*, Potsdam: IEEE, Jul. 2010, pp. 1–4. doi: 10.1109/ICSD.2010.5568072.

[68] M. W. Khemici, N. Doulache, A. Gourari, and M. Bendaoud, 'Contribution to the Study of the Enthalpy Relaxation of Polyesters by DSC Experiments', *Int. J. Polym. Anal. Charact.*, vol. 17, no. 5, pp. 358–370, Jul. 2012, doi: 10.1080/1023666X.2012.668641.

[69] S. Souilem, N. Doulache, M. W. Khemici, and A. Gourari, 'TSDC and DSC Study of Effects of Physical Aging on Polybutylene Terephthalate (PBT)', *Int. J. Polym. Anal. Charact.*, vol. 19, no. 2, pp. 175–188, Feb. 2014, doi: 10.1080/1023666X.2014.873610.

[70] A. R. Ramos, J. M. Hutchinson, and A. J. Kovacs, 'Isobaric thermal behavior of glasses during uniform cooling and heating. III. Predictions from the multiparameter KAHR model', *J. Polym. Sci. Polym. Phys. Ed.*, vol. 22, no. 9, pp. 1655–1696, Sep. 1984, doi: 10.1002/pol.1984.180220909.

[71] L. C. E. Struik, 'On the rejuvenation of physically aged polymers by mechanical deformation', *Polymer*, vol. 38, no. 16, pp. 4053–4057, Aug. 1997, doi: 10.1016/S0032-3861(96)01002-6.

[72] G. Levita and L. C. E. Struik, 'Physical ageing in rigid chain polymers', *Polymer*, vol. 24, no. 8, pp. 1071–1074, Aug. 1983, doi: 10.1016/0032-3861(83)90162-3.

[73] L. C. E. Struik, 'The mechanical enhancement of physical aging', *Polymer*, vol. 21, no. 8, pp. 962–967, 1980.

[74] J. M. Hutchinson, S. Smith, B. Horne, and G. M. Gourlay, 'Physical Aging of Polycarbonate: Enthalpy Relaxation, Creep Response, and Yielding Behavior', *Macromolecules*, vol. 32, no. 15, pp. 5046–5061, Jul. 1999, doi: 10.1021/ma981391t.

[75] H. Yoshida, 'Relationship between enthalpy relaxation and dynamic mechanical relaxation of engineering plastics', *Thermochim. Acta*, vol. 266, pp. 119–127, Nov. 1995, doi: 10.1016/0040-6031(95)02437-9.

[76] R. Peredo-Ortiz, M. Medina-Noyola, T. Voigtmann, and L. F. Elizondo-Aguilera, '"Inner clocks" of glass-forming liquids', *J. Chem. Phys.*, vol. 156, no. 24, p. 244506, Jun. 2022, doi: 10.1063/5.0087649.

[77] B. R. Frieberg, E. Glynos, G. Sakellariou, M. Tyagi, and P. F. Green, 'Effect of Molecular Stiffness on the Physical Aging of Polymers', *Macromolecules*, vol. 53, no. 18, pp. 7684–7690, Sep. 2020, doi: 10.1021/acs.macromol.0c01331.

[78] Y. Guo and R. D. Bradshaw, 'Long-term creep of polyphenylene sulfide (PPS) subjected to complex thermal histories: The effects of nonisothermal physical aging', *Polymer*, vol. 50, no. 16, pp. 4048–4055, Jul. 2009, doi: 10.1016/j.polymer.2009.06.046.

[79] P. Cortés and S. Montserrat, 'Effect of previous thermal history on physical aging of amorphous poly (ethylene terephthalate)', in *Makromolekulare Chemie. Macromolecular Symposia*, Wiley Online Library, 1989, pp. 279–287.

[80] C. G. Robertson, J. E. Monat, and G. L. Wilkes, 'Physical aging of an amorphous polyimide: Enthalpy relaxation and mechanical property changes', *J. Polym. Sci. Part B Polym. Phys.*, vol. 37, no. 15, pp. 1931–1946, Aug. 1999.

[81] A. D. Drozdov, 'The effect of temperature on physical aging of glassy polymers', *J. Appl. Polym. Sci.*, vol. 81, no. 13, pp. 3309–3320, Sep. 2001, doi: 10.1002/app.1787.

[82] Z. Terzopoulou, M. Wahbi, N. Kasmi, G. Z. Papageorgiou, and D. N. Bikiaris, 'Effect of additives on the thermal and thermo-oxidative stability of poly(ethylene furanoate) biobased polyester', *Thermochim. Acta*, vol. 686, p. 178549, Apr. 2020, doi: 10.1016/j.tca.2020.178549.

[83] S. J. D. Smith, R. Hou, K. Konstas, A. Akram, C. H. Lau, and M. R. Hill, 'Control of Physical Aging in Super-Glassy Polymer Mixed Matrix Membranes', *Acc. Chem. Res.*, vol. 53, no. 7, pp. 1381–1388, Jul. 2020, doi: 10.1021/acs.accounts.0c00256.

[84] H. Zhou, E. A. Lofgren, and S. A. Jabarin, 'Effects of microcrystallinity and morphology on physical aging of poly(ethylene terephthalate): Physical Aging of PET', *J. Appl. Polym. Sci.*, vol. 106, no. 5, pp. 3435–3443, Dec. 2007, doi: 10.1002/app.26779.

[85] H. Zhou, E. A. Lofgren, and S. A. Jabarin, 'Effects of microcrystallinity and morphology on physical aging and its associated effects on tensile mechanical and environmental stress cracking properties of poly(ethylene terephthalate)', *J. Appl. Polym. Sci.*, vol. 112, no. 5, pp. 2906–2917, Jun. 2009, doi: 10.1002/app.29822.

[86] Y. Tanaka and N. Sakamoto, 'Analysis of TNM model calculation for enthalpy relaxation based on the fictive temperature model and the configurational entropy model', *J. Non-Cryst. Solids*, vol. 473, pp. 26–32, Oct. 2017, doi: 10.1016/j.jnoncrysol.2017.07.023.

[87] L. Andreozzi, M. Faetti, F. Zulli, and M. Giordano, 'Connecting Shear Stress Relaxation and Enthalpy Recovery in Polymers through a Modified TNM Approach', *Macromolecules*, vol. 37, no. 21, pp. 8010–8016, Oct. 2004, doi: 10.1021/ma049334p.

[88] H. Vogel, 'Das temperaturabhangigkeitsgesetz der viskositat von flussigkeiten', *Phys Z*, vol. 22, pp. 645–646, 1921.

[89] G. S. Fulcher, ‘Analysis of recent measurements of the viscosity of glasses’, *J. Am. Ceram. Soc.*, vol. 8, no. 6, pp. 339–355, 1925.

[90] G. Tammann and W. Hesse, ‘The dependence of viscosity upon the temperature of supercooled liquids’, *Z Anorg Allg Chem*, vol. 156, no. 1, pp. 245–257, 1926.

[91] G. Adam and J. H. Gibbs, ‘On the temperature dependence of cooperative relaxation properties in glass-forming liquids’, *J. Chem. Phys.*, vol. 43, no. 1, pp. 139–146, 1965.

[92] P. A. O’Connell and G. B. McKenna, ‘Arrhenius-type temperature dependence of the segmental relaxation below Tg’, *J. Chem. Phys.*, vol. 110, no. 22, pp. 11054–11060, Jun. 1999, doi: 10.1063/1.479046.

[93] J. Zhao and G. B. McKenna, ‘Temperature divergence of the dynamics of a poly(vinyl acetate) glass: Dielectric vs. mechanical behaviors’, *J. Chem. Phys.*, vol. 136, no. 15, p. 154901, Apr. 2012, doi: 10.1063/1.3701736.

[94] M. Pracella, L. Rolla, D. Chionna, and A. Galeski, ‘Compatibilization and properties of poly(ethylene terephthalate)/polyethylene blends based on recycled materials’, *Macromol. Chem. Phys.*, vol. 203, no. 10–11, pp. 1473–1485, Jul. 2002.

[95] W. Loyens, ‘Ultimate mechanical properties of rubber toughened semicrystalline PET at room temperature’, *Polymer*, vol. 43, no. 21, pp. 5679–5691, Oct. 2002, doi: 10.1016/S0032-3861(02)00472-X.

[96] X. Q. Cheng *et al.*, ‘Hyper-Cross-Linked Additives that Impede Aging and Enhance Permeability in Thin Polyacetylene Films for Organic Solvent Nanofiltration’, *ACS Appl. Mater. Interfaces*, vol. 9, no. 16, pp. 14401–14408, Apr. 2017, doi: 10.1021/acsami.7b02295.

[97] M. B. M. Mangion and G. P. Johari, ‘Relaxations in thermosets. VI. Effects of crosslinking on sub- T_g relaxations during the curing and aging of epoxide-based thermosets’, *J. Polym. Sci. Part B Polym. Phys.*, vol. 29, no. 4, pp. 437–449, Mar. 1991, doi: 10.1002/polb.1991.090290406.

[98] S. D. Kelman *et al.*, ‘Crosslinking poly[1-(trimethylsilyl)-1-propyne] and its effect on physical stability’, *J. Membr. Sci.*, vol. 320, no. 1–2, pp. 123–134, Jul. 2008, doi: 10.1016/j.memsci.2008.03.064.

[99] B.-W. Wang, H. Liu, J. Ying, C.-T. Liu, C.-Y. Shen, and Y.-M. Wang, 'Effect of Physical Aging on Heterogeneity of Poly(ε-caprolactone) Toughening Poly(lactic acid) Probed by Nanomechanical Mapping', *Chin. J. Polym. Sci.*, vol. 41, no. 1, pp. 143–152, Jan. 2023, doi: 10.1007/s10118-022-2806-1.

[100]C. Fang, X. Lu, and J.-P. Qu, 'Preparation and properties of biodegradable poly (lactic acid)/ethylene butyl acrylate glycidyl methacrylate blends via novel vane extruder', *Plast. Rubber Compos.*, vol. 48, no. 8, pp. 364–373, Sep. 2019, doi: 10.1080/14658011.2019.1630541.